BACTERIA-DOPED AEROGEL PREPARATION FOR POLLUTANTS REMOVAL FROM WASTEWATER

Thesis

Submitted by

DEBOJYOTI BASAK

[Exam Roll No: M4BPE24001]

[Class Roll No: 002210303001]

[Reg no. 144481 of 2018-2019]

Under the guidance of

Prof. (Dr.) PAPITA DAS

MASTER OF BIO-PROCESS ENGINEERING

DEPARTMENT OF CHEMICAL ENGINEERING

JADAVPUR UNIVERSITY

JADAVPUR, KOLKATA-700032

Declaration of originality and compliance with Academic Ethics

I hereby declare that this thesis contains the literature survey and original research work by the undersigned candidate, as a part of his Master of Bio-Process Engineering Studies. All information in this document has been obtained and presented per academic rules and ethical conduct.

I also declare that, as required by these rules and conduct, I have fully cited and referenced all material and results that are not original to this work.

Name: Debojyoti Basak

Roll No: 002210303001

Thesis Title: **Bacteria-doped Aerogel preparation for Wastewater Treatment**

Signature: Debojyoti Basak.

Date: 06/08/2024.

CERTIFICATE

This is to certify that the thesis entitled "**BACTERIA-DOPED AEROGEL PREPARATION FOR POLLUTANTS REMOVAL FROM WASTEWATER**" has been carried out by Debojyoti Basak in the fulfillment of the requirements for the Degree of the Master of Bio-Process Engineering from Jadavpur University, Kolkata is recorded as bona fide work that has been conducted under the supervision of Prof. (Dr.) Papita Das. The contents embodied in the thesis have not been submitted to any other University for the award of any degree or diploma.

Papita Das 6/8/24

Prof. (Dr.) Papita Das
Thesis Supervisor
Chemical Engineering Department
Jadavpur University
Kolkata- 700032

Dr. Papita Das
Professor
Dept. of Chemical Engineering
Jadavpur University, Kolkata

Papita Das 6/8/24

Prof. (Dr.) Papita Das
Head of The Department
Chemical Engineering Department
Jadavpur University
Kolkata- 700032

HEAD
CHEMICAL ENGINEERING DEPARTMENT
JADAVPUR UNIVERSITY
Kolkata-700 032

Dipak Laha 06/8/24

The Dean, Faculty of Engineering and Technology
Jadavpur University
Kolkata- 700032

DEAN
Faculty of Engineering & Technology
JADAVPUR UNIVERSITY
KOLKATA-700 032

ACKNOWLEDGEMENT

This thesis would not have been possible without the guidance and help of several individuals during the preparation and completion of this study.

First and foremost, I would like to show my sincere and utmost gratitude to my supervisor Dr. Papita Das, Professor, of the Department of Chemical Engineering, at Jadavpur University, Kolkata for her kind and valuable pieces of advice during the completion of this research work.

I am also very much grateful to the research scholars of my lab in the Chemical Engineering Department, Subhasis Ghosh, Sayan Mukherjee, Sampad Sarkar, Sk. Aakash Hossain, Poushali Chakraborty, Swastika Saha and Dr. Sandipan Bhattacharya for their kind and hearty cooperation. Whenever I found myself in difficulty, their ever-helping attitudes have given me the courage to proceed further.

I am grateful to my colleagues, seniors, and staff in the Department of Chemical Engineering, Jadavpur University, Kolkata, for their kind cooperation and moral support.

It would be incomplete if I did not mention my affable gratitude towards my family without whose constant support and enthusiasm this thesis would not have been completed.

Debojyoti Basak

Department of Chemical Engineering

Jadavpur University

Kolkata- 700032

TABLE OF CONTENTS

Abstract

1. Introduction **1-8**

2. Literature review **10-15**

2.1. Dye removal methods, Technologies **10-11**

2.2. General Aspect of Adsorption Process, one of the Emerging removal processes for wastewater treatment **12-13**

2.3. Aerogel as a Possible and widely used safe adsorbent **14**

2.4. Microbial-infused Aerogels for enhancing Adsorption encapsulating with bioremediation **14-15**

3. Aims and Objectives **17-18**

3.1. Aims of the study **17**

3.2. Objectives of the study **18**

4. Materials and methods **20-27**

4.1. Materials **20-21**

4.2. Preparation of Fillers **21-23**

4.2.1. Preparation of Biochar **21**

4.2.2. Preparation of Cellulose **22**

4.2.3. Preparation of Silica **23**

4.3. Preparation of Gel-Matrix of PVA-supported Aerogel **23-24**

4.3.1 Sol-gel Process of Hydrogel Synthesis 23

4.3.2. Lyophilization for converting Hydrogel to Aerogel 24

4.4. Isolation of micro-organisms 25

4.5. Preparation of Microbial Solution for Bioremediation 25

4.6. Immobilizing Micro-organisms inside the gel matrix of PVA Aerogel 25-26

4.7. Batch adsorption studies 26

4.8. Batch Biodegradation studies 26

4.9. Batch removal studies using bacteria-doped aerogel 27

5. Characteristics of aerogels 29~31

5.1. Analysis of functional groups and chemical bonds 29

5.2. Crystallographic structure analysis 29

5.3. Microscopic analysis 29

5.4. Calculation of Density 30

5.5. Calculation of Porosity 30

5.6. Swelling test 30

5.7. Moisture content of aerogels and effect of temperature 31

5.8. Effect of salinity 31

5.9. Effect of pH 31

6. Results and Discussions 33~104

6.1. Properties and Characteristics of Fillers: 33~34

6.1.1. Anthrone Test for characterization of cellulose 33~34

6.2. Properties and Characteristics of Aerogel 35~51

6.2.1. Density Analysis 35

6.2.2. Porosity Analysis 36

6.2.3. Moisture Content 37

6.2.4. Swelling Test 38

6.2.5. Degradation over pH changes and presence of salinity 39~40

6.2.5.1. Observation of Aerogel Degradation data 40

6.2.6. Scanning Electron Microscopy (SEM) of Aerogel 41

6.2.7. EDAX analysis 42~44

6.2.8. Thermogravimetric Analysis 45~47

6.2.9. FTIR analysis 48~49

6.2.10. Crystallographic Structure Analysis using XRD 50~51

6.2.10.1. Calculation of hkl and d_{hkl} value using Bragg' Law 51

6.3. Adsorption Studies of dyes and Other organic Components 52~67

6.3.1. Adsorption by Fillers 52~53

6.3.1.1. Sorting of Fillers for preparation of Aerogel 53

6.3.2. Adsorption by Aerogels 53~67

6.3.2.1. Effects of various parameters on adsorption 53~61

6.3.2.1.1. Contact Time 53~54

6.3.2.1.2. Effect of pH 55~57

6.3.2.1.3. Effect of Solution Temperature 57~58

6.3.2.1.4. Effect of Adsorbent Dosage 59~60

6.3.2.1.5. Effect of Pollutant Concentration 61~62

6.3.2.2. Optimization of Pollutant Removal by PVA and its derivatives aerogel 63~67

6.4.Concentration-Dependent Inhibition of Microbial Growth by Pollutants 67~70

6.5. Bioremediation of Pollutants 71~80

6.5.1. Effect of Different Parameters on Bioremediation 71~79

6.5.1.1. Effect of Contact Time 71~72

6.5.1.2. Effect of Temperature 73~74

6.5.1.3. Effect of pH 75~76

6.5.1.4. Effect of Pollutant Concentration 77~78

6.5.1.5. Effect of Microbial Dose 77~79

6.5.2. Sorting of bacteria for immobilization in Aerogel Matrix 80

6.6. Removal of Pollutants using Bacteria-doped Aerogel 80~87

6.6.1. Effects of various parameters on removal of pollutants 80~87

6.6.1.1. Effect of Contact Time 80~81

6.6.1.2. Effect of Temperature 82~83

6.6.1.3. Effect of solution pH 84~85

6.6.1.4. Effect of Pollutants Concentration 86

6.6.1.5. Effect of Adsorbent dosage 87

6.7. Comparative Analysis of Bacteria immobilized Aerogel with Base Aerogel on the removal process of pollutants 88~89

6.8. Modelling of Adsorption Process 90~98

6.8.1. Adsorption Isotherm 90~94

6.8.1.1. Langmuir Isotherm 91~92

6.8.1.2. Freundlich Isotherm 93~94

6.8.1.3. Significance of Isotherm analysis of Adsorption process by Aerogel 94

6.8.2. Adsorption Kinetics 94~96

6.8.2.1. Pseudo first Order kinetics 94~95

6.8.2.2. Pseudo second order kinetics 95~96

6.8.2.3. Analysis of Adsorption Kinetics of Adsorption process by Aerogel 96

6.8.3. Adsorption Thermodynamics 97~98

6.8.3.1. Conclusion of Thermodynamics analysis of the adsorption process 98

6.9. Kinetics of Bioremediation 99~100

6.9.1. Monod Kinetics 99~100

6.10. Toxicity analysis 101~104

6.10.1. Toxicological analysis based on germination of Moong Dal (*Vigna radiata*) seeds **101~104**

7. Conclusion and Future perspective **106**

List of Figures

Chapter 1:

Fig 1. Effects of various water-soluble textile dyes on human health (R Al-Tohamy et al., 2022)

Chapter 2:

Fig 2. Types of wastewater Treatments (Rápó, E., & Tonk, S, 2021).

Fig 3. Bonds formed during adsorption on the adsorbent surface (Rápó, E., & Tonk, S, 2021).

Chapter 4:

Fig 4. Biochar used as fillers for preparation of PVA derivatives Aerogels (A) SDBC, (B) RHBC, (C) GO.

Fig 5. Cellulose used as filler for the preparation of PVA derivatives Aerogels (A) RHC (b) SDC

Fig 6. Materials used for (A) PVA Silica Derivatives aerogel preparation, (B) Gel matrix preparation.

Fig 7: Hydrogel: (A) PVA Silica Hydrogel, (B) PVA Hydrogel

Fig 8: Aerogel: (A) PVA Saw Dust Aerogel, (B) PVA-APTES Aerogel

Chapter 6.

Fig 9. Anthrone test on a) Saw Dust and b) Rice Husk prepared using various Alkaline and Acid treatments.

Fig 10. Moisture Content of Aerogel

Fig 11. Swelling test of Aerogel

Fig 12. Aerogel Degradation over (A) pH changes and (B) presence of 10% NaCl solution

Fig 13. SEM image of (A) PVA, (B) PVA-Si, (C) PVA-SDC, (D) PVA-RHC, (E) PVA-GO, (F) PVA-RHBC, (G) PVA-SDBC, (H)PVA-MO

Fig 14. FESEM cross-sectional micrograph for EDAX analysis of PVA and its derivatives Aerogels (A) PVA, (B) PVA-Si, (C) PVA-APTES, (D) PVA-SDC, (E) PVA-RHC, (F) PVA-GO, (G) PVA-RHBC, (H) PVA-SDBC.

Fig 15. EDAX mapping of PVA and its derivatives aerogels: (A) PVA, (B) PVA-Silica, (C) PVA-APTES, (D) PVA-SDC, (E) PVA-RHC, (F) PVA-GO, (G) PVA-SDBC, (H)PVA-RHBC

Fig 16. TGA of PVA-RHC aerogel with region based on temperature variation

Fig 17. TGA of Aerogels (A) PVA, (B)PVA-Silane, (C)PVA-Silica, (D)PVA-SDC, (E)PVA-GO, and (F) PVA-MO

Fig 18. (A) FTIR analysis of PVA and its derivatives aerogels, (B) FTIR analysis of PVA with peak value

Fig 19. XRD spectroscopy data of PVA and its derivatives aerogel for Crystallographic Structure Analysis

Fig 20. Removal by fillers: (A) Congo Red, (B) Methylene Blue, (C) Pyrene, and (D) Anthracene

Fig 21. Effect of contact time with the Removal % of (A) Congo Red (B) Methylene Blue (C) Pyrene and (D) Anthracene using PVA and derivatives aerogel. Conditions: concentration 5mg/L, temperature 30^0C and pH-7.

Fig 22. Effect of pH on the Removal % of (A) Congo Red (B) Methylene Blue (C) Pyrene and (D) Anthracene using PVA and its derivatives aerogel. Conditions: concentration 5 mg/L of pollutant in aqueous solution, Adsorbent Dosage- 1g/L, temperature 30^0C, pH- 2, 7, 10.

Fig 23. Effect of Temperature with the Removal % of (A) Congo Red (B) Methylene Blue (C) Pyrene and (D) Anthracene using PVA and derivatives aerogel. Conditions: concentration 5mg/L of pollutant in aqueous solution, Adsorbent Dosage- 1g/L solution, temperature 20^0C, 30^0C, 40^0C and solution pH-7.

Fig 24. Effect of Adsorbent Dosage on the Removal % of (A) Congo Red (B) Methylene Blue (C) Pyrene and (D) Anthracene using PVA and derivatives aerogel. Conditions: concentration 5 mg/L of pollutant in aqueous solution, Adsorbent Temperature- 30^0C, Dosage variation 0.5g/L, 1g/L, 2g/L and solution pH-7.

Fig 25. Effect of pollutant concentration on the Removal % of (A) Congo Red (B) Methylene Blue (C) Pyrene and (D) Anthracene using PVA and its derivatives aerogel. Conditions: concentration 5mg/L, 10mg/L, and 20mg/L of pollutants in the solution, Adsorbent Dosage-1g/L solution, temperature 30^0C, and solution pH-7.

Fig 26. The Plot showing the relation between the prediction data points and the experimental data points as per the RSM model. (B) The 3D plot showing the interaction between the pH of the experimental solution and Dose of PVA-SDBC and their effect on the percentage removal of Methylene Blue, (C) The 3D plot showing the interaction between the pH of solution and concentration of Methylene Blue and their effect on the removal percentage of the pollutant, (D) The 3D plot showing the interaction between the Concentration of adsorbate and dosage of PVA-SDBC and their effect on the percentage removal of Methylene Blue.

Fig 27. The plot showing optimum value of adsorption process based on perturbation graph as per the RSM model. (B) The Contour graph showing the interaction between pH of the solution and Dosage of PVA-SDBC and their effect on the percentage removal of Methylene Blue, (C) The Contour plot showing the interaction between the pH of solution and concentration of Methylene Blue and their effect on the removal percentage of the pollutant, (D) The Contour plot showing the interaction between the Concentration of adsorbate and dosage of PVA-SDBC and their effect on the percentage removal of Methylene Blue.

Fig 28. 1) Concentration-dependent inhibition of A) WMO, B) *Lysinibacillus sp.*, C) *Bacillus subtilis*, D) *Pseudomonas sp.*, and E) SMO against Methylene Blue Dye

2) Concentration-dependent inhibition of A) *Bacillus subtilis*, B) *Lysinibacillus sp.*, C) *Pseudomonas sp.*, D) SMO, and E) WMO against Congo Red Dye

3) Concentration-dependent inhibition of A) *Bacillus subtilis*, B) *Lysinibacillus sp.*, C) *Pseudomonas sp.*, D) SMO, and E) WMO against Pyrene

4) 4) Concentration-dependent inhibition of A) WMO, B) SMO, C) *Pseudomonas sp.*, D) *Lysinibacillus sp*, and E) *Bacillus subtilis* against Anthracene

Fig 29. Effect of contact time with the Removal % of (A) Congo Red (B) Methylene Blue (C) Pyrene and (D) Anthracene using bioremediation process by bacterial strain culture *Bacillus subtilis*, *Pseudomonas sp.*, Soil white Micro-organism and Water Micro-organism. Conditions: concentration 5mg/L, temperature 30^0C and pH-7.

Fig 30. Effect of temperature on the Removal of (A) Congo Red (B) Methylene Blue (C) Pyrene and (D) Anthracene using bioremediation process by bacterial culture *Bacillus subtilis*, *Pseudomonas sp.*, Soil white Micro-organism and Water Micro-organism. Conditions: concentration 5mg/L, temperature 20^0C, 30^0C, 40^0C and pH-7.

Fig 31. Effect of pH on the Removal of (A) Congo Red (B) Methylene Blue (C) Pyrene and (D) Anthracene using bioremediation process by bacterial culture *Bacillus subtilis*, *Pseudomonas sp.*, Soil white Micro-organism and Water Micro-organism. Conditions: concentration 5mg/L, temperature 30^0C and pH-2, 7, 10.

Fig 32. Effect of Pollutants Concentration on the Removal of (A) Congo Red (B) Methylene Blue (C) Pyrene and (D) Anthracene using bioremediation process by bacterial culture *Bacillus subtilis*, *Pseudomonas sp.*, Soil white Micro-organism and Water Micro-organism with variable Concentration of 5 mg/L , 10 mg/L, and 20 mg/L where other parameters maintained at same condition Dosage of Bacteria: 1 µl/ml , pH-7 and Temp-30^0C.

Fig 33. Effect of Bacterial Dose on the Removal of (A) Congo Red (B) Methylene Blue (C) Pyrene and (D) Anthracene using bioremediation process by bacterial culture *Bacillus subtilis*, *Pseudomonas sp.*, Soil white Micro-organism and Water Micro-organism with variable dosage of 100 µl, 300 µl and 1ml where other parameters maintained at same condition Concentration of pollutants: 5mg/L, pH-7 and Temp-30^0C.

Fig 34. Effect of contact time on removal of the Pollutants: (A) Congo Red, (B) Methylene Blue, (C) Pyrene, and (D) Anthracene using PVA and derivatives aerogels immobilized by *Pseudomonas sp.* bacteria while maintaining conditions viz. Pollutants concentrations 5 mg/L, Dosage- 1g/L and Temperature-30^0C and pH-7.

Fig 35. Effect of Solution temperature on the Removal of (A) Congo Red (B) Methylene Blue (C) Pyrene and (D) Anthracene using *Pseudomonas sp.*-doped PVA and its derivatives Aerogel with variable Temperature of 20^0C and 40^0C where other parameters maintained at same condition Adsorbent Dosage: 1g/L, pH-7 and Conc-5 mg/L.

Fig 36. Effect of Solution pH on the Removal of (a) Congo Red (b) Methylene Blue (c) Pyrene and (d) Anthracene using *Pseudomonas sp.*-doped PVA and its derivatives Aerogel with variable pH of 2 and 10 where other parameters maintained at same condition Adsorbent Dosage: 1g/L, temperature-30^0C and Conc-5 mg/L.

Fig 37. Effect of Pollutants concentration on the Removal of (A) Congo Red (B) Methylene Blue (C) Pyrene and (D) Anthracene using *Pseudomonas sp.*-doped PVA and its derivatives Aerogel with variable conc 5, 10 and 20 mg/L where other parameters maintained at same condition Dosage: 1g/L, temperature-30^0C and pH- 7.

Fig 38. Effect of Adsorbent dosage on the Removal of (A) Congo Red (B) Methylene Blue (C) Pyrene and (D) Anthracene using *Pseudomonas sp.*-doped PVA and its derivatives Aerogel with variable dosage of 0.5, 1, 2 g/L and where other parameters maintained at same condition Concentration-5mg/L, temperature-30^0C and pH- 7.

Fig 39. (A) Methylene Blue Dye removal by PVA-SDBC immobilized with *Pseudomonas sp.* with mechanism of removal process with time difference. (B) comparative analysis of Bacteria-immobilized aerogel with Base aerogel.

Fig 40: A) Monod equation of Methylene Blue bioremediation using *Pseudomonas sp.* Bacteria, B) Double-reciprocating equation

List of Tables:

Chapter 6.

Table 1. Density of Aerogels:

Table 2. Porosity of PVA and its derivatives aerogels.

Table 3. Moisture content of PVA and its derivatives aerogel:

Table 4. Swelling test of PVA and its derivatives aerogel:

Table 5. Degradation of PVA and its derivatives aerogel with the changes of pH:

Table 6. Degradation of Aerogel in the presence of 10% NaCl Solution:

Table 7. Elemental compositions of different aerogels determined by EDAX analysis:

Table 8: hkl and d_{hkl} values of PVA and its derivatives aerogel using XRD analysis:

Table 9. ANOVA for Quadratic model for RSM analysis:

Table 10: ANNOVA for Quadratic Model:

Table 11. Langmuir isotherm significance of Methylene Blue removal by PVA-SDBC aerogel:

Table 12. Freundlich Isotherm significance of Methylene Blue by PVA-SDBC aerogel:

Table 13. Significance of pseudo first order kinetics of Methylene Blue by PVA-SDBC:

Table 14. Significance of pseudo second order kinetics of Methylene Blue removal by PVA-SDBC:

Table 15. Thermodynamics analysis on Methylene Blue removal by PVA-SDBC aerogel:

Table 16. Parameters analysis of Methylene Blue bioremediation by *Pseudomonas sp.* using Monod eqn:

Table 17. Toxicity analysis of bacteria immobilized PVA and its derivatives aerogel on germination process of Moong seeds.

Abstract

Emerging pollutants and large volumes of unused dyes from various industries create serious problems for water bodies. This work introduces a scalable approach to the application on purifying the water by adsorption of various dyes such as Congo Red (CR), Methylene Blue (MB), and some organic pollutants Pyrene and Anthracene from an aqueous solution using bacteria-doped modified aerogel with Sol-gel method of aerogel production focusing on both conventional and complex materials used as adsorbent during the process of removal of soluble waste. Key factors influencing adsorption efficiency, removal percentages such as surface characteristics, pore structure, and surface chemistry with chemical and structural stability of the adsorbents, are discussed. The mechanisms governing the adsorption, including physical, chemical interactions between adsorbates and adsorbents, are examined to provides insight into optimizing treatments processes.

The results from the studies show the high removal percentages in most of the experimental runs provide evidence of excellent performance of the adsorbent and the adsorption holds a higher adsorption capacity for PVA-Saw Dust Biochar-immobilized with Pseudomonas aeruginosa micro-organism on cationic, anionic and even organic pollutants. The preparation of aerogel was also done through recycling the waste materials and aerogels gave excellent removal percentage of > 85% along with the toxicology study of bacteria-doped aerogel on the germination of Moong Dal (Vigna radiata) to ensure toxic effects on the environment's living entities to ensure immobilized aerogels are suitable to implicates in removal process or not. This study shows the potential of bacteria-doped aerogel adsorbents in wastewater treatments along with the possible potential hazard generated during the adsorption.

Chapter 1: Introduction

1. Introduction

India has only 4% of global water resources, mainly from lakes, rivers, and ponds, while supports 18% of the world's population. Moreover, as an agrarian country, India is undergoing massive urbanization, with an urban population from 28% in 2000 to 35.9% in 2023 (Nager et al.,2020). Despite average GDP growth of 6.5% and increasing life expectancy, India's pharmaceuticals, automotive, chemical, petrochemical, and other manufacturing industries face severe water scarcity (Moussavi et al., 2018; Roshan and Kumar, 2020). The problematic situation of the water crisis is increasing with the increase of population in India and also by the rapid urbanization exponentially and a deep-research from the Department of Water Resources shows out of 7089 assessment units in the country 1006 units are so-called 'over-exploited' in the year 2022 and the situation is increasing more chaotic day-by-day and also the 'over-exploited' number was 909 in 2017 (reported at 9th Nov 2022 by PIB Delhi). That means the amount and quality of usable water are decreasing. But the reasons for the water crisis are not single. Various Emerging contaminants in the water source from multiple industries such as industrial chemicals, textiles, pharmaceuticals, hospital waste, and pesticides pose a significant hazard to water quality and amount (Amaly et. al., 2022; Ma, J et al.,2017; Prabha et al.,2017). These contaminations harm the ecosystem, and even trace amounts of specific chemicals can have a substantial impact (Gogoi, A. et al.,2018; Rathi et al, 2021).

The increase in population and urbanization has led to a rapid demand for synthetic dyes and the expansion of various industries viz. textile, plastic, paper, pulp, color photography, pharmaceutical, and other industries. It's estimated that about 7 x 10^5 -1 x 10^6 tons of dyes are produced annually (Parmar et al., 2021; Wan, Y et al.,2019). There are many types of dyes viz. Acid dye (viz. Acid orange 7), Basic dye (viz. Methylene blue and Basic yellow), Direct dye (viz. Congo Red and Direct Black 38), VAT dye (viz. Vat blue 1, and Vat acid

blue 74), and Nitro dye (viz. Naphthol yellow (II)), etc. (Dutta Soumi, 2021). However, most of the dyes are toxic (Bani-Atta, S. 2022) and the wastewater from industries must be treated before discharging into water bodies to remove water pollutants (Wang et al.,2020). Discharge of contaminated water poses a significant environmental concern. Around 40-45 % of dyes are contaminated with water during the dying process and 15-20% are rejected as wastewater, which changes water color (Drumond Chequer, F. M. et al.2011). Most of the dyes are carcinogenic, mutagenic, and also known as endocrine disruptors, which not only affect microbes and aquatic animals present in water but also create unfavorable conditions for plants and human life. In Fig 1. The effect of the textile dyes on human organs is shown.

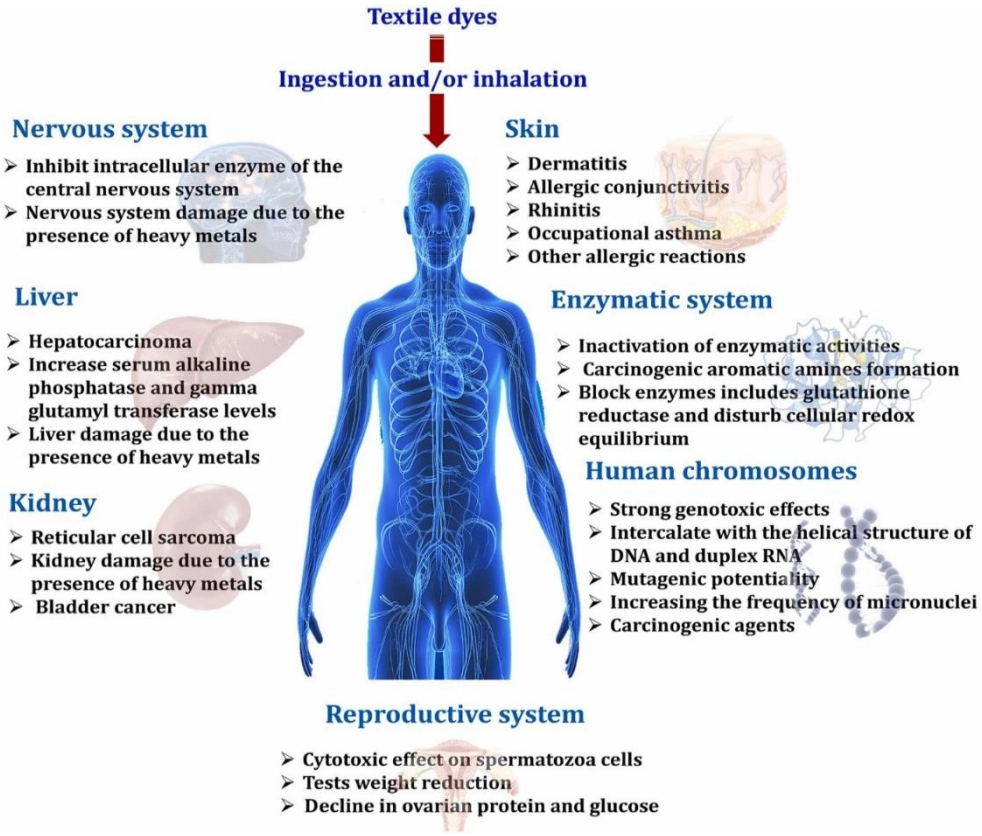


Fig 1: Effects of various water-soluble textile dyes on human health (R Al-Tohamy et al., 2022).

The accumulation of organic dyes in water bodies can also hinder light penetration, which can impede the natural process of decontamination and photosynthesis (Chowdhury et al., 2011). Except from all of the dyes organic waste materials also show various hazardous

problems in human bodies for example naphthalene which is considered as a carcinogenic, mutagenic agent along with acute kidney injuries and poisoning to children's bodies. Naphthalene can cause mutation in insects but not in bacteria and or cultured human lymphoblastoid cells (Sasaki et al., 1997; Grosovsky et al., 1997; NTP 2002). And can cause other types of genetic damage in the same but not all test systems. In the case of cultured mammalian cells, it causes chromosomal aberrations, sister chromatid exchange, and formation of kinetochore-negative micronuclei, but does not cause DNA strand break, formation of kinetochore, or cell transformation. And due to inhalation of naphthalene in rat bodies, can cause oxidative stress and also DNA damage, and liver and brain tissue damage (IARC 2002; NTP 2002). It's proved that organic and inorganic dyes can also affect plant cells vigorously. As an example, in the presence of 0.78mM naphthalene on 20-day-old pea plants with a light illumination of 15µmol photons.m^{-2}.s^{-1} decreases the maximum PS-2 quantum efficiency and noticeable changes in polyphasic induction kinetics of fluorescence and delays the fluorescence of Chlorophyll a (Lankin et al., 2014). Also, as in the case of Methylene Blue, it gives acute toxicity in Chlorella vulgaris and Spirulina platensis as Growth inhibition, Chl-a, Chl-b, Carotinoid, and protein production (Moorthy Abarna et al., 2021). Dyes are not the only serious problem for wastewater stream that ends up in natural water bodies. Also, these are large-scale organic waste products generated from pharmaceutical industries. For example, drug molecules such as antibiotics, anti-inflammatories, fat/lipids regulators, and also hormones. Their effects are spread throughout the whole human body and also affect the central nervous system (Frank et al., 2005) due to alteration of the metabolic system and modulation of receptors' working processes present in the nervous systems which cause the mutation of chromosomes (Maimon M and Cohen Ph. D., 1969), and long-term consumption of drug-contaminated water can cause lung, throat, and tongue cancer (Pignatti, Francesco et al., 2011; Bishop et al., 2004). And to an estimation, by WHO 6% of the world's humans are affected by cancer

and also the data from 2020 18,084,176 million cases were diagnosed globally. In India, cancer cases are not a negligible problem as in 2022, over 14 lakh new cases and 9 lakh deaths were reported. And, even most cancer patients are contaminated with the dangerous disease due to the consumption and usage of industrial wastewater viz. pharmaceuticals. So, the removal of inorganic and organic harmful wastes is an essential process to maintain the cleanliness of the water. Various treatments are also used to remove the pollutants such as dyes from water just as membrane filtration, flocculation, advanced oxidation, ozonation, and also some biological processes. However, some of these methods are challenging because of the high costs of operation and large volumes of sludge generation (Geyikci et al., 2012). Unfortunately, existing conventional methods cannot remove all these types of elements, so alternative treatment methods are required (Hassani et al.,2015). However, except all of these processes, adsorption is a low-cost, easy-to-design and operate method, with no production of toxic by-products, efficient in different conditions for different pollutants in wastewater, minimal chemical usage, and is able to treat wastewater at different pHs and temperatures that's why adsorption is one of the best processes to remove pollutants from wastewater.

For adsorption, Aerogels are one of the most interesting materials of the century (Barrios et al., 2019). They have gained considerable interest because of their unique properties such as high porosity, low density, high surface area, and excellent heat noise insulations. The highly porous nanostructured materials were first created by Kistler in 1931 (Kistler, 1931; Nita et al. 2020). As for definition, Aerogels are a class of synthetic porous ultralight material derived from a gel, in which the liquid component has been replaced with gas viz. air or liquid nitrogen, without significant collapse of the gel structure. They can be produced by the creation of a colloidal suspension of solid particles known as "sol" and followed by two methods lyophilization or super-critical drying. In both processes, the microporous structure of the material is preserved. Therefore, this material is highly porous

has extremely low density, and has high surface area. The first aerogel produced by Kistler was a silica aerogel obtained through super-critical drying. However, the precursors used in the production of silica aerogels are toxic and the resulting aerogel is not biodegradable and has unsatisfactory strength (Katti et al., 2006).

The materials used for the production of aerogel can be divided into three types inorganic, organic, or hybrid (Nita et al. 2020; Novak et al.1994). Organic aerogels can be produced from biopolymers that are based on renewable raw materials as the most abundant materials viz. cellulose because of various advantages i.e. biodegradability, biocompatibility, and low toxicity. As the inorganic aerogels are highly toxic and non-biodegradable, biological celluloses are given extra attention rather than inorganic ones. Examples of these types of components for the preparation of aerogel include various sources such as inorganic materials (viz. silica), artificial polymers (viz. PVA and formaldehyde) (Zhang L.et al.,2019), organic waste viz. (sawdust and rice husk), carbon-based materials (viz. graphene oxide and biochar) (Chen Y et al., 2019) even from polyamides and polystyrene (Ganesamoorthy, R., 2021) through the sol-gel polymerization process, in this process monomers react with other monomers to form 'sol' or a solid suspended collided solution that consists of bonded molecules, by cross-linking with each other. This crosslinking gives high structural strength and stability along with a more active site for adsorption. For example, Aerogels prepared from PVA monomers can withstand an impressive pressure viz. 12.7 MPa due to the presence of Hydrogen bonds which have bond-breaking energy of more than 23kJ/mol, and after doping with Graphene oxide and Ni with PVA aerogel they can withstand more pressure of about 172.2 MPa pressure. Also, Aerogels have a high surface area which allows a greater number of active sites available for adsorption, making them more efficient at removing contaminants from water. But the reason behind low thermal conduction and density is the 'Knudsen effect' where the reduction of thermal conductivity in gases when the size of the cavity encompassing the gas becomes

comparable to the means free path. Due to low density and high surface area make aerogels suitable for the adsorption process.

But not only the physical and chemical processes are enough for the removal of dyes especially organic ones because of their complex structures. That's why Bioremediation and adsorption make a better condition for removing waste from water. However, Bioremediation is another process where micro-organisms (considering bacteria, fungi, and algae) viz. free-cell, biofilm, or aggregates (or activated sludge flocs) play an important role in providing a greener, cost-effective, and sustainable solution toward the treatment of wastewater. Apart from the conventional direct application of micro-organisms wherein the organisms are freely exposed to contaminated water, an alternative approach can be used where microbial cells are cultured and immobilized or encapsulated in a permeable polymeric gel matrix, and the microbes immobilized in a gel matrix are exposed in contaminated media indirectly (Mehrotra et al., 2021).

Historically, immobilized microbes were first developed for in-situ production of enzymes. Back in 1969, the immobilized enzymes (Aminoacylase) were first used industrially for continuous production of L-amino acids from acyl-DL-amino acids (R. Singh *et al., 2000*). From then immobilized bacterial solutions are heavily used for enzyme production for in-situ conditions due to the disadvantages of free bacterial cell culture usage viz. low biomass concentration in a particular space/time, easy washout of microbes during the application, and susceptibility to external stressors also in case of application of bioremediation the encapsulated bacterial cells have specific advantages over free forms as examples, efficient separation of biomass from treated water, effective spatial-temporal control of biomass within the contaminated media, longer survivability, stability and reusability without loss of activity (Kang et al., 2005). That's why the modification of aerogel by bacterial doping also gives advantages during the removal process of pollutants rather than normal adsorption by aerogel.

This study can enlighten the crucial part of the preparation of bacteria-doped modified aerogel with the sol-gel method and removal efficiency of dyes in aqueous solution along with the characterization of aerogel using TGA, FTIR, XRD, EDAX and SEM. Also, the effect of several parameters, using adsorbent dosage, contact time, pH, temperature, and initial dye concentration was determined for removal efficiency. To optimize the experimental system, response surface methodology (RSM) constructed on Box- Behnken design (BBD) was used as an operative statistical and mathematical method to identify the effectiveness of different parameters concurrently assessed (Ganesamoorthy et al.,2021; Liu, M. et al.,2021; Malika, M. and Sonawane, S.,2021). Process optimization was then used to determine the optimal combination of input variables that result in the maximum or minimum response. With analysis of toxicological effects on the water through the germination process of seeds. The novelty of the study lies in its innovative approach to combatting water pollution caused by an emerging pollutant from various dye industries along with pharmaceutical industries' waste. By introducing a scalable approach involving the use of bacteria-doped aerogel along with the properties of the modification of aerogel to achieve remarkable contaminant removal efficiencies. This study presents a highly effective, cutting-edge solution with board implications for addressing complex water pollution challenges in various industrial and environmental contexts.

Chapter 2: Literature review

2. Literature review:

2.1. Dye removal methods, Technologies:

Dye removal methods have been summarized in review articles by many authors (Hessel C. et al., 2007; Singh P.K. and Singh R.L., 2017). The importance of removing dyes is driven by various factors; they are hazardous for health and the environment, often mutagenic or carcinogenic, inhibit the photosynthetic activity in aqueous solution, and even at low levels (< 1 mg/L) are highly visible and undesirable in water bodies, with color being the most obvious parameter affecting water quality (Chikri R. et al., 2020; Crini G., 2006). Hessel et al. described the percentage of non-fixed dye that may be discharged in the effluent as a function of dye classes from EPA and OECD legislation.

Throughout recent years, numerous investigations have been made to find the ideal technology for dye wastewater purification. Even though a wide range of methods have been studied in the past 30 years, only several and truly being implemented by the concerned industries these days due to the limitations they possess (Katheresan V., et al., 2018).

As it appears in the review articles referred the above, dye removal technologies can be divided into three main categories viz. physical, chemical, and biological treatments. Under all categories, there are various techniques for pollutant removal such as coagulation, chemical oxidation, membrane separation process, electrochemical, and aerobic and anaerobic microbial degradation. Each of the processes has its advantages and limitations (Ghoreishi S and Haghighi R. et al.,2003). In Fig 1. as a summary, three categories are briefly explained along with the advantages and disadvantages of the methods (Samsami S. et al., 2020).

Review articles exclusively analyze and compare paint removal methods. Often, published studies are used to illustrate the effectiveness of the methods presented. In these studies, several methods are classified into three main categories of pollutant removal (Bhatia D. et al., 2017; Madhav S. et al., 2018). As an example, physical treatments can be divided into various types viz. Adsorption, membrane separation, Ino exchange, ultrasonic mineralization, non-remediation, and reverse osmosis etc. Along with chemical treatments such as catalyst reduction, coagulation/flocculation, electrochemical reduction, etc. and biological methods can be divided into phytoremediation and microbial remediation (Bacterial, fungi, enzyme degradation, and phycoremediation) (Bhardwaj D. and Bharadvaja N., 2021).

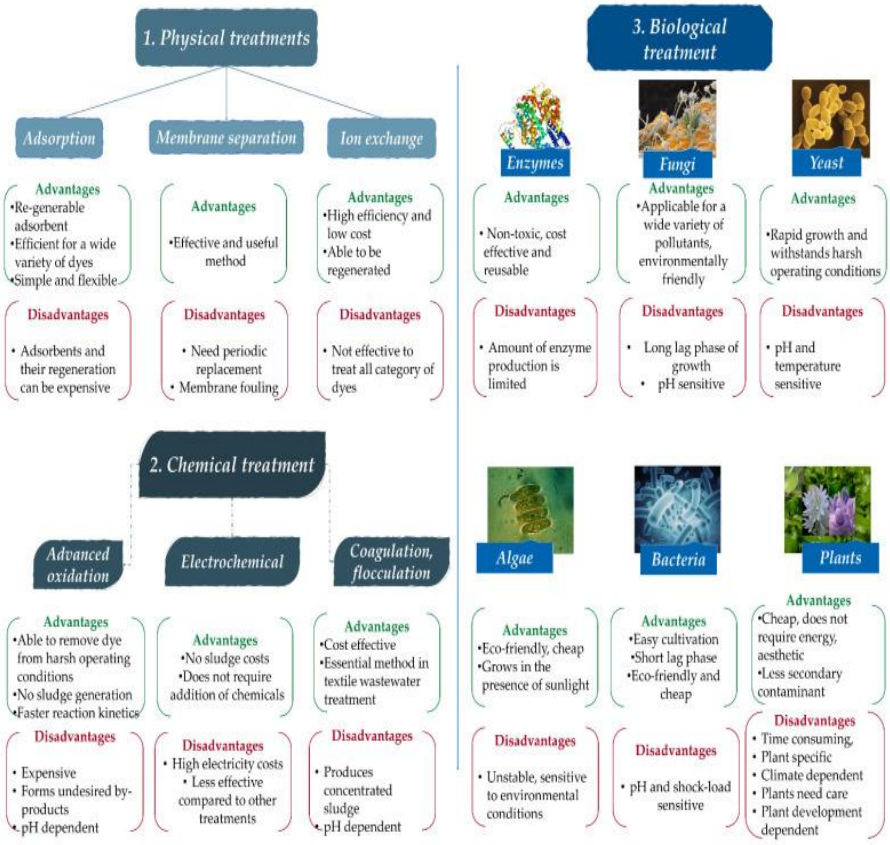


Fig 2: Types of wastewater Treatments (Rápó, E., & Tonk, S, 2021)

2.2. General Aspect of Adsorption Process, one of the Emerging removal processes for wastewater treatment:

The term adsorption was first used in 1881 by the German physicist Heinrich Kayser (Choudhary A., 2017). The past decade has seen a boom in environmental adsorption studies on the adsorption removal of pollutants from the aqueous phase. It is preferred over other methods because of its relatively simple design, operation, cost-effectiveness, and energy efficiency (Tan K.L. and Hameed B.H., 2017).

As definition of Adsorption is a mass transfer process or adhesion of atoms, ions, or molecules from a gas or liquid phase to form a mono-layer or multilayer on the adsorbent surface. That means the atoms or molecules by some physical, chemical, or biological forces prepare bonds with the surface of the adsorbents but can't penetrate the adsorbent surface. In practice, adsorption is performed as an operation, either in batch or in continuous mode, in a packed bed column with porous adsorbents (Abebe B. et al., 2018).

The adsorption process is sometimes confused with the absorption process which is an irreversible process where the molecules or atoms are taken by the volume, not by surface. A more common difference between adsorption with absorption is that in absorption the molecules penetrate a three-dimensional matrix, while in adsorption the molecules in a two-dimensional matrix (Qi Y. et al., 2017; Sims R.A. et al., 2018). The process is usually reversible, so the adsorption is responsible for the extraction of the substances but also for their release (Al-Ghouti M.A. and Da'ana D.A., 2020).

Like surface tension, adsorption is a consequence of surface energy. In a bulk material, all the bonding requirements of the constituent atoms of the material are fulfilled by another atom in the material. Depending upon the bonding presence between the adsorbents and adsorbates adsorption process can be divided into two parts: physisorption and another is chemisorption.

The process of adsorption happens due to forces existing between molecules and the forces can be primarily two types viz. Physical and Chemical bond force as a result of surface energy. In Fig 3. The nature of the bonds that can be formed during the adsorption of pollutants is described by their characteristics (Ruthven D.M., 1986; Kamaya Parashar, 2021; Terry P.A., Noble R.D., 2004).

Since adsorption is one of the common phenomena in natural biological, physical, and chemical systems, therefore various industries mostly wastewater treatment industries can take advantage of its benefits. The use of the adsorption process nowadays increasing rapidly on the pollutants contaminated water from various factories (Guo X. and Wang J., 2019; Al-Ghouti M.A. and Da'ana D.A., 2020). And currently become one of the most important and useful processes for the removal of low-concentration and non-degradable dyes and organic components from groundwater, drinking water production, and process water, or tertiary treatments (EMIS, 2018).

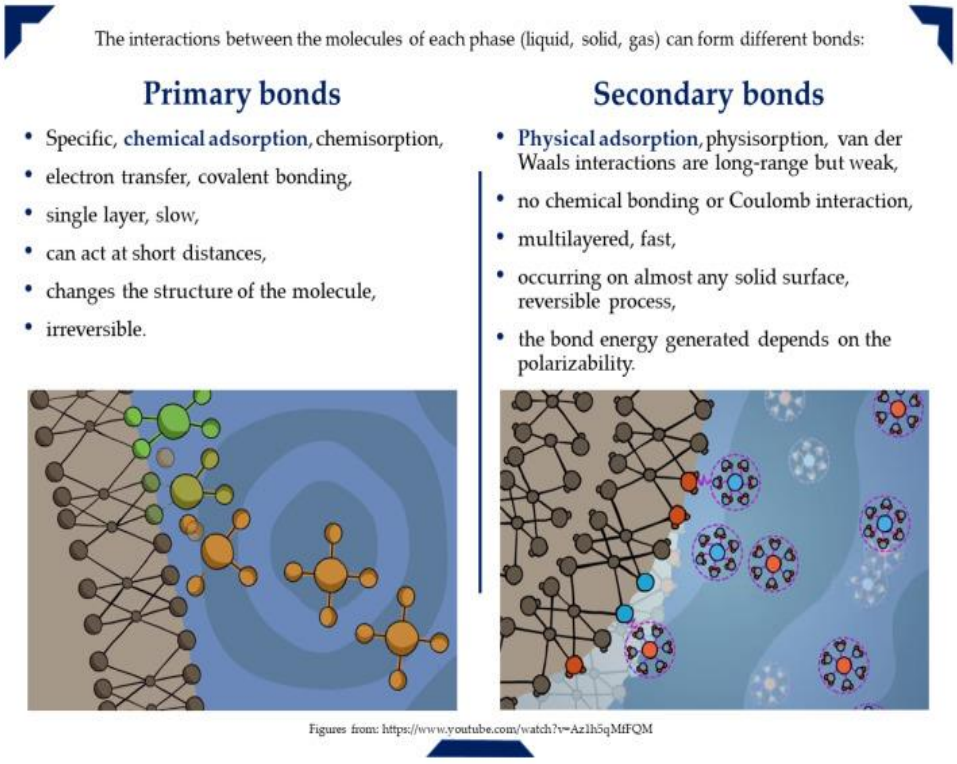


Fig 3: Bonds formed during adsorption on the adsorbent surface (Rápó, E., & Tonk, S, 2021).

2.3. Aerogel as a Possible and widely used safe adsorbent:

Aerogel was first created by Samuel Stephens Kistler in 1931 after replacing the liquid inside with gas and was given the name ‘Aerogel’ but till the time to 1960s, aerogel was not a popular pollutant removal agent in wastewater treatment plants because of the low strength of the aerogel structure and high cost of production. Then from the 1970s to the early 1980s after the initiation of the sol-gel technique production became quite simple from the technological side. In the year 2001, the ‘casting process’ was utilized for the preparation of the aerogel composite blanket, which involved the application of silica gel onto fiber batting, followed by supercritical drying, to enhance the strength the matrix strength. But in October 2002, the first commercially viable method of aerogel was prepared by using the compound ‘Polyvinyl Alcohol (PVA) as a binder since 2007 (Lee, 2020). Since that time the application of the sol-gel technique on the binder component viz. PVA with filler components like metal or carbonic oxide not only enhances the adsorption efficiency but also increases the strength and stability of the aerogel matrix structure (Erkey, 2011; Kreek, Kristiina, et al., 2014).

2.4. Microbial-infused Aerogels for enhancing Adsorption encapsulating with bioremediation:

Recent research has highlighted the promising potential of bacteria-immobilized aerogels as safe and effective adsorbents in various environmental and industrial applications. Aerogels, known for their high surface area and structural porosity, provide an ideal matrix for immobilizing bacteria due to their biocompatibility and structural stability along with pollutants degrading selectivity and transforming them into less harmful elements. According to research conducted by Akhavan et al., 2011, wrapping bacteria isolated from the environment into a Graphene nanosheet can influence the activity of removal of soluble dye from the wastewater by encapsulating two processes into the mechanism of one

adsorbent. Also, the selective biodegradation of oils in wastewater treatment processes is proved by the research of L Chen et al., 2024 using Micro-organisms immobilized hydroxyethyl cellulose/luffa composite sponge from this study it was observed that removal effects of immobilized degrading bacteria on nutrients in wastewater is better than that of suspended bacteria (L Chen et al., 2024). Studies have demonstrated the efficacy of such bio-functionalized aerogels in removing pollutants viz. organic pollutants, heavy metals, and even pathogens from the aquatic environments. Ongoing advancements in material science and microbiology continue to refine the design and performance of the bacteria-immobilized aerogels, paving the way for widespread adoption in environmental remediation and beyond.

Chapter 3: Aims and Objectives

3. Aims and Objective

3.1. Aims of the study:

The aim of this study is to synthesize Aerogel and to be doped with Micro-organism to aerogel matrix to form bacteria-doped aerogel for wastewater remediation. Nowadays water pollution has become an increasingly important problem in the world, because of this problem wastewater remediation is one of the foremost solutions to reduce wastewater problems. Wastewater is polluted with different types of organic and inorganic pollutants that if not removed can cause harmful effects not only on human health but also on animal and plant life mostly in aquatic life. To counter these problems many methods and techniques are being used. But out of them, the use of bacteria-doped aerogels has gained much attention due to their versatility, stability, and also for their mechanism of removal. Normal adsorption and adsorption processes still require the precursor material to be removed from the waterway as they still hold the contaminant in them that has a risk of being desorbed in the water defeating their original purpose. Bacteria-doped aerogel, on the other hand, can completely disintegrate the pollutant based on encapsulating two processes viz. adsorption by aerogel and bioremediation by bacteria immobilized inside the aerogel matrix and stay inert compounds in the water system causing no harm to the aquatic life cycle make it a feasible solution for wastewater remediation. In this study, we will see the effects of bacteria-doped aerogels on the Organic dyes also called Azo Dyes, we will comprehend the effects of bacteria-immobilized aerogel on these dyes, as how long it takes to remove them, what concentration they can be removed at the end the amount of bacteria-doped aerogel required to remove them along with the toxicological effects during the wastewater processing by the bacteria immobilized aerogel.

3.2. Objectives of the study:

The broad objective was to study the synthesis and test the productivity and effects of the bacteria-doped aerogels against the organic dye pollutants under favorable environmental conditions for immobilized micro-organism growth considering the low toxic effects on animals and plants mostly on aquatic species.

The specific objectives of the study were:

- To prepare a structurally stable aerogel doped with micro-organisms to make a complex aerogel structure.
- To examine the structural, and chemical properties of the bacteria-immobilized aerogel and comparative study against subsequent aerogel without doping.
- To determine the removal capacity of the pollutants using these complex adsorbents.
- To study the toxicological analysis of the by-product generated from the biodegradation of pollutants and social acceptance of bacteria-immobilized aerogel.

Chapter 4: Materials and Methods

4. Materials and Methods

4.1. Materials:

The chemicals used in the experiment, including Polyvinyl alcohol (PVA), HCl, and glutaraldehyde which were required for the 'gel matrix' of the aerogel, Biochar, combined treated Cellulose, Graphene oxide (GO), and (2-aminopropyl) triethoxysilane (APTES) in aerogel preparation were either prepared from renewable waste materials or any analytical-grade compounds. Biochar and Alkaline Acid treated cellulose were prepared from sawdust and rick husk wastes using 'Pyrolysis' and 'Delignification' processes respectively. And APTES [$C_9H_{23}NO_3Si$, 98%], Methylene Blue, and Pyrene (98%) were of analytical grade purchased from HiMedia Laboratories Pvt. Ltd. (India) Along with the PVA [$(C_2H_4O)n$, 99 %] and Anthracene (98 %) were kindly provided by Loba Chemie Pvt Ltd (India). And GO (>99 %) from Platonic Nanotech Private Limited (India) with HCl (35 %) and glutaraldehyde (25 %) were from Merck (Germany). For isolated bacterial culture Nutrient Media and Nutrient Agar are commercially purchased from Merck (Germany). However, GO and APTES were used to prepare the aerogel to compare the efficiency of removal of dyes in an aqueous solution of Congo Red, Methylene Blue, Anthracene, and Pyrene.

Bacterial Strains used in the studies are either isolated from different sources or commercially purchased. The commercially purchased bacterial viz. *Pseudomonas sp., Bacillus subtilis* and *Lysinibacillus sp.* are supplied by MTCC and Water and Soil Micro-organisms are isolated from Swargadwar and East Kolkata Wetlands using serial dilution methods.

Except for the chemicals and bacterial cultures, other instruments were used such as Erlenmeyer flasks (BOROSIL, India), test tubes (Slisco, India), measuring cylinders (BOROSIL, India), digital weighing balance (Sky Technologies, India), magnetic stirrer

REMI 2HML (REMI, India), centrifuge (REMI, India), incubator-shaker (GB Enterprise, India), Spectrophotometer (Shimizu Corporation, Japan), FTIR (Perkin-Elmer, USA), Scanning Electron Microscope (Zeiss, Germany), and TGA (Perkin-Elmer, USA).

4.2. Preparation of Fillers:

4.2.1. Preparation of Biochar:

Saw Dust and Rice Husk were taken to convert biochar using the pyrolysis process which is a partial thermal degradation of carbonaceous materials under various temperature differences from 400-800^{0}C (Jenkins et al.2016) without the presence of oxygen or in an oxygen-free atmosphere (Cory et al.,2009). Based on the yield of biochar at the temperatures of 400, 600, and 800^{0}C, shown in Fig 4. were taken for the preparation of Aerogel. The heating rate in this pyrolysis process is maintained at 20^{0}C per second to optimize the reaction for converting raw materials into biochar.

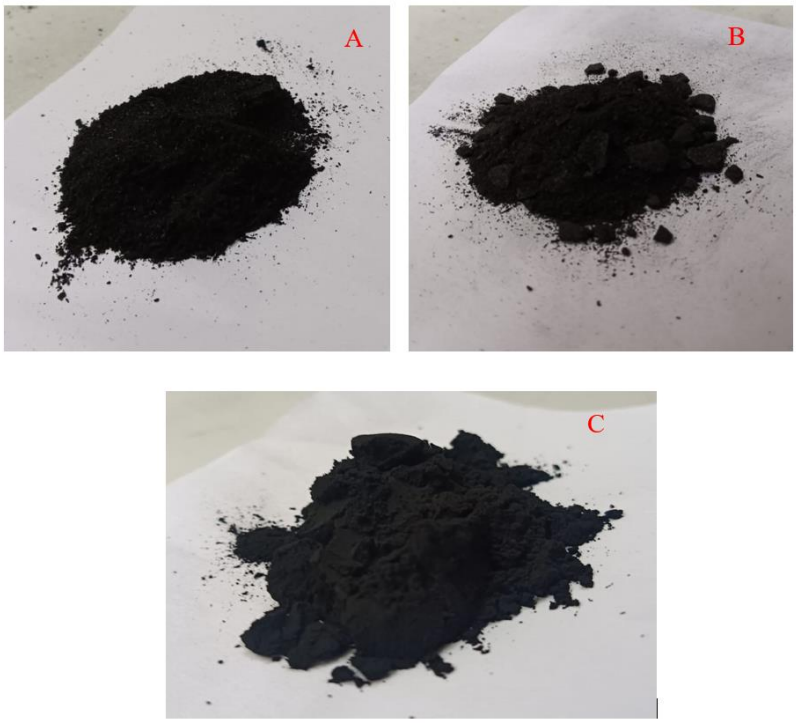


Fig 4: Biochar used as fillers for preparation of PVA derivatives Aerogels (A) SDBC, (B) RHBC, (C) GO.

4.2.2. Preparation of Cellulose:

Cellulose preparation involved extraction from lignin using acidic and alkaline treatments using variable % of NaOH or H_2SO_4 solution with dilution % viz. 2, 4, and 6 % on the waste of Saw dust and Rice husk followed using 4% HNO_3 for removal of non-cellulosic components in the mixture Sonicated Raw materials to obtain optimized cellulose preparation for the production aerogel. The process of making alkaline treated cellulose using NaOH is called Alkaline 'delignification' of Saw dust and Rice husk and on another hand, the using of H_2SO_4 is called Acidic 'delignification'. For Alkaline and Acidic treatments for cellulose preparation, the pH of the solution is maintained appx. 2-4 and 11-13 respectively (Cavali, Matheus, et al., 2020; Baksi et al.2019), and temperature is maintained at room temperature at 25 ± 5^0C. The preparation of cellulose was followed by the "Anthrone" test for quantifying and quantifying the presence of carbohydrates in the Saw Dust and Rice Husk cellulose. In Fig 5. The image of the cellulose extracted from Saw Dust and Rice Husk raw materials using Alkaline media viz. 6% NaOH is shown.



Fig 5: Cellulose used as filler for the preparation of PVA derivatives Aerogels (A) RHC (B) SDC

4.2.3. Preparation of Silica:

Economical silica preparation was done through an 'Acid precipitation' process where raw material and biological waste rice husk were burned at 600^0C temperature. Then with heating ash of Rice Husk was treated with 4% NaOH to prepare Sodium silicate. After cooling the liquid part of the solution was titrated with diluted HCl or H_2SO_4 to extract Silica from Rice Husk followed by washing and drying. In Fig 6: A) fillers prepared for the preparation of PVA-Silica Aerogels.

4.3. Preparation of Gel-Matrix of PVA-supported Aerogel:

4.3.1 Sol-gel Process of Hydrogel Synthesis:

As a typical sol-gel synthesis process, an aqueous mixture of PVA was prepared along with a heating and stirring effect until a homogeneous and transparent solution was achieved. In this process amount of PVA is taken (10±0.4) g per 200ml of water. Heating is done for 90 min and temperature is maintained about 80^0C or above. After the transparent solution appeared mixture was cooled at room temperature along with components for fillers taken at a ratio of 100:1 (w/w) but for APTES amount was 200µg. And stirred until a homogeneous mixture was achieved then HCl and Glutaraldehyde were mixed at an amount of 100µg each then heating was done at 80^0C until the gel was formed. According to the fillers used for Aerogel making they were named PVA, PVA-Silica, PVA-APTES, PVA-GO, PVA-Rice husk Cellulose, PVA-Saw Dust Cellulose, PVA-Graphene Oxide, PVA-Rice Husk Biochar and PVA-Saw Dust Biochar.



Fig 6: Materials used for (A) PVA Silica Derivatives aerogel preparation, (B) Gel matrix

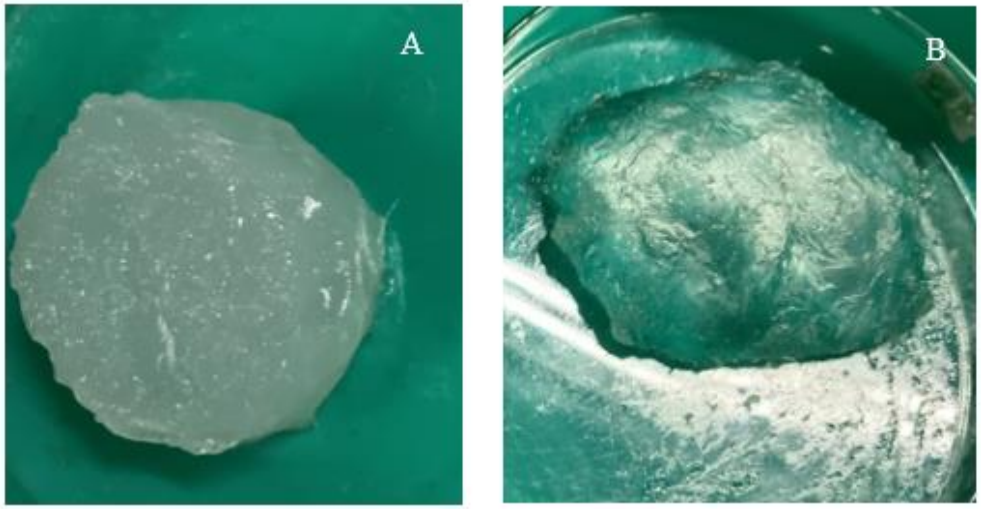


Fig 7: Hydrogel: (A) PVA Silica Hydrogel, (B) PVA Hydrogel

4.3.2. Lyophilization for converting Hydrogel to Aerogel:

After Hydrogels are prepared from the sol-gel process, a drying method is required where the phase boundary between the liquid and gas phase does not exist and thus the capillary pressure does not play an important role, which is called freeze-drying. Here, the solvent must be exchanged with a low expansion coefficient and a high sublimation pressure. The pore liquid is frozen and sublimed under vacuum (Husing et al., 1998). Material obtained in this way is called a cryogel. Unfortunately, freeze-drying has many disadvantages including the fact that the aging period has to be prolonged for stabilization of the network and, in some cases; the network may not be stable due to crystallization of the solvent in the pores.

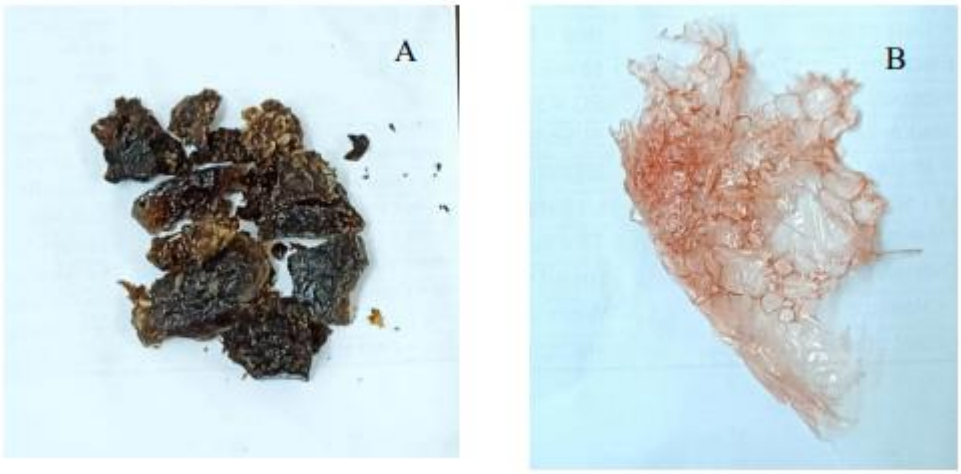


Fig 8: Aerogel: (A) PVA Saw Dust Aerogel, (B) PVA-APTES Aerogel

4.4. Isolation of microorganisms:

The micro-organisms are isolated from soil and water using serial dilution process and kept in a sterile nutrient broth media taken in Erlenmeyer Flask and incubated at 35^0C.

4.5. Preparation of Microbial Solution for Bioremediation:

For the Bioremediation of the pollutants in wastewater, microbial growth plays a vital role because of this reason media act as a suitable environment. For bacterial growth, Minimal media was used whereas components 3.5gram of Dipotassium Hydrogen Phosphate, 1gram of Potassium Dihydrogen Phosphate, 50 mg of Magnesium Sulphate, and 500 mg of Ammonium Sulphate were taken in 500ml of water. After dividing this solution into five microbial strain cultures were prepared which were *Bacillus subtilis*, *Pseudomonas sp.*, *Lysinibacillus sp*, Water Micro-Organism, and Soil Micro-Organism.

4.6. Immobilizing Micro-organisms inside the gel matrix of PVA Aerogel:

After cultivating the desired amounts of microbial colonies in minimal media solution, sterilization of aerogels and equipment was done to prevent unwanted microbial growth

during the entire process. Then Aerogels were mixed with bacterial suspension or directly introduced to the structure to prepare Bacteria-doped aerogel. However, throughout the process, some chemical stabilizations needed to be maintained to prevent structural damage of the aerogels.

4.7. Batch adsorption studies:

Adsorption was determined by the batch method, which permits convenient evaluation of parameters that influence the adsorption process. In the batch method, the aerogel was mixed with the specific volume of the solution (100 ml)and constantly agitated at 303 K in incubator for 3hr and after a constant time interval 1ml sample collected and centrifuged at 14000 rpm for 5 min on a centrifuger. Then the liquid was collected and concentration of the pollutants in the medium was determined using a spectrophotometer (Shimizu Corporation, Japan). This experiment was conducted three times, and the mean value was considered the result.

4.8. Batch biodegradation studies:

The 100 ml of prepared each Pollutants media were taken in Erlenmeyer flask and inoculated with the five different microorganisms and incubated. The readings were noted for every 24,48,72,96 and 120 hours interval to study the bioremediation patterns. Various parameters were altered viz., Pollutants concentrations (10mg/l, 30mg/l and 50mg/l); microbial dosage (100µl, 300 µl and 1ml); pH (2,7 and 10); temperatures (20^0C, 30^0C and 40^0C). The readings were taken at every 24-hour interval for 5 days. The baseline study was done with 10 ppm pollutants concentration, 100 µl microbial dosage and at pH 7 incubated at 30^0C. The five-day data was spectrophotometrically analyzed and degradation curve was obtained for different microbes with different parameters to find the optimum conditions for degradation. This experiment was conducted three times, and the mean value was considered the result.

4.9. Batch removal studies using Bacteria-doped Aerogel:

Removal studies of Immobilized aerogels were determined by the batch method, which permits convenient evaluation of parameters that influence the removal process. In the batch method, the immobilized aerogel was mixed with the specific volume of the solution (100 ml) and constantly agitated at 303 K in incubator for 120hr and after a constant time interval two 1ml of each sample collected and one sample was centrifuged at 14000 rpm for 5 min on a centrifuge. Then the liquid was collected from the centrifuged sample and concentration of the pollutants in the medium was determined using a spectrophotometer (Shimizu Corporation, Japan) and for the bacterial growth of immobilized aerogel sample was collected from the sample and their growth were measured using spectrophotometer at wavelength of 600nm. This experiment was conducted three times, and the mean value was considered the result.

Chapter 5.Characterization of Aerogels

5. Characterization of aerogel

5.1. Analysis of functional groups and chemical bonds:

The functional groups and chemical bonds present on the surface of aerogels are analyzed by attenuated total reflectance-Fourier transform infrared spectroscopy or ATR-FTIR (Perkin Elmer, Model- Spectrum 2, UK). For this analysis, a wavelength range of 500–4500 cm^{-1} was considered with a resolution of 4 cm^{-1}.

5.2. Crystallographic structure analysis:

To analyze the crystallographic structure of the prepared aerogels, an X-ray diffractometer or XRD (Bruker D-8 advanced, USA) was used. All six types of aerogels were studied by this characterization process to compare the effect of different modification agents on the crystallinity of aerogels. The percentage of crystallinity was calculated according to Eq. 1 as mentioned. Surface morphology and elementary composition analysis. The surface morphology of the aerogels was analyzed by scanning electron microscopy (SEM) (ZEISS EVO MA-10, Germany) using gold platting. It is a microscopic technique performed by shooting an electron beam on the surface of the sample and preparing an image by the detector. To understand the elementary composition of the aerogels, energy-dispersive X-ray spectroscopy (EDAX) analysis was performed.

$$\%\ of\ crystallinity = \frac{Area\ under\ the\ crystallinity\ curve}{Total\ area\ under\ curve} x\ 100 \quad \text{.....(1)}$$

5.3. Microscopic analysis:

A fluorescent microscope (Dewinter, model: Fluorex-LED) was used to observe the microscopic structure of the prepared aerogels. By using this analysis, the evenness of the aerogel surface and the presence of pores were observed.

5.4. Calculation of density:

Fifty milliliters of water was taken in a measuring cylinder. One gram of each aerogel was submerged in the water, and the final volume of water was measured. The density of aerogel was calculated by using Eq 2. This experiment was conducted thrice, and the mean value was considered the result.

$$Density\ of\ aerogel = \frac{Mass\ of\ aerogel}{Final\ volume\ of\ water - Initial\ volume\ of\ water} \quad \text{.....(2)}$$

5.5. Porosity analysis:

The formula used to calculate the porosity is mentioned as Eq. 3 and used in previous studies (Ferrero, F., 2007).

$$Porosity\ of\ aerogel = 1 - \frac{Density\ of\ aerogel}{Skeletal\ density\ of\ modefication\ agent} \quad \text{.....(3)}$$

The density of aerogels was calculated by using Eq. 2, and the skeletal density was calculated in the laboratory by measuring the weight of modification agents along with their volume. In this experiment, 1 g of each component was taken, and the gap between the particles was decreased by applying pressure. In this condition, the volume of the substance was measured, and skeletal density was calculated. This experiment was conducted thrice, and the mean value was considered the result.

5.6. Swelling test:

To understand the water absorption capacity of the prepared aerogels, the swelling test was performed. For this study, 1 g of each aerogel was submerged into water for 2 h, and the final weight was recorded. The percentage of weight difference or water uptake was calculated using Eq: 4. This experiment was conducted three times, and the mean value was considered the result.

$$\%\ of\ water\ uptake = \frac{Weight\ difference}{Initial\ weight} x100 \quad \text{.....(4)}$$

5.7. Moisture content of aerogels and effect of temperature:

To determine the moisture content of the aerogels, 1 g of each aerogel was placed inside a hot air oven at 333 K for 1 h. After heat treatment, the final weight of the aerogels were recorded. The moisture content in the aerogels was calculated by using Eq. 5. The equation is mentioned in the supplementary section. This experiment was conducted three times, and the mean value was considered the result. To understand the effect of temperature on the prepared aerogels, the heat-treated aerogels were characterized by ATR-FTIR.

$$Moisture\ content = \frac{Weight\ before\ heating - Weight\ after\ heating}{Initial\ weight} x100 \quad \text{.....(5)}$$

5.8. Effect of salinity:

To monitor the effect of salinity on aerogels, a 10% (W/V) NaCl solution was prepared, and 1 g of each aerogel was submerged into the solution for 2 h. After the treatment was completed, they were dried in a hot air oven at 333 K for 1 h. The final weight was recorded to calculate the percentage of weight difference, and the changes in functional groups were studied by ATR-FTIR analysis. To calculate the percentage of weight difference, Eq. 4 was used as mentioned "Swelling test" section. This experiment was conducted three times, and the mean value was considered the result.

5.9. Effect of pH:

To determine the effect of pH on aerogels, five different pH were considered viz., 2, 4, 6, 8, and 10. One gram of each aerogel was taken and submerged in the solution. After 2 and 24 h, the samples were collected and dried in a hot air oven at 333 K for 1 h, and the final weight was recorded. The percentage of degradation was calculated by using Eq. 3 as mentioned in the "Porosity Analysis" section. This experiment was conducted three times, and the mean value was considered the result.

Chapter 6: Results and Discussions

6. Results and Discussions

6.1. Properties and Characteristics of Fillers:

Characterization of fillers for aerogel preparation involves several parameters to ensure the optimal performance and properties of the final aerogel materials (Salimian, S., et al., 2018). Fillers play a crucial role in enhancing specific properties of aerogels. Characterization of fillers mainly involved Chemical and Physical Characterization. Chemical Characteristics are more important for examining the fillers' structure, for an example, the Anthrone test for Cellulose, prepared by the 'delignification' process, which is the most important for sorting out the fillers for optimizing the adsorbent preparation.

6.1.1. Anthrone Test for characterization of cellulose:

Anthrone test is a chemical test used to detect the presence of carbohydrates and quantify them in the fillers viz. Sawdust and Rice Husk cellulose are prepared from the Acid and Alkaline 'delignification' process. The process of the Anthrone test consists of 3 crucial steps of the reaction:

1. Hydrolysis of polysaccharides to monosaccharide
2. Dehydration of monosaccharide to furfural
3. Reaction of furfural with Anthrone reagents

Anthrone reagent is a solution of dissolved naphthol in concentrated sulfuric acid and needed to be freshly prepared for the test, mainly 2g of naphthol needed to be dissolved in 1 liter of concentrated sulfuric acid. After mixing the polysaccharide in the Anthrone reagents heating needed to be done at 90^0C for 20 minutes. After cooling the sample Optical Density is measured at 625nm against a blank solution to quantify the presence of carbohydrates in the filler samples.

In Fig 9. The Anthrone test results on acid and alkaline-treated Rice Husk and Saw dust Cellulose are shown along with the compare studies for sorting the fillers and optimizing the process. And form the graphical representation it can be easily determined that using high acid and alkaline solutions increases the cellulose extraction by the delignification process. However, the alkaline treatments on Saw Dust and Rice Husk show the highest concentration of cellulose presence in the sample causing the selection of NaOH-treated cellulose for preparation of Aerogel can optimize the process of adsorption with the highest removal efficiency.

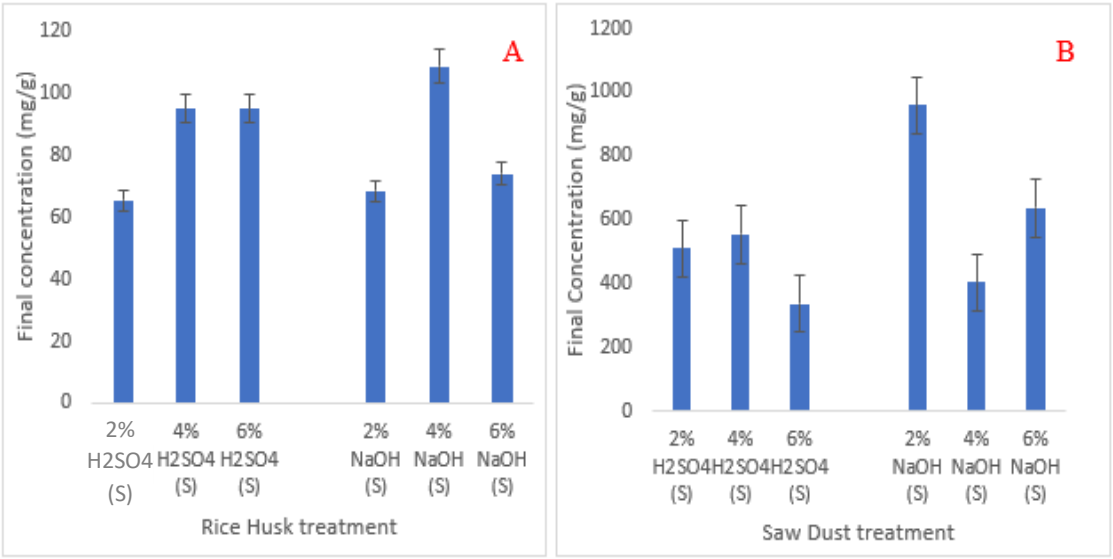


Fig 9: Anthrone test on a) Saw Dust and b) Rice Husk prepared using various Alkaline and Acid treatments.

6.2. Properties and Characteristics of Aerogel:

Aerogels prepared from the sol-gel technique have some unique properties which make them attractive in science and technology, as given in the below tables with various aerogels. Due to these unique properties, aerogels can be used in various applications, and also because of the preparation of aerogel from waste products makes it biodegradable and environment friendly.

6.2.1. Density Analysis:

The density of Aerogels is naturally low because of the use of supercritical drying or cryogenic drying process to replace the liquid portion of hydrogel with gas or air making it completely low dense and giving one of its unique properties. Some of the previous research work shows the density of aerogel is situated between 0.05 to 0.2 g/cm^3 (KH Lee et al., 1995). Also, the density of PVA and its derivatives aerogel show some impressive low-dense properties as given in Table 1.

Table 1: Density of Aerogels:

Aerogel	Density (g/cm^3)
PVA	0.124
PVA-Silica	0.1091
PVA-Silane	0.094
PVA-Rice Husk Cellulose	0.1605
PVA-Saw Dust Cellulose	0.16
PVA-Graphene Oxide	0.1371
PVA-Rice Husk Biochar	0.2629
PVA-Saw Dust Biochar	0.1325

6.2.2. Porosity Analysis:

Aerogels have high overall porosity and overall good pore accessibility. For low density of aerogel and replacement of liquid with air makes it high pore creation. As from the previous research works on aerogels show that the porosity of aerogels exists between 90 to 99.5% (Zheng, Qifeng, et al., 2018). Silica aerogels have porosity that is very high as much as 99% with an average pore diameter of ~20nm.

One most important aspects of the aerogel pore network is its "open" to nature and interconnectivity. In open-pore structures, however, the fluids can flow pore to pore, with a limited restriction, and eventually travel through the entire material (Dorcheh, A. et al., 2008). The porosity of the PVA and its derivatives aerogels is given in Table 2.

Table 2: Porosity of PVA and its derivatives aerogels.

Aerogels	Porosity (%)
PVA	90.46
PVA-Silica	97.05
PVA-Silane	95.95
PVA-Rice Husk Cellulose	93.58
PVA-Saw Dust Cellulose	94.07
PVA-Graphene Oxide	95.58
PVA-Rice Husk Biochar	83.57
PVA- Saw Dust Biochar	92.21

6.2.3. Moisture Content:

Aerogels have low moisture content properties and because of the freeze-drying process used for preparing the aerogel, most of the aerogels have a moisture content of less than 20%. Aerogels are typically 95%- 99% air by volume makes them ultralight and porous. Because of this reason of high air content low amount of liquid is present in the structure also the low moisture presence in the aerogel makes it low thermal conductive. In Table 3 and Fig 10. the moisture content of PVA and its derivatives are shown:

Table 3: Moisture content of PVA and its derivatives aerogel:

Aerogel	Moisture Content (%)
PVA	16.0
PVA-Silica	8.12
PVA-Silane	11.61
PVA-Rice Husk Cellulose	12.65
PVA-Saw Dust Cellulose	14.26
PVA-Graphene Oxide	16.60
PVA-Rice Husk Biochar	11.13
PVA-Saw Dust Biochar	12.43

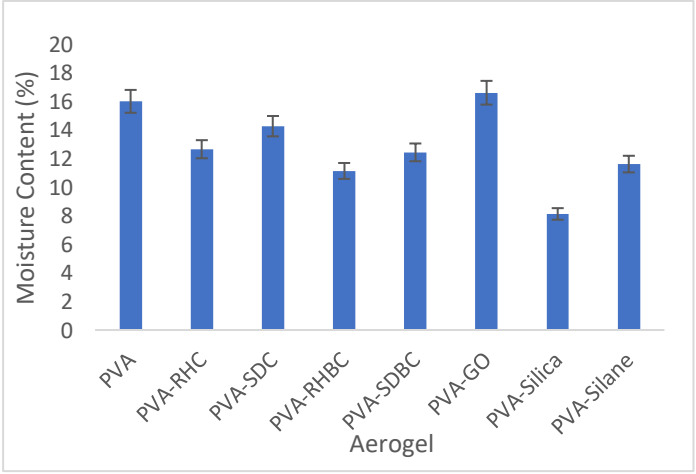


Fig 10: Moisture Content of Aerogel

6.2.4. Swelling Test:

The swelling test of aerogels shows the amount of pore and size of the pore present in the aerogel and the amount of water absorbed is directly proportional to the pore size and air present in the aerogel structure. The previous research work shows that most aerogels have swelling properties of more than 90% (H Lu et al., 2022). The capability of high swelling properties indicates high adsorption and absorption nature in aerogel structure. In Table 4 and Fig 11. the results of the swelling test on PVA and its derivatives aerogels are shown.

Table 4: Swelling test of PVA and its derivatives aerogel:

Aerogel	Swelling test
PVA	118.34 %
PVA-Silica	187.25
PVA-Silane	276.94
PVA-Rice Husk Cellulose	121.05
PVA-Saw Dust Cellulose	74.92
PVA-Graphene Oxide	80.73
PVA-Rice Husk Biochar	145.147
PVA-Saw Dust Biochar	258.511

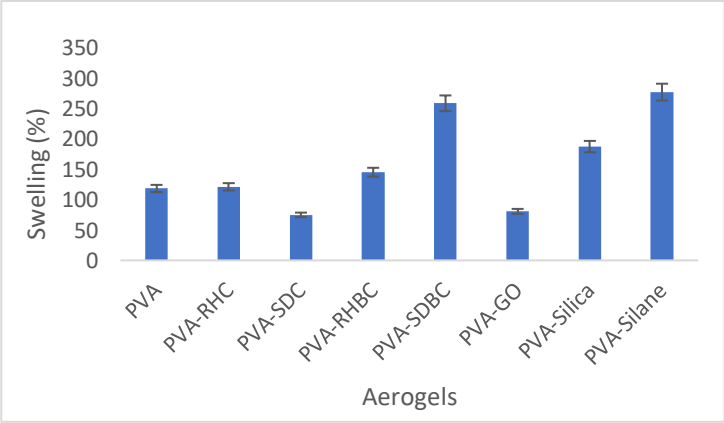


Fig 11: Swelling test of Aerogel

6.2.5. Degradation over pH changes and presence of salinity:

Aerogels have structural instability with changes in pH and Salinity. Because the change in pH strongly affects the intermolecular structural morphology of the aerogel. According to the research works by Khedkar, Mangesh V., et al., at pH~5 the silica aerogel shows better quality than other pH Solutions and the change in pH affects the density, Thermal Stability, pore size, and pore structure. Also, the salinity changes have the same effect on aerogel as pH changes and some of the changes can be observed even in the adsorption of dyes by the aerogel (Zhang, Yongmin, et al., 2022). In Tables 5 and 6, the 24-hour degradation study of aerogel with an initial weight of 1 gram in the presence of 10% NaCl and with the pH changes are shown respectively, and through Fig 12: the comparison between the degradation of aerogels can be examined,

Table 5: Degradation of PVA and its derivatives aerogel with the changes of pH:

Aerogel	Degradation with pH changes				
	pH 2	pH 4	pH 6	pH 8	pH 10
PVA	7.4	3.9	3.1	8	4
PVA-Silica	4.8	2.5	2.3	3.8	3.5
PVA-Silane	98.5	97.3	95.6	48.5	5.6
PVA-Rice Husk Cellulose	8	2.9	3.8	7.9	3.3
PVA-Saw Dust Cellulose	1.8	2.8	3.9	3.8	4.1
PVA-Graphene Oxide	1	0.5	18	1.1	4
PVA-Rice Husk Biochar	0.8	1.4	1.6	2.8	3.1
PVA-Saw Dust Biochar	1.1	3.8	1.1	1.3	2.9

Table 6: Degradation of Aerogel in the presence of 10% NaCl Solution:

Aerogel	Degradation of Aerogel
PVA	9.68
PVA-Silica	15.77
PVA-Silane	-56.76
PVA-Rice Husk Cellulose	4.67
PVA-Saw Dust Cellulose	3.05
PVA-Graphene Oxide	-25.88
PVA-Rice Husk Biochar	8.40
PVA-Saw Dust Biochar	16.33

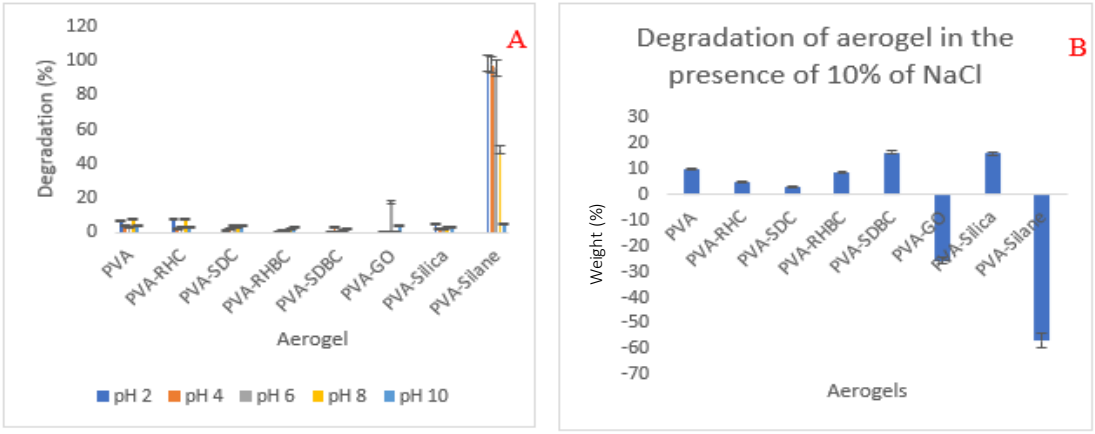


Fig 12: Aerogel Degradation over (A) pH changes and (B) presence of 10% NaCl solution

6.2.5.1. Observation of Aerogel Degradation data:

Degradation studies of Aerogel were done under different pHs from basic to Acidic conditions along with the application of salinity by applying 10% of NaCl solution on the initial 1-gram weighted samples. Throughout the process, temp is maintained at 30^0C. After the studies, it was observed that PVA-Silane showed the highest structural degradation over the pH changes and the presence of salinity was higher than other aerogels which was more than 90%

6.2.6. Scanning Electron Microscopy (SEM) of Aerogel:

Fig. 13 shows SEM photographs of PVA and its derivatives aerogels along with one of the bacteria-doped aerogels. From Fig 13 (H), it can be observed that bacteria doping in aerogel with no physical and chemical deformation presence of mesopores and excessive presence of surface responsible for adsorption. As like state above, it is possible to observe the microchemical and physical states in aerogel and the filler presence in its structure.

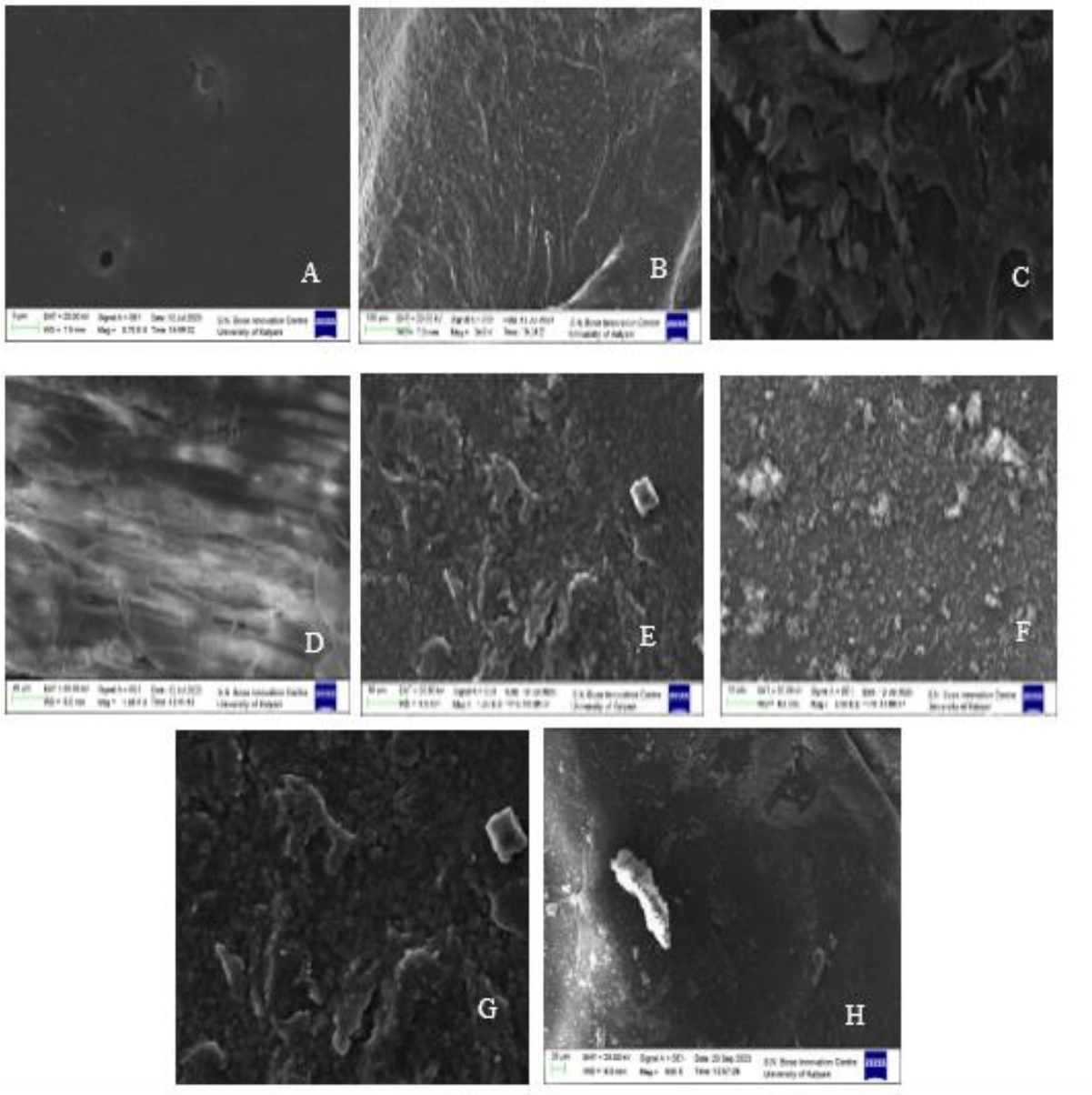


Fig 13: SEM image of (A) PVA, (B) PVA-Si, (C) PVA-SDC, (D) PVA-RHC, (E) PVA-GO, (F) PVA-RHBC, (G) PVA-SDBC, (H)PVA-MO

6.2.7. EDAX analysis:

Table 7. Elemental compositions of different aerogels determined by EDAX analysis:

Aerogel	C wt%	O wt%	Si wt%
PVA	100	_	_
PVA-SDC	62.04	37.96	_
PVA-RHC	64.77	35.23	_
PVA-SDBC	57.68	42.32	_
PVA-RHBC	57.58	42.42	_
PVA-Si	51.13	40.10	8.78
PVA-APTES	57.62	29.43	12.95
PVA-GO	56.68	43.32	_

EDAX patterns of PVA and its derivatives in PVA aerogels are shown in Table 7, and Fig 15. which indicate the presence and weight percentage of molecules in Aerogels (Meddouri, Malaaz, et al, 2014). PVA, PVA-Saw Dust Cellulose, PVA-Rice Husk Cellulose, PVA-Graphene Oxide, PVA-Saw Dust Biochar, and PVA-Rice Husk Biochar shows the presence of C wt% about 100, 62.04, 64.77, 57.68, 57.58, 56.68 respectively with O wt% of about 35 to 45 %. The ratio of [Si]/[C] is 0.178 for PVA-Silica and 0.225 for PVA-APTES respectively which shows no presence of other impurities in the aerogel structure.

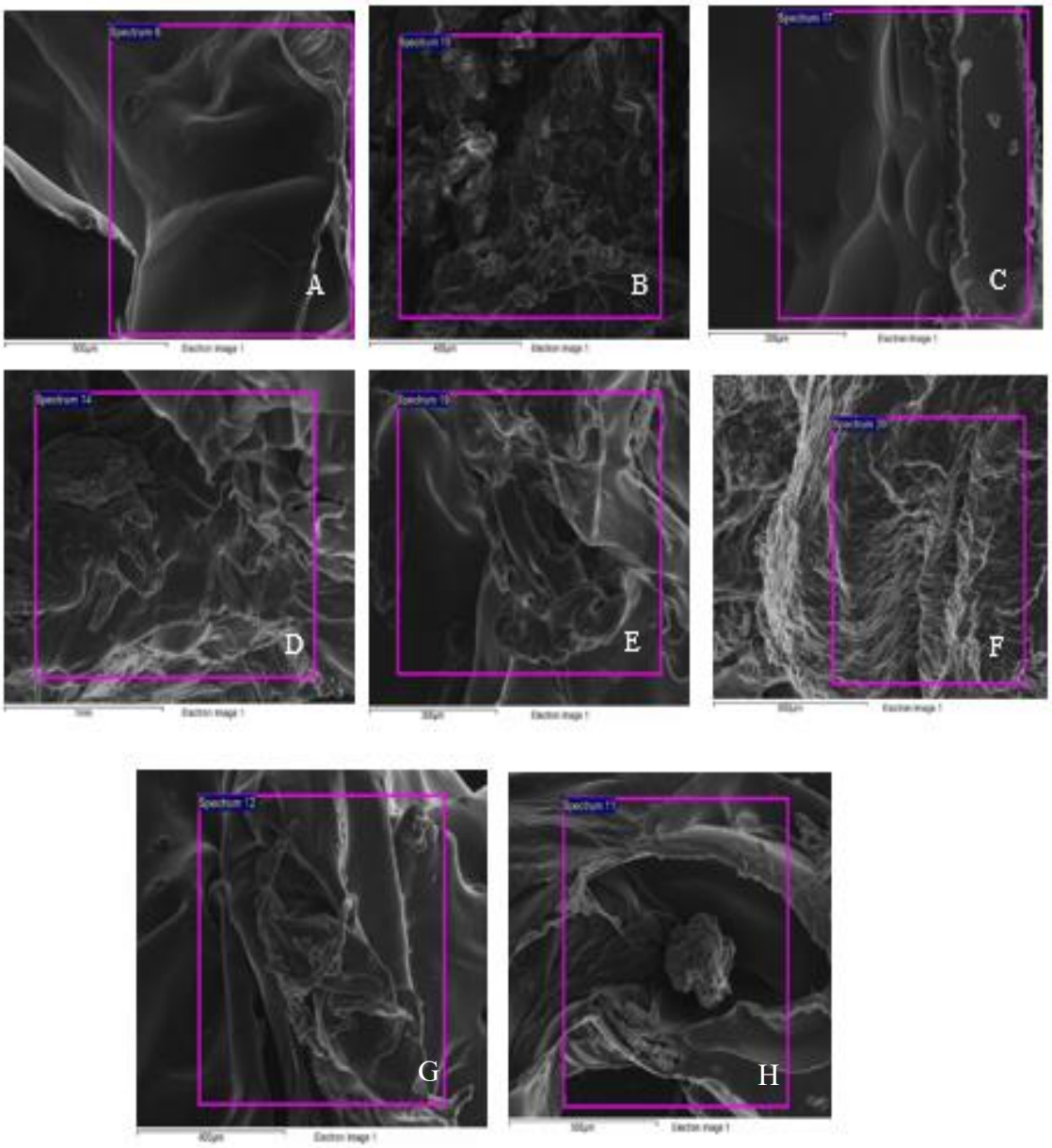


Fig 14: FESEM cross-sectional micrograph for EDAX analysis of PVA and its derivatives Aerogels (A) PVA, (B) PVA-Si, (C) PVA-APTES, (D) PVA-SDC, (E) PVA-RHC, (F) PVA-GO, (G) PVA-RHBC, (H) PVA-SDBC.

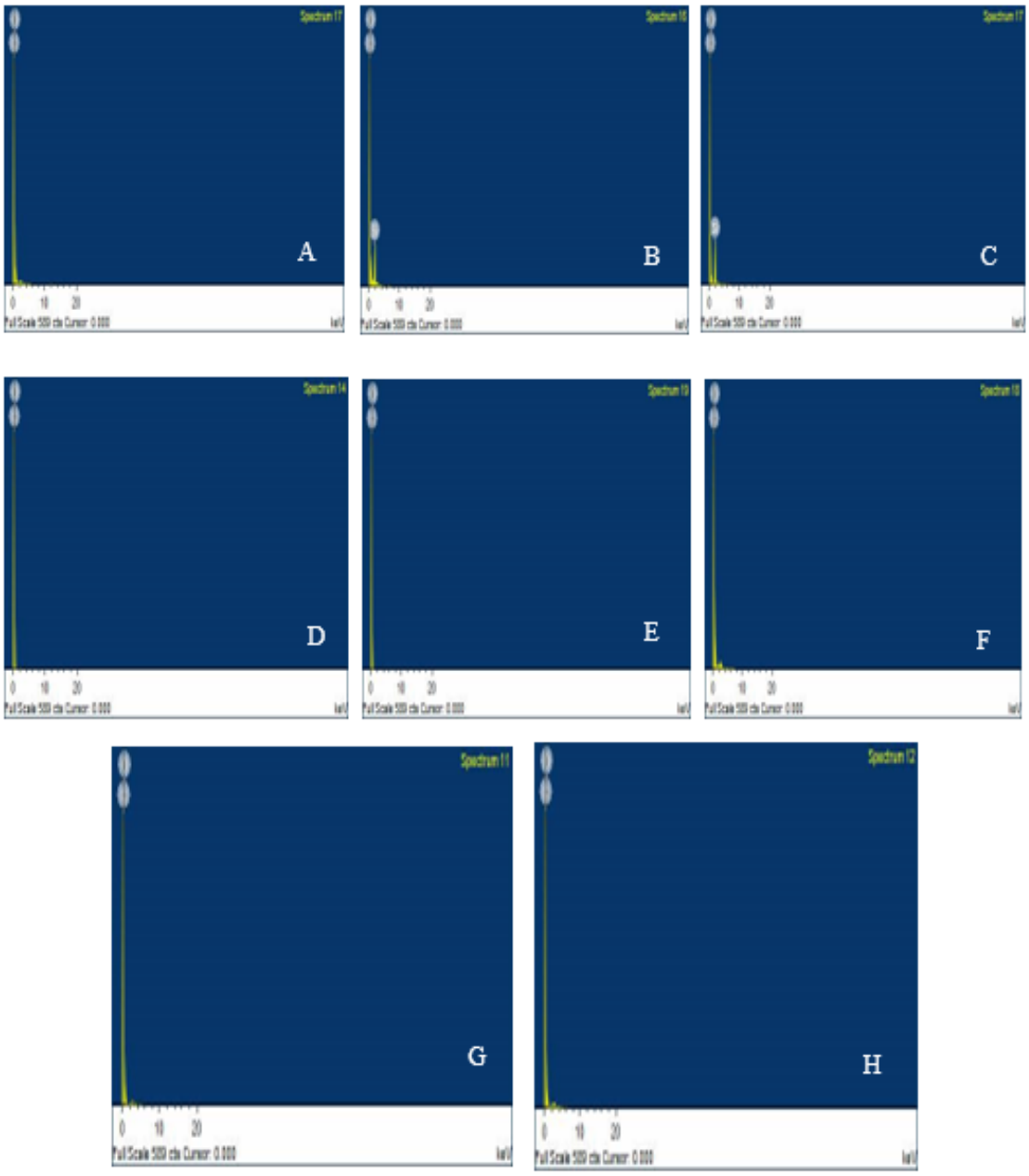


Fig 15: EDAX Mapping of PVA and its derivatives aerogels: (A) PVA, (B) PVA-Silica, (C) PVA-APTES, (D) PVA-SDC, (E) PVA-RHC, (F) PVA-GO, (G) PVA-SDBC, (H)PVA-RHBC

6.2.8. Thermogravimetric Analysis:

Thermogravimetric analysis is a thermal analysis in which the mass of a sample is measured over time as the temperature changes as it undergoes programmed heating (or cooling) controlled in inter or oxidized atmospheric conditions in presence of nitrogen or argon flow. In Fig 17. TGA analysis of PVA and its derivatives are shown with a scanning temperature range from room temp up to 900^0C. The TGA graphical representation of the aerogels can be divided into some regions based on temperature variation and subsequent weight loss percentages which conjugately form a step-like pattern shown in Fig 16.

Region I: The weight loss from room temperature to 250^0C happened due to the evaporation of volatile molecules. During the initial increase of temperature, a common phase of weight loss happened due to the evaporating of residual water or solvent present inside the gel structure that was not known to correspond with any chemical changes in the structure of the Aerogels.

Region II: Further increasing of temperature from 250^0C to 450^0C results a rapid change in weight loss due to evaporation of low volatile components or polymers presence inside the gel structure. This increase in temperature abruptly changed the pore volume and surface area of the aerogel sample.

Region III: Increasing the sample temperature from 450^0C to 850^0C during thermal Analysis in TGA, results combustion of carbon and other similar components to evaporate in gaseous form causing structural fragility and deformation.

Region IV: Further increasing sample temperature from $>850^0$C shows negligible changes in the weight loss graph with temperature changes. As the residual contains Ash, full of minerals oxide viz. Silica, Zinc Oxide, etc. present as a trace amount in the aerogel structure.

From the regional temperature increasing during the TGA analysis of PVA doped aerogel with Rice Husk Cellulose sample, the percentage of high, low volatile, carbon black and ash contains can be obtained which were about 15.62%, 46.82%, 25.85%, and 11.7% respectively. On another hand, PVA-Saw Dust Cellulose had a material composition of about 10.25%, 36.87%, 22.53%, and 19.09% respectively which were quite similar to PVA-RHC aerogel except for the amount of Ash content. However, due to the present of negligible amounts of impurities in PVA, the TGA graph of the aerogel shows a negative percentage trend after increasing temperature from 176^{0}C, and the graphical representation of PVA immobilized Aerogels by Bacterial also has the same trends except that the negative percentage in retained weight % started from 274^{0}C. As shown in Fig 17. C) The TGA study showed the thermal stability of PVA-Silica aerogel throughout the temperature scanning and this phenomenon can be described by the presence of High-energy chemical bonds within the structure such as Si-O, Si-C, and C-H bonds (Y Zhao et al., 2018), which were ascribed to chemical stability. The loss of mass up to 300^{0}C was caused by Si-OH bonds that persisted after the sol-gel process (G.G. Kaya, & H. Deveci, 2020). As most of the bonds were converted to the Si-O-Si network, unreacted group reactions at high temperatures did not affect the mechanical characteristics of the PVA-Silica aerogel (M Kucharek et al., 2020).

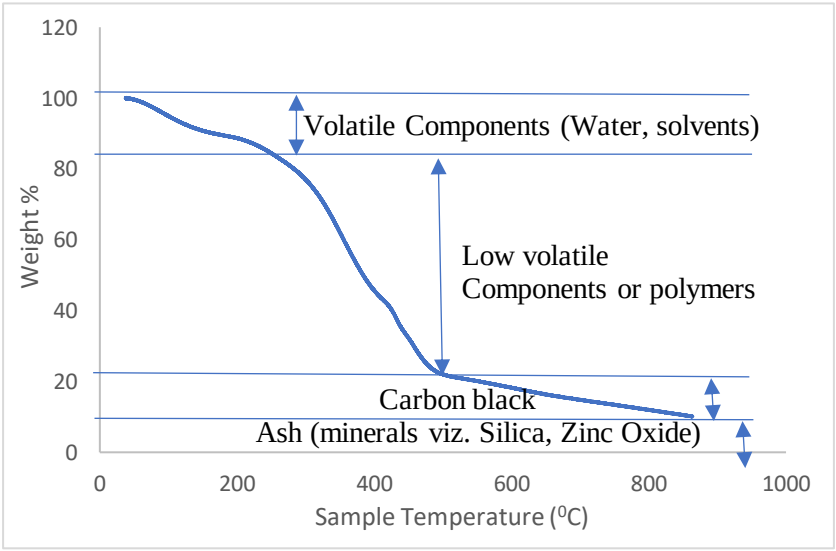


Fig 16: TGA of PVA-RHC aerogel with region based on temperature variation

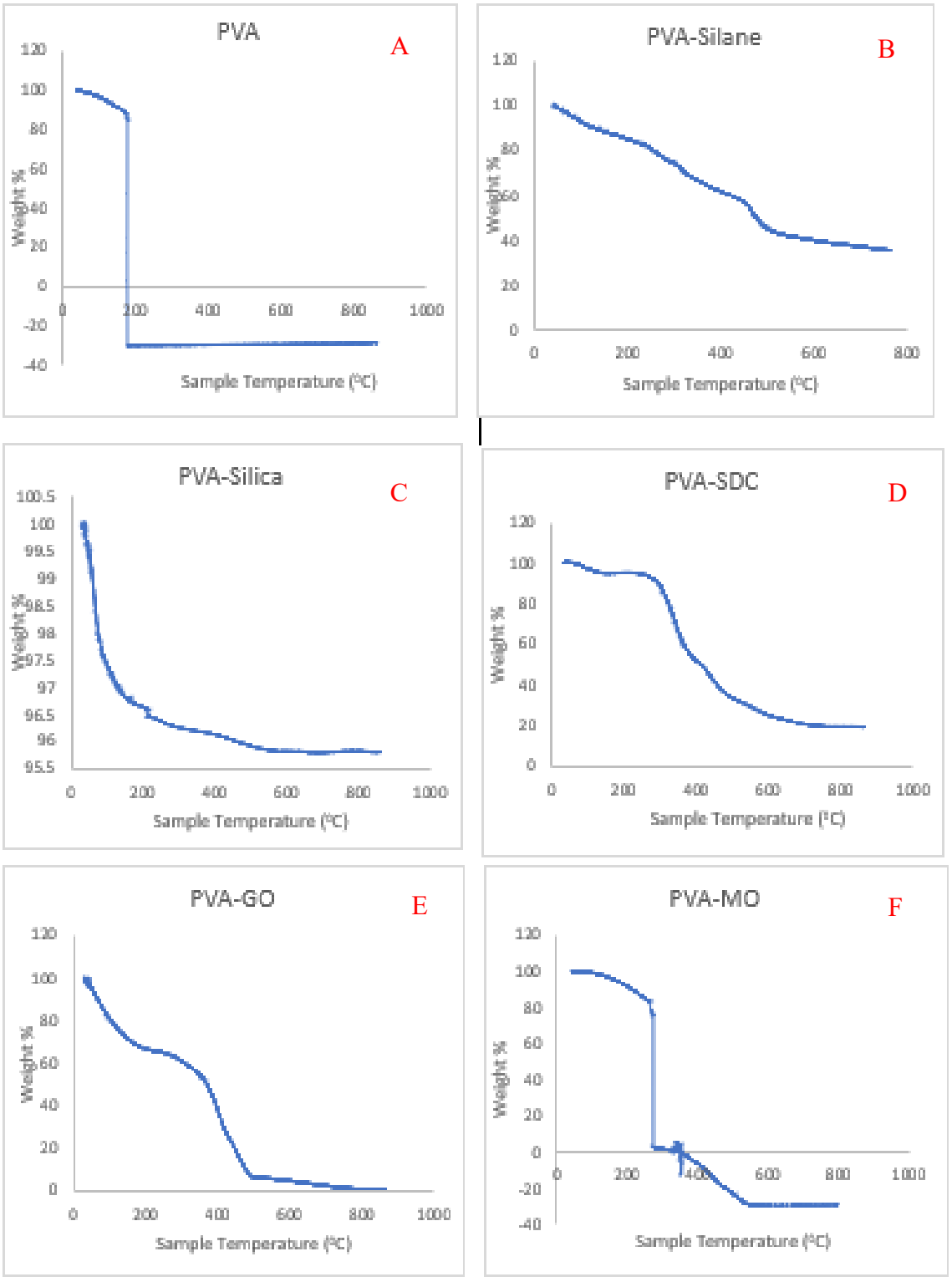


Fig 17: TGA of Aerogels (A) PVA, (B)PVA-Silane, (C)PVA-Silica, (D)PVA-SDC, (E)PVA-GO, and (F) PVA-MO

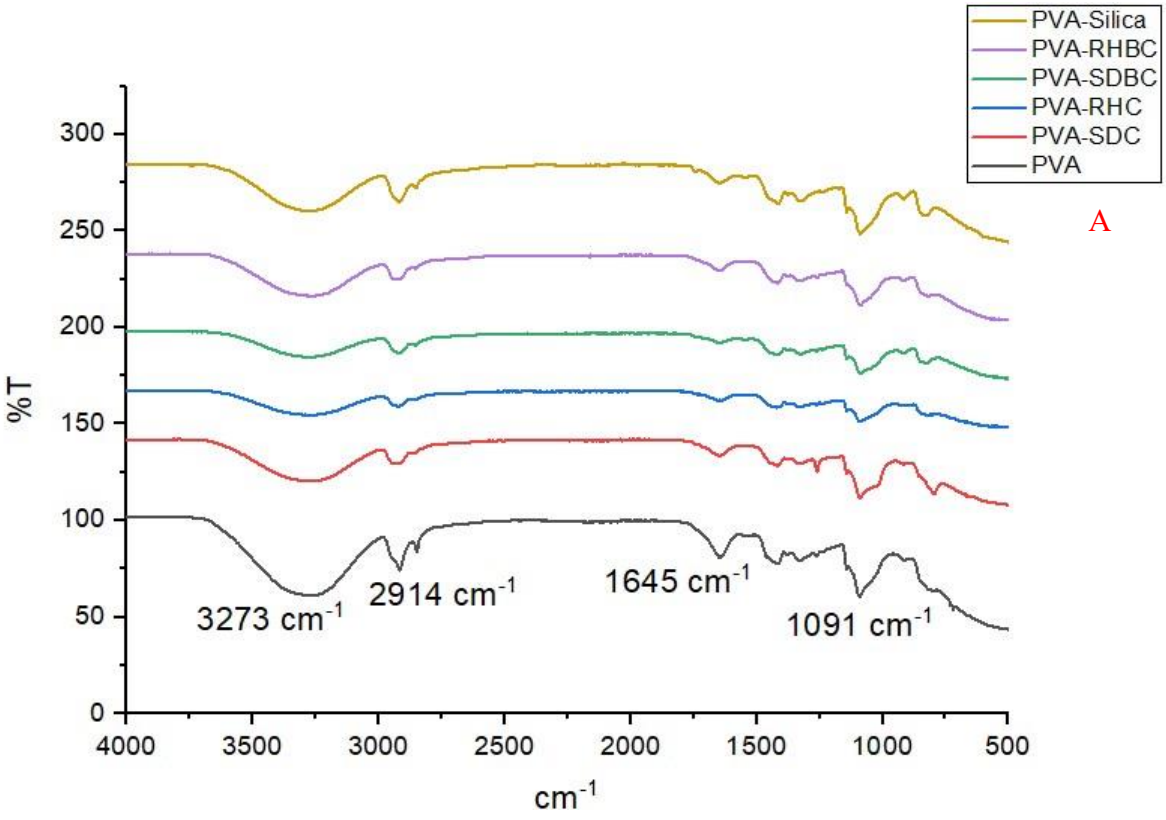
6.2.9. FTIR analysis:

In order to assess the chemical groups between the PVA and its fillers viz. GO, Cellulose, Biochar, and Silica for the preparation of the PVA and its derivatives aerogel and investigate the synthesis mechanism of porous microspheres the FTIR spectrums of the aerogels were obtained and shown in Fig 18. The FTIR spectrum of PVA had a broad band at 3300-3800 cm^{-1} with strong Hydrogen-bonding between intra-molecular o inter-molecular of PVA and other several characteristics peaks at 2914 cm^{-1} related to C-H stretching and 1645 cm^{-1} assigned to C=C stretching vibration due to polymerization between intermolecular homogeneous polymerization between PVA molecules or heterogeneous polymerization between PVA or other fillers molecules (E.S. Costa-Júnior et al., 2009; El-Shamy et al., 2020). FTIR spectrum of PVA and its aerogels included several peaks at 1645 cm^{-1}, and 1091 cm^{-1} attributed to alkanes and aliphatic amines the peak at 2914 cm^{-1} was attributed to C-H stretching vibration and a strong broad peak appears at 3273 cm^{-1} which was due to O-H stretching vibration presence in aerogel surface with strong OH bond rich and another region range from 1000 cm^{-1} to12000 cm^{-1}, 1091 cm^{-1} related to C-O stretching also 1421 cm^{-1} attributes to C-C aromatic ring (MR Gandhi, S Meenakshi, 2012; Zheng, 2011).

After adding the fillers in the aerogel preparation process the wavelength of OH stretching was slightly high with the decrease in the intensity which indicated the inter-molecular hydrogen bond of PVA was slightly weaker after the process (E.S. Costa-Júnior et al., 2009).

Also, the wavelength 804 cm^{-1} indicates the C-H (rock) alkanes bond which was generated between PVA and Saw dust Cellulose during polymerization or sol-gel technique which was also the same as indicated in PVA-Rice husk Cellulose aerogel formation.

Additionally, the crystallization should change in the whole frequency region with similar spectral changes or appearance of sharp bands doing occur and crystallization of microspheres occurring all of them are examined by XRD (x-ray diffraction spectroscopy) analysis (Habiba, Umma, et al. 2017).



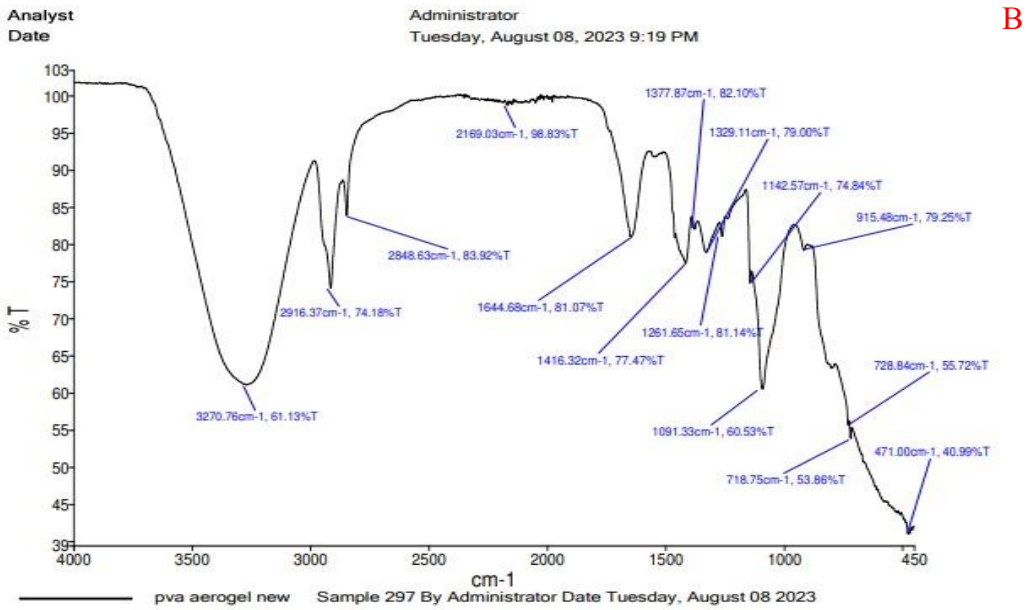


Fig 18: (A) FTIR analysis of PVA and its derivatives aerogels, (B) FTIR analysis of PVA with peak value

6.2.10. Crystallographic Structure Analysis using XRD:

The XRD patterns of pure PVA and its derivatives aerogels are depleted in Fig 19. The PVA diffraction patterns presented three major peaks at 19.5^0, 23.01^0, and 40.5^0 which were the crystalline parts of PVA molecules due to the strong intra-molecular or inter-molecular hydrogen bonding and other broad regions presenting amorphous structure, which indicated that PVA was semi-crystalline (Yang, Guanghui, et al., 2016; Gamal El-Shamy, 2019).

And from the Fig 19. It is quite observable that the intensity of the peak of 19.5^0 increases with the formation of PVA derivatives aerogel. No shift of the peak $2\Theta = 19.5^0$ was observed where the total peak area of crystallinity is highest of PVA-Rice Husk Cellulose aerogel with a crystallinity % of 8.75 and for other aerogel viz. PVA-SDBC, PVA-RHBC, and PVA-SDC come up with 7.03 %, 5.83 %, and 7.49 % of crystallinity.

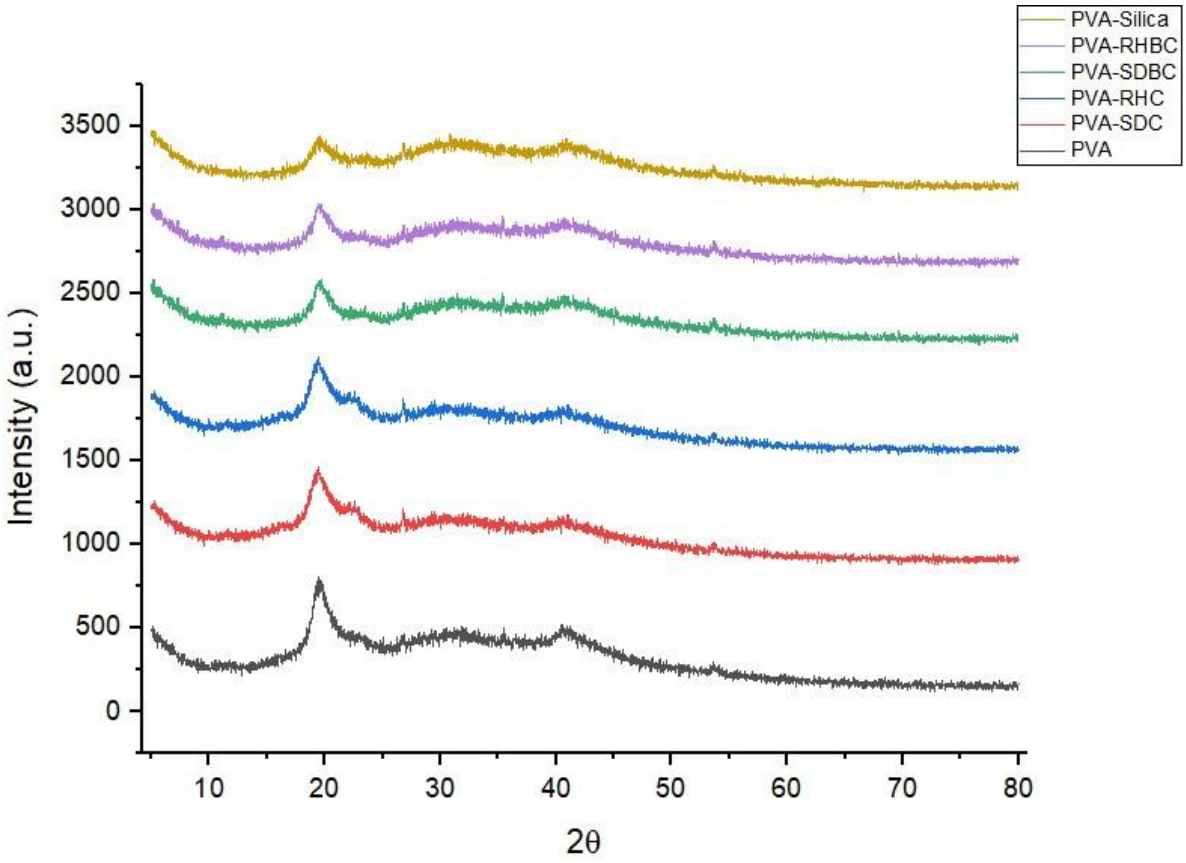


Fig 19: XRD spectroscopy data of PVA and its derivatives aerogel for Crystallographic Structure Analysis

Using Bragg's Law, the geometric function of the size and shape of a unit cell can be evaluated which is denoted by d_{hkl}, and this is a vector drawn from the origin to the plane (hkl) at a 90^0 angle and this is a vector magnitude, is the distance between parallel planes of the atoms in the family (hkl) (Humphreys, C. J., 2013).

6.2.10.1. Calculation of hkl and d_{hkl} value using Bragg's Law:

According to the Bragg's Law,

$$\lambda = 2d_{hkl} \sin \Theta$$

where 2Θ = diffraction angle to d_{hkl}

and λ= wavelength of X-ray $=1.5481\times10^{-10}$ m or 1.5481 Å.

From the Fig 19. Three major peaks of the XRD graph are detected from which the values of hkl and d_{hkl} are shown in Table 8.

Table 8: hkl and d_{hkl} values of PVA and its derivatives aerogel using XRD analysis:

λ (wavelength)	2Θ (diff angle)	Θ	h, k, l	d_{hkl} (Å)
1.5481×10^{-10} (nm)	19.5	9.75	(5 0 0)	4.57
	31.4	15.7	(0 3 0)	2.86
	40.6	20.3	(2 0 0)	2.23

6.3.Adsorption Studies of dyes and Other organic Components:

6.3.1. Adsorption by Fillers:

As previously discussed in various research papers fillers are the components used for aerogel preparation where there are two parts used in the preparation of aerogel chemically. Here are some Graphical representations of the removal percentage of one cationic and anionic dyes and other organic components by the fillers shown in Fig 20. by maintaining temperature of the solution at 30^0C and pH 7 on 5 mg/L concentration of pollutants where the data were taken after 3hr.

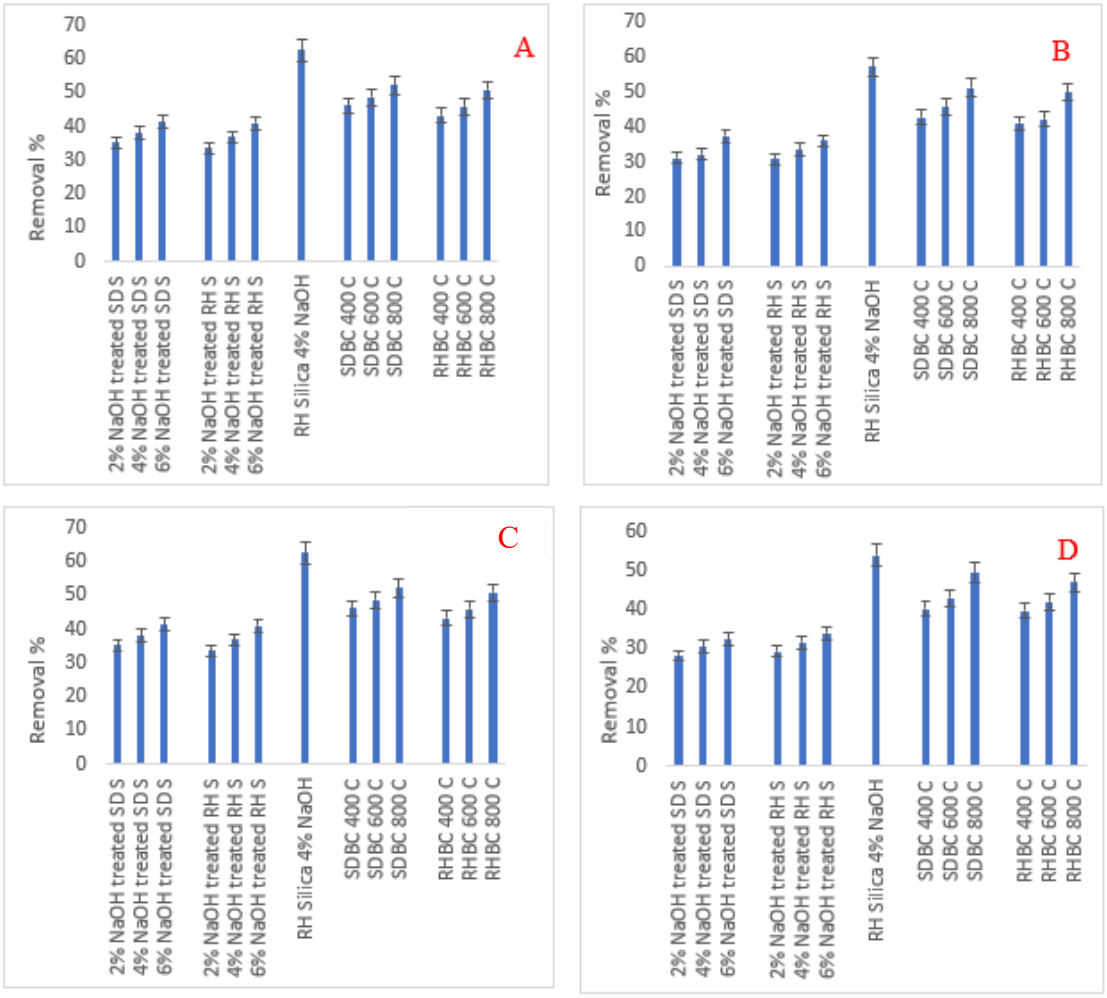


Fig 20: Removal by fillers: (A) Congo Red, (B) Methylene Blue, (C) Pyrene, and (D) Anthracene

6.3.1.1. Sorting of Fillers for preparation of Aerogel:

The above experimental results proved that the extraction process affects the adsorption operation, and the comparative studies of the adsorption by the fillers sorting processes were done by considering the highest removal percentage of the pollutants and fillers viz. 6% NaOH treated Saw Dust Sonicated, 6% NaOH treated Rice Husk Sonicated, Rice Silica 4% NaOH, Saw Dust Biochar 800^{0}C and Rice Husk Biochar 400^{0}C were sorted out for PVA aerogels preparation as adsorbents to conduct further process of Aerogel preparation using PVA molecule by sol-gel technique and further experiments were conducted for examine the enhance of adsorption and removal efficiency by converting them into aerogel.

6.3.2. Adsorption by Aerogels:

6.3.2.1. Effects of various parameters on adsorption:

The adsorption process is a surface phenomenon and the binding of the adsorbates on the adsorbent surface is dependent on various parameters viz. Temperature, Dose of Adsorbents, Concentration of Adsorbates, pH, and Types of Adsorbents.

The removal % of the adsorbates can be determined from Eq. 6 (Yagub, Mustafa T., et al., 2014).

$$\text{Degradation\%}=\frac{(\gamma o-\gamma e)}{\gamma o} * 100\% \ldots\ldots\ldots\ldots\ldots\ldots\ldots\ldots\ldots\ldots\ldots\ldots\ldots\ldots(6)$$

Where γ_o and γ_e are the initial and final mass concentrations of adsorbates.

6.3.2.1.1. Contact Time:

The Effect of contact time between pollutants viz. Congo Red, Methylene Blue, Pyrene, and Anthracene with PVA and its derivatives aerogel where the concentration of Pollutants was 5 mg/L. The Experiments were performed at 30^{0}C adjusting the pH at 7. It was observed that the adsorption of a large quantity of dyes and organic pollutants onto the

aerogels after a short contact time where more than 40% of dyes were adsorbed by Aerogels. Fig 21. presents the effect of contact time on the dyes' adsorption.

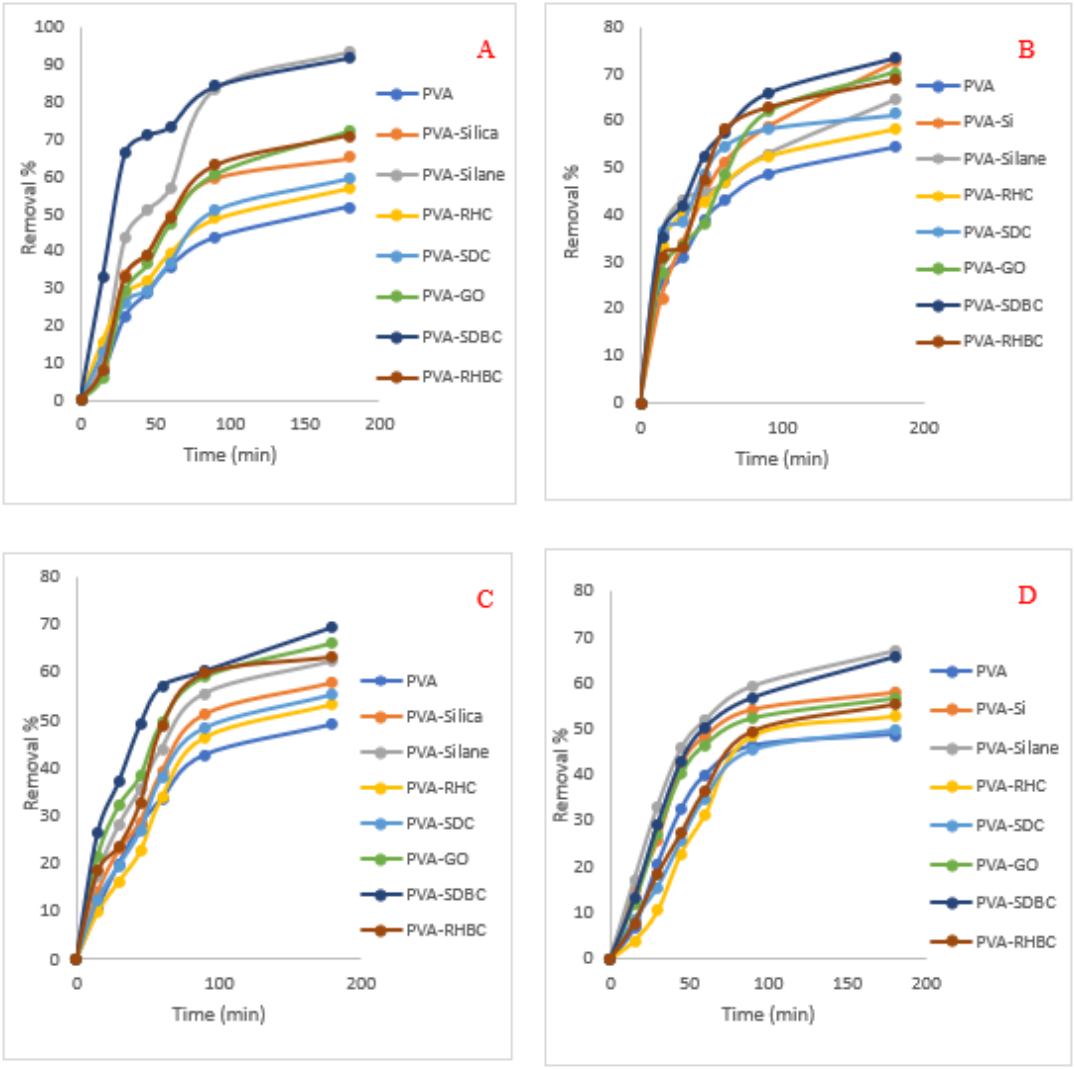


Fig 21: Effect of contact time with the Removal % of (A) Congo Red (B) Methylene Blue (C) Pyrene and (D) Anthracene using PVA and derivatives aerogel. Conditions: concentration 5 mg/L, temperature 30^0C, adsorbent concentration 1 g/L, and pH-7.

6.3.2.1.2. Effect of pH:

According to several papers, the key parameter in almost all adsorption processes is the pH of the pollutant solution. This factor affects the capacity of the adsorbent and the efficiency of the process.

The pH affects the solution chemistry of the contaminants, the activity of the functional groups in the adsorbents, the competition with coexisting ions in the solution, and the surface charge of the adsorbents (Khasri A. et al., 2021). The pH of the aqueous medium can influence the properties of the adsorbents, the adsorption mechanism, and the dissociation of dye molecules. Not only the adsorbents but also the chemical structure of the dye can be altered by the pH of the solution. The pH changes the surface charges and the degree of ionization of the adsorbed ion (Rápó E. et al., 2018; Kanwal A. et al.,2017, and Brito M.J. et al.,2018).

Practical applications in Fig 22. demonstrate that anionic dyes bind more effectively to the adsorbent surface in acidic media, whereas cationic dyes bind more effectively in basic media. Usually, the pH of the aqueous dye solution is adjusted with HCl and NaOH.

- When HCl is added to the solution, the surface of the adsorbents in the solution is promoted, allowing the anionic dye to bind more efficiently on its surface, due to the electrostatic attraction.
- Conversely, in a basic medium, the addition of NaOH deprotonates the aerogel surface, resulting in a repulsive force between the anionic dye and aerogels. This reverse phenomenon is observed for cationic dyes.
- Simultaneously, for organic pollutants pH affects less than other anionic or cationic dyes.

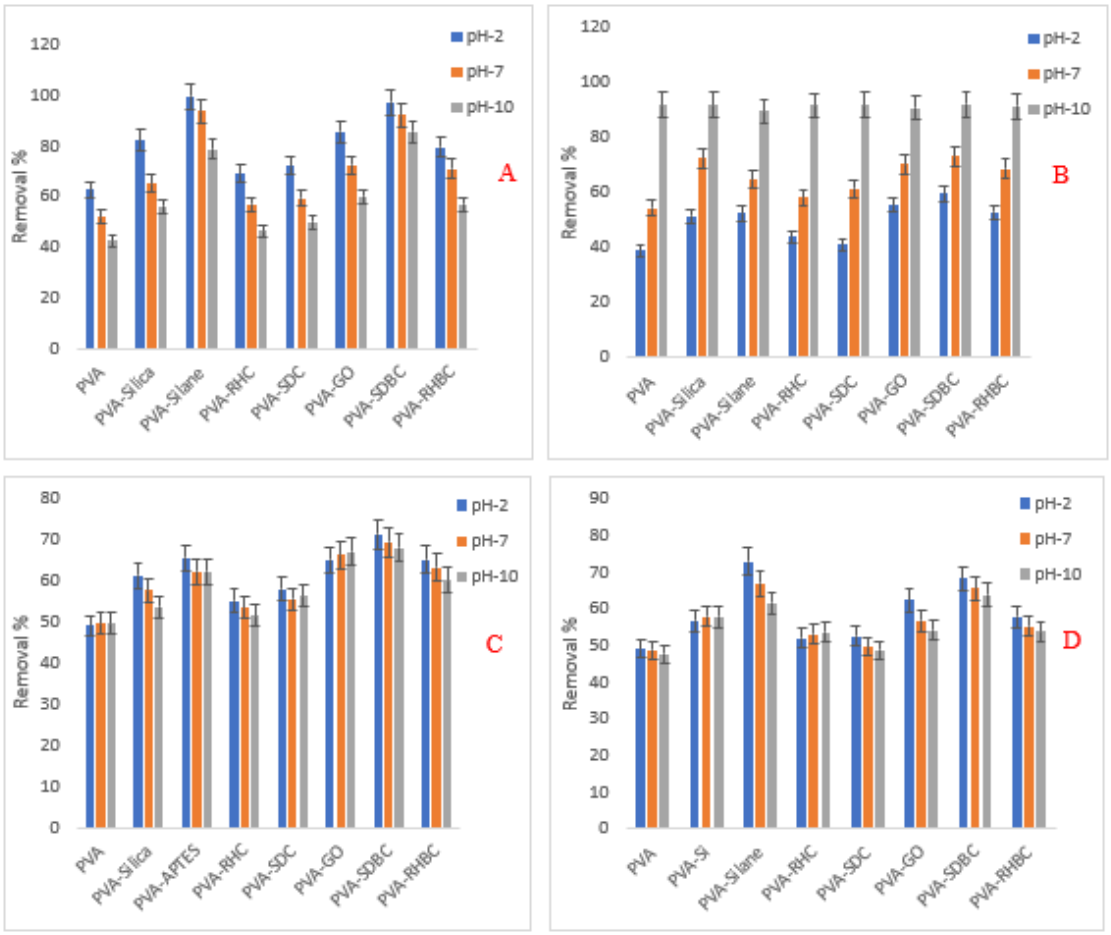


Fig 22: Effect of pH on the Removal % of (A) Congo Red (B) Methylene Blue (C) Pyrene and (D) Anthracene using PVA and its derivatives aerogel. Conditions: concentration 5 mg/L of pollutant in aqueous solution, Adsorbent Dosage- 1 g/L, temperature 30^0C, pH- 2, 7, 10.

Fig 22. clearly display the pH effects on Methylene Blue and Congo red removal by PVA and its derivatives aerogel. As increase with pH, removal rate of Methylene Blue increased as opposite with Congo Red. As the pH increased, surface of the adsorbents becomes negatively charged and this surface repulses the negatively charged dyes viz. Congo Red but the positively charged dyes viz. Methylene Blue gets attracted more, and due to the high electrostatic interaction between adsorbate and adsorbents pH played a crucial role in the charged dye adsorption process. However, the organic pollutants viz. Pyrene and Anthracene have less affinity to the pH changes still presence of π bonds and π electrons in their structure have less affinity to the pH changes still presence of π bonds and π

electrons in their structure slightly affects their affinity to the adsorbents' surface however these interactions are negligible.

6.3.2.1.3. Effect of Solution Temperature:

The effect of solution temperature is also a significant physicochemical factor as affects the treatment process by shifting the nature of the reaction from endothermic to exothermic, or vice versa (Yeow P.K. et al., 2020). Moreover, it has a strong effect on adsorption as it can increase or decrease the removal % (Badawy A.A. et al., 2020).

The temperature can affect the efficiency of the sorption differently depending on the adsorbent and the pollutant. In general, it enhances the biosorption of adsorption impurities by increasing the surface activities and kinetics energy of the adsorbates, but it can damage the physical structure of the biosorbent.

- As the temperature rises, the rate of the chemical reaction also increases, so if the sorption process is chemisorption ($\Delta H_{chemisorption}$= -200kJ/mol), then higher sorption efficiency will be seen at higher temperatures (this would eventually reach the equilibrium).
- On the other hand, if the process is physical adsorption ($\Delta H_{physisorption} \approx$ -20kJ/mol), then the higher temperature will negatively affect the adsorption. Temperature can chemically alter the adsorbent, and its adsorption site and activities (Szende T. et al.,2020).

In adsorption studies, a static batch method in Fig 23. is demonstrated by the application of PVA and its derivatives aerogel on cationic, anionic dyes and organic pollutants with a temperature range of 20^0C to 40^0C with the application of dye concentration of 10mg/L, dosage 1 g/L and pH at 7.

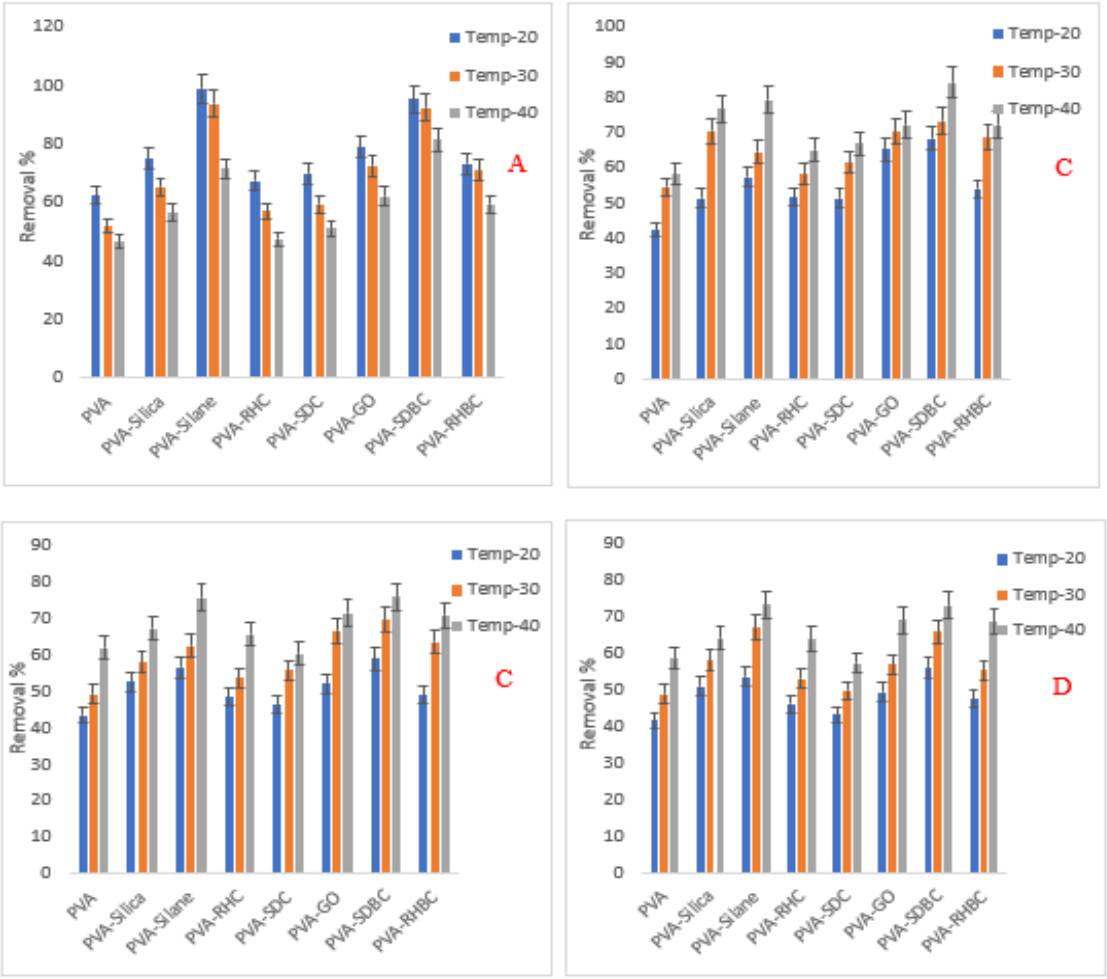


Fig 23: Effect of Adsorbent Dosage on the Removal % of (A) Congo Red (B) Methylene Blue (C) Pyrene and (D) Anthracene using PVA and derivatives aerogel. Conditions: concentration 5 mg/L of pollutant in aqueous solution, Adsorbent Dosage- 1 g/L solution, temperature 20^0C, 30^0C, 40^0C and solution pH-7.

Through the batch study analysis by Aerogel on pollutants in aqueous solution shown in Fig 23. It is quite observable that with increasing of temperature of the solution and environment the removal rate of adsorption increases. Because of this increase in kinetic energy of the sample, the diffusivity of dye molecules on the water caused the increase of their movement into the pores of aerogel. For this reason, adsorption is an exothermic process. There were some exceptions viz. Congo Red whose adsorption showed the opposite of Other experimented dyes, which can be considered as an endothermic process.

6.3.2.1.4. Effect of Adsorbent Dosage:

The amount of adsorbent is an important parameter that influences the adsorption process, through the quantitative ratio of adsorbent to adsorbent. Since the adsorbent determines the adsorbent capacity for a given initial concentration, the dosage of the adsorbent is an important parameter (Şentürk İ. and Alzein M., 2020). According to Kroeker's rule, the specific adsorbed volume, for a constant volume, for a constant initial concentration, decreases with increasing adsorbent mass (Pernyeszi T. et al., 2019). Thus, increasing the adsorbent dose is positively correlated with the efficiency and performance of dye removal. With increasing the adsorbent dosage, at a fixed contaminated concentration, a more active surface area is available for adsorption, and more active adsorption sites are available (Ma C.M. et al., 2020).

As the biomass concentration increases, the efficiency of the pollutant removal increases, but there is no direct proportionality between the amount of biomass and the amount of pollutant removal. In contrast, as the concentration of biosorption increases, the amount adsorbed per species decreases. This can be attributed to the fact that the shape of the sorption isotherm changes with the increasing biosorbent concentration. The decrease in the specific adsorbed amount is probably due to the fact that some of the surface or surface groups may be saturated in the more concentrated suspensions (Neag E. et al., 2018; Esmaeili H. et al.,2020 and Salahshour R. et al.,2020).

During the dye removal process, the capacity may decrease for two reasons (Popa S. et al.,2021):

- Adsorption sites remain unsaturated while the number of sites available for adsorption increases; or
- Aggregation or agglomeration of adsorbent particles may occur, reducing the available surface area and increasing the diffusion path length.

Several studies also report that this increase in efficiency lasts until a saturation state is reached and then steadily decreases, sometimes slightly. This fact can be explained by the fact that after a certain adsorbent dose, maximum adsorption is reached and the amounts of ions bound to the adsorbent and the amounts of free ions remain constant, even with the further addition of adsorbent (Rápó E. et al.,2020; Rápó E. et al.,2019 and Hamza W. et al., 2018). The Studies of PVA and its derivatives Aerogel adsorption are shown in Fig 24. The process was done based on the aerogel amount of 0.5 and 2 g/L of adsorbate using temperature at 30^0C and pH at 7 along with pollutants concentration of 5 mg/L.

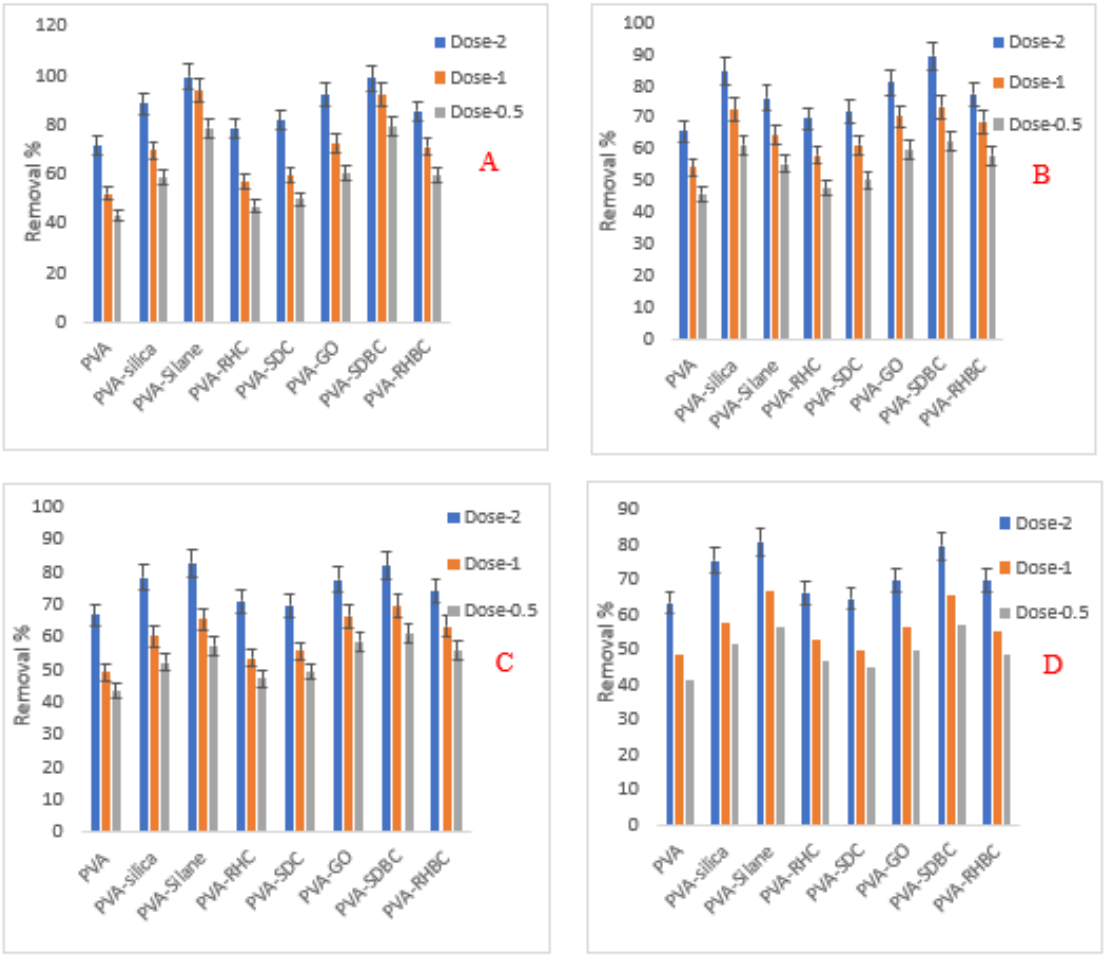


Fig 24: Effect of Adsorbent Dosage on the Removal % of (A) Congo Red (B) Methylene Blue (C) Pyrene and (D) Anthracene using PVA and derivatives aerogel. Conditions: concentration 5 mg/L of pollutant in aqueous solution, Adsorbent Temperature- 30^0C, Dosage variation 0.5g/L, 1g/L, 2g/L and solution pH-7.

6.3.2.1.5. Effect of Pollutant Concentration:

The initial pollutant concentration is perhaps one of the most important factors influencing the adsorption process, as it indirectly affects the efficiency of the dye removal by reducing or increasing the availability of the binding sites on the adsorbent surface. The initial concentration of solute acts as a driving force for the adsorption processes, favoring diffusion and mass transfer from the solution (with a high amount of pollutant in the solution) (Seow T.W., Lim C.K. et al., 2016). In such water treatment systems, the efficiency of the pollutant removal and the maximum amount of the maximum amount of dye bound in equilibrium are directly related to the initial dye concentration (Yagub M.T., 2018; Terangpi P. and Chakraborty S., 2017). By examining the effect of dye concentration, three trends can be observed (Al-Ghouti M.A. et al.,2020):

- The removal efficiency decreases as the initial concentration increases;
- Removal efficiency increases as the initial concentration increases; and
- No significant change in removal efficiency.

Most often, the percentage of dye removal decreases with increasing initial pollutant concentration. This phenomenon can be explained by the saturation of adsorption sites on the adsorbent surface. And the case of a low initial concentration of pollutants the presence of a high amount of binding site for the adsorbates and trends slow down with the increasing of pollutant concentration in the solution. At low concentrations, the ratio of active sites to dye molecules can be high, allowing all molecules to interact with the adsorbent and be removed from the solution almost instantaneously (de Farias Silva C.E. et al., 2020).

Fig 25. Shows the effect of the initial concentration of pollutants on the removal of pollutants by PVA and its derivatives aerogel.

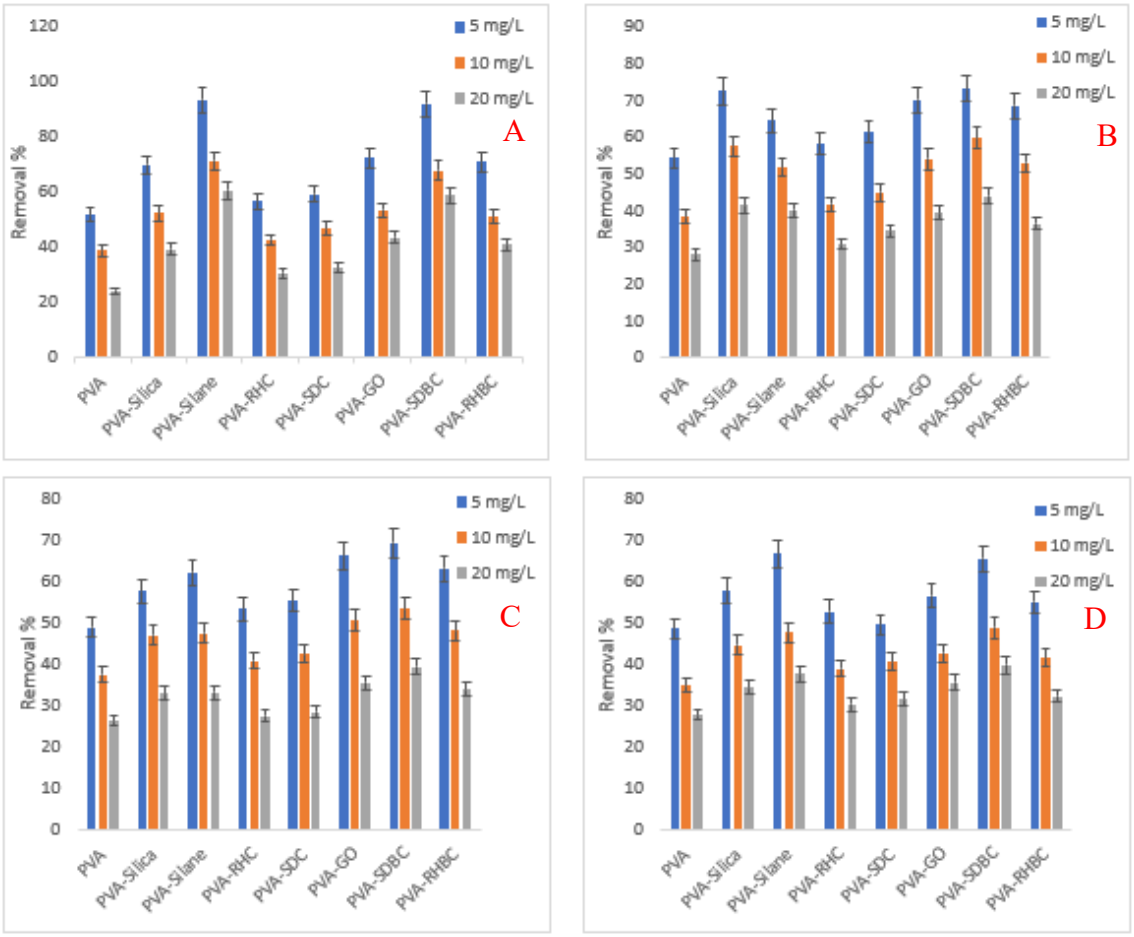


Fig 25: Effect of pollutant concentration on the Removal % of (A) Congo Red (B) Methylene Blue (C) Pyrene and (D) Anthracene using PVA and its derivatives aerogel. Conditions: concentration 5 mg/L, 10 mg/L, and 20 mg/L of pollutants in the solution, Adsorbent Dosage- 1 g/L solution, temperature 30^0C, and solution pH-7.

From the data displayed in Fig 25. the significant decrease of removal percentage with increasing of pollutant concentration throughout the process can be observed. For example, during Congo Red removal at 5 mg/L concentration by PVA-SDBC, the removal percentage was about 92.19 % but increasing of concentration to 10 mg/L decrease the percentage to 67.98% and further increase to 20 mg/L the removal percentage was shown at about 59.02%. This result can be explained by the increased competition in the adsorption media. As the concentration increased, the number of adsorbate molecule faced an increased competition to occupy the available binding sites on the adsorbent. That leads the active sites to be exhausted and a decreased of removal percentage (Ghosh et al., 2024).

6.3.2.2. Optimization of Methylene Blue Removal by PVA-SDBC aerogel:

Building upon our previous research, a parametric study was conducted to investigate the impact of individual parameters on the removal rate of Pollutants, and this study involved systematically varying a single parameter while keeping other parameters constant in the overall process. To optimize the overall process of pollutant removal by adsorption Response Surface methodology is done, which is a subset of Design of Experiments (DOE) and used to explore the relationship between several explanatory variables and one or more response variable. RSM is done by considering some steps viz. Identification of Factors, selecting the factors level, and choosing Experimental design (Central composite, Box-Behnken and Definite Screen) (Bezerra, M. A. et al., 2008). RSM can be used for optimizing result of adsorption process by Developing adsorption model by describing the relation between various variables, Experimental design phase by suggesting a series of experiments, optimizing removal capacity of adsorption process. Response-surface methods also have some unique experimental-design issues, due to the emphasis on iterative experimental and need for relatively sparse designs that can be built-up piece-by piece according to the evolving needs of the experimenter (Lenth, R. V., 2010). In Fig 26. And Fig 27. The graphical and mathematical representations of RSM are shown on the basis of the highest removed adsorbate by PVA-derivatives aerogel maintaining various conditions viz. concentration from 5 to 20 mg/L, Dosage from 0.5 to 2 g/L and pH from 2 to 10. And shown in the Fig 26. (A) the relation between the experimental data obtained and the predicted data points. It can be observed that the experimental data shows high correlation with the predicted data. The result of ANOVA is shown in Table 9. where the sum of squares, mean value, corresponding F and P value are examined. A very high F value (74.02, much higher than unity) and a very low value of P meant the model was highly significant, the experimental values showed a strong correlation with experimental

value. The contour plots shown in Fig 27. show the interaction of independent variable with the pollutant removal rate.

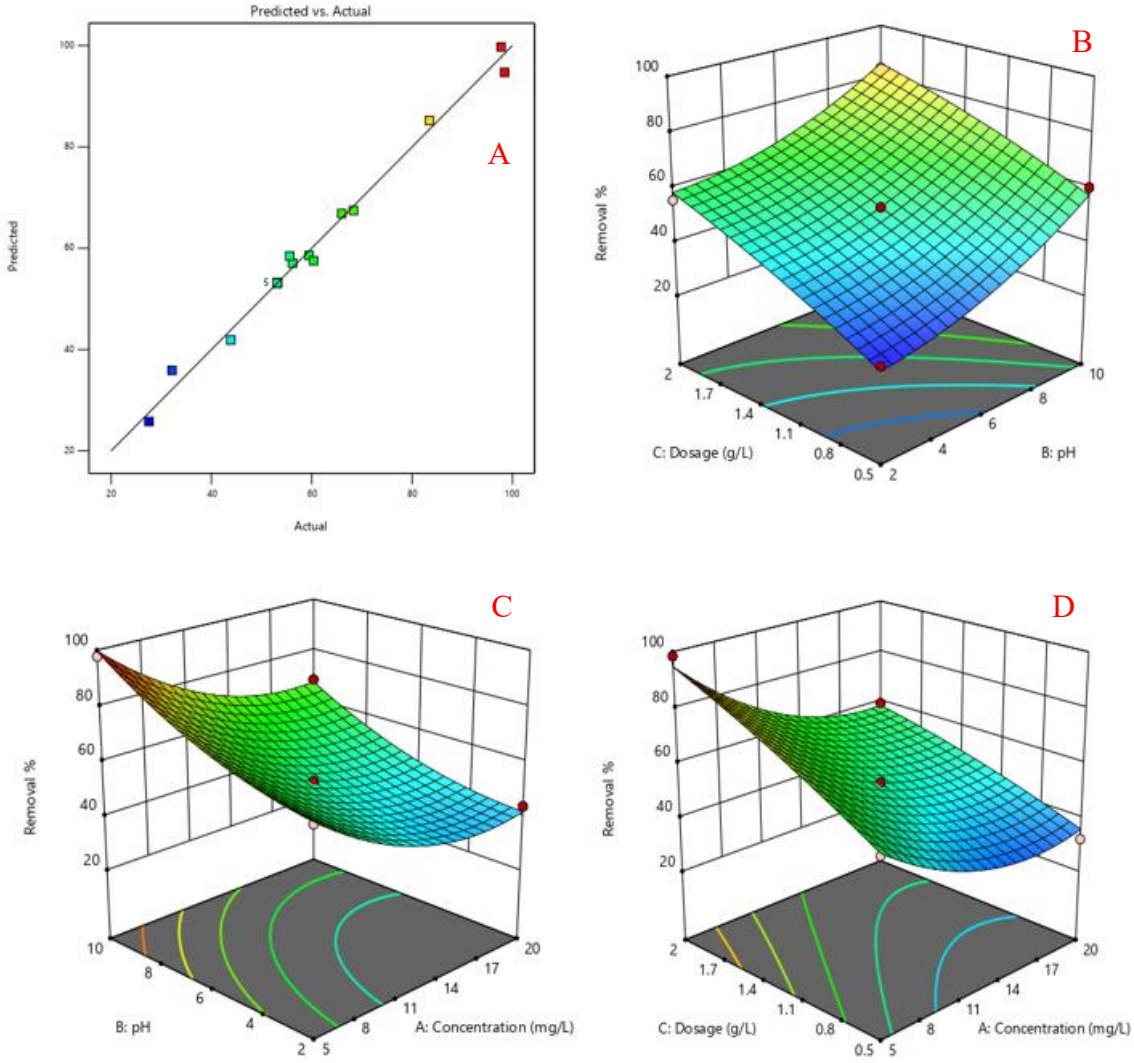


Fig 26: The Plot showing the relation between the prediction data points and the experimental data points as per the RSM model. (B) The 3D plot showing the interaction between the pH of the experimental solution and Dose of PVA-SDBC and their effect on the percentage removal of Methylene Blue, (C) The 3D plot showing the interaction between the pH of solution and concentration of Methylene Blue and their effect on the removal percentage of the pollutant, (D) The 3D plot showing the interaction between the Concentration of adsorbate and dosage of PVA-SDBC and their effect on the percentage removal of Methylene Blue.

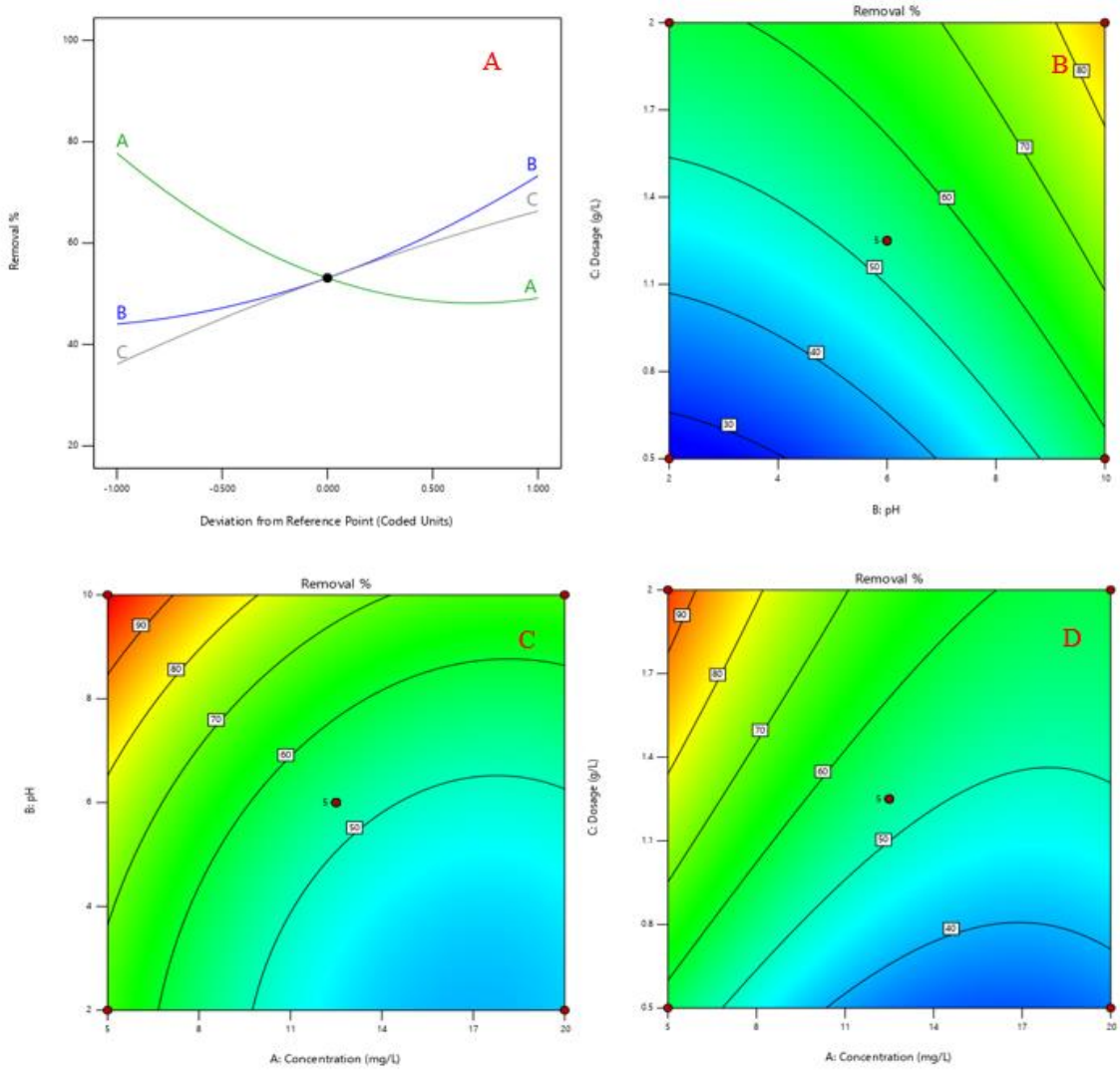


Fig 27: The plot showing optimum value of adsorption process based on perturbation graph as per the RSM model. (B) The Contour graph showing the interaction between pH of the solution and Dosage of PVA-SDBC and their effect on the percentage removal of Methylene Blue, (C) The Contour plot showing the interaction between the pH of solution and concentration of Methylene Blue and their effect on the removal percentage of the pollutant, (D) The Contour plot showing the interaction between the Concentration of adsorbate and dosage of PVA-SDBC and their effect on the percentage removal of Methylene Blue.

Table 9. ANOVA for Quadratic model for RSM analysis:

R^2 value	Adjusted R^2 value	f-value	Probability value P
0.9896	0.9762	74.02	<0.0001 Significant

Table 10: ANNOVA for Quadratic Model:

Source	Sum of Squares	df	Mean square	F-value	p-value	
Model	5854.33	9	650.48	74.02	<0.0001	significant
A-Conc	1640.21	1	1640.21	186.64	<0.0001	
B-pH	1708.20	1	1708.20	194.38	<0.0001	
C-Dose	1821.36	1	1821.36	207.25	<0.0001	
AB	13.36	1	13.36	1.52	0.2574	
AC	55.95	1	55.96	6.37	0.0396	
BC	6.18	1	6.18	0.7027	0.4296	
A^2	449.30	1	449.30	51.13	0.0002	
B^2	128.41	1	128.41	14.61	0.0065	
C^2	15.20	1	15.20	1.73	0.2299	
Residual	61.52	7	8.79			
Lack of Fit	61.52	3	20.51			
Pure Error	0.0000	4	0.0000			
Cor Total	5915.85	16				

%Removal=47.70632–5.30367×Concentration+0.790417×pH+39.35889×Dose-0.060917×Concentration×pH+0.664889×Concentration×Dose-0.414167×pH×Dose+0.183644×$Concentration^2$+0.345156×pH^2-3.37778× $Dose^2$

The optimal value of pH, Concentration and Dose 6.87, 12.5, 1.25 respectively and removal (%) was 53.14, which closed to RSM data 52.38%, in which the RSM model can better represented the experimental data.

6.4.Concentration-Dependent Inhibition of Microbial Growth by Pollutants:

The minimal inhibitory concentration (MIC) is the lowest concentration of pollutants (such as a dye) that inhibits the visible growth of a microorganism after overnight incubation. It's a crucial measure in determining the effectiveness of Pollutants against specific microbes.

MIC testing involves exposing the microorganism to varying concentrations of the antimicrobial agent in a controlled environment, such as a laboratory setting. The concentration at which growth was inhibited and these were recorded as the MIC.

Importance of MIC in microbial analysis for some reason but out of them most importance is the “Resistance detection of Microbes to pollutants” as the MIC experiment was done with increased concentration of pollutants toxic effects on the microbial survival rate can be effectively observed.

MIC is typically performed using standardized methods such as dilution methods or the agar-based method and microbial stain was tested in a suitable medium until it reached a specific density, typically equivalent to a 0.5 McFarland standard, which corresponds to approximately 1-2 × 10^8 colony-forming units per milliliter (CFU/mL). Microbial stain inoculation is done with different concentration pollutants for testing with incubation periods of usually 18-24hrs.

The MIC was recorded as the lowest concentration of the pollutants that prevents visible growth. The results are interpreted according to established breakpoints, which classify the microorganism as susceptible, intermediate, or resistant to the pollutants.

Upon conducting MIC testing using broth dilution method shown in Fig 28, it was observed that the growth of *Lysinibacillus sp* was inhibited at a concentration of 100 mg/L of Congo Red, and Pyrene indicating its effectiveness in inhibiting bacterial growth at minimal concentration. Except from the above-mentioned micro-organism (*Lysinibacillus sp*), any of above microbes didn't show any growth inhibitory effects against any dyes or organic components used for removal process by bacteria immobilized aerogels. And based on the Fig 28., *Lysinibacillus sp* bacteria was sorted out from bioremediation process performed against the aqueous solution of the pollutants used during the studies.

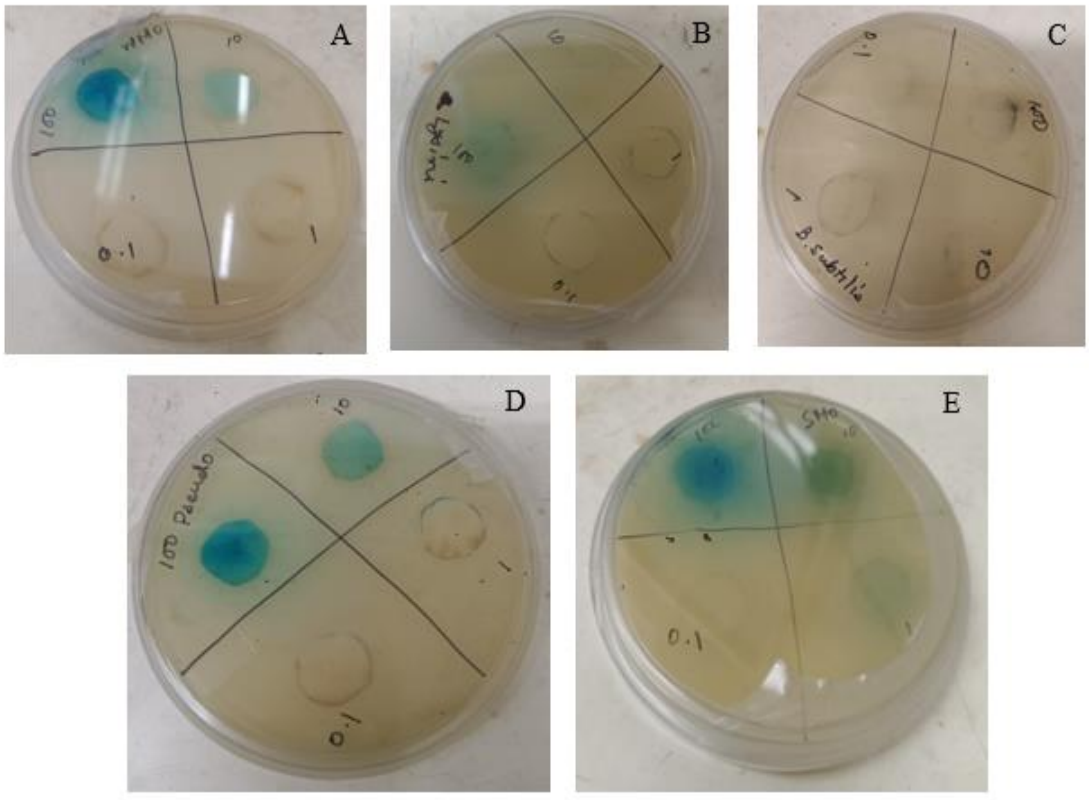


Fig 28: 1) Concentration-dependent inhibition of A) WMO, B) *Lysinibacillus sp.*, C) *Bacillus subtilis*, D) *Pseudomonas sp.*, and E) SMO against Methylene Blue Dye

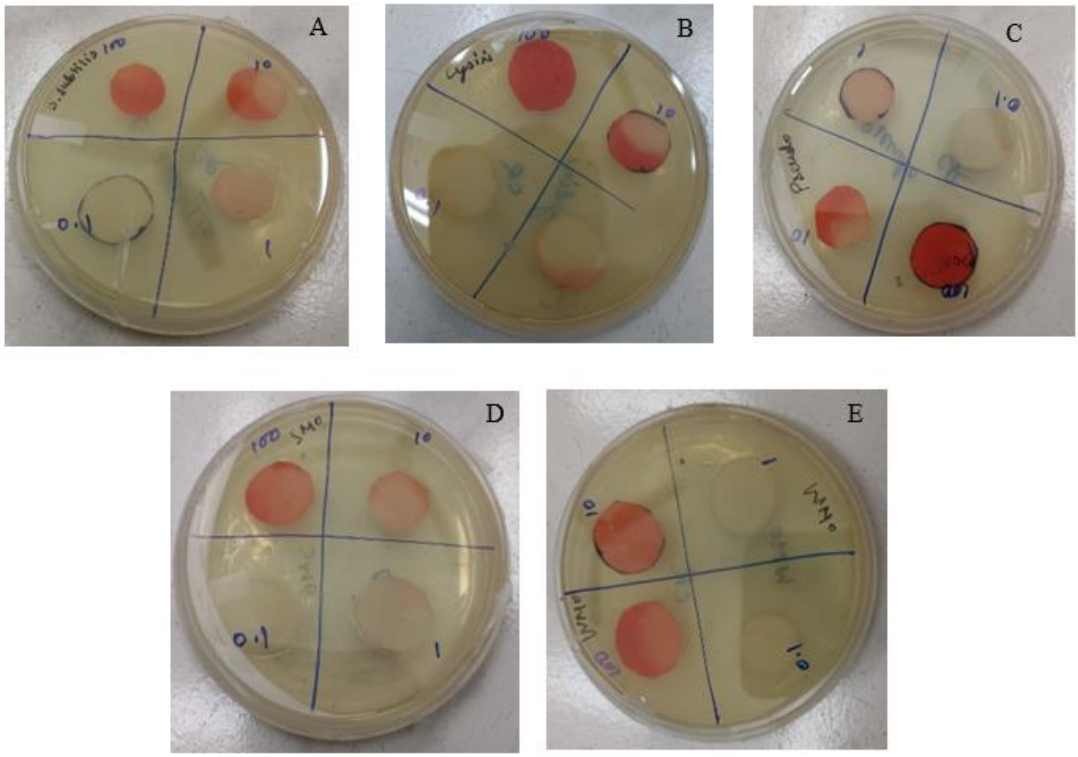


Fig 28: 2) Concentration-dependent inhibition of A) *Bacillus subtilis*, B) *Lysinibacillus sp.*, C) *Pseudomonas sp.*, D) SMO, and E) WMO against Congo Red Dye

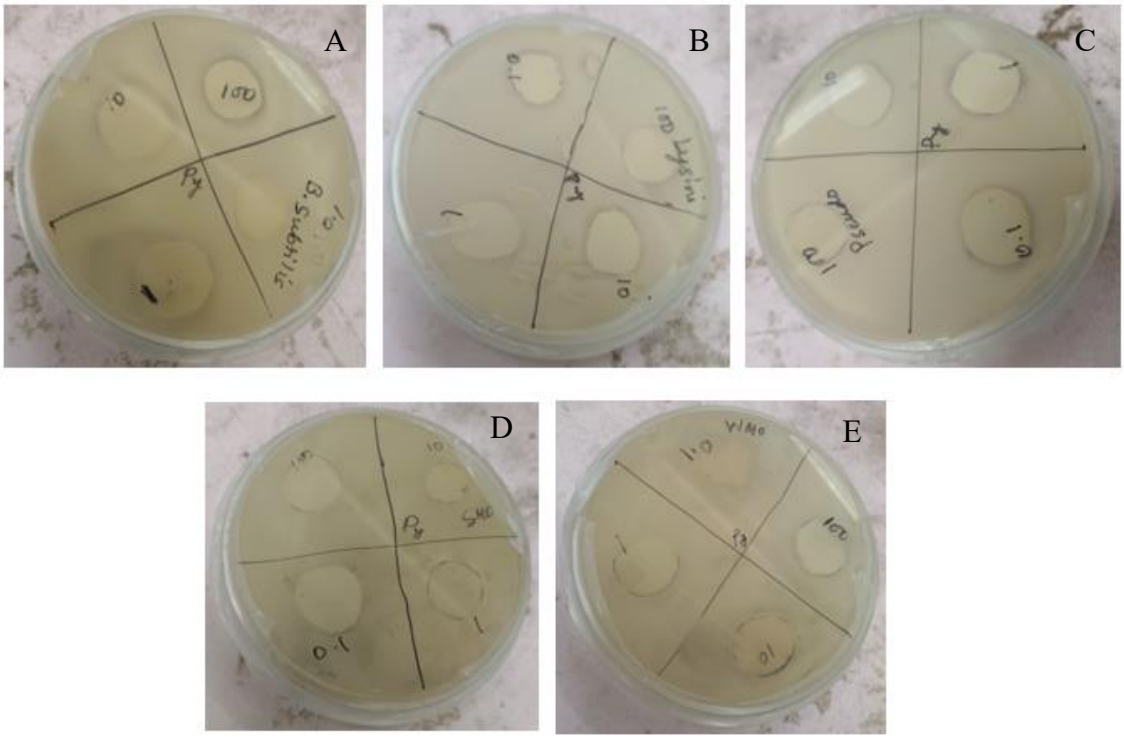


Fig 28: 3) Concentration-dependent inhibition of A) *Bacillus subtilis*, B) *Lysinibacillus sp.*, C) *Pseudomonas sp.*, D) SMO, and E) WMO against Pyrene

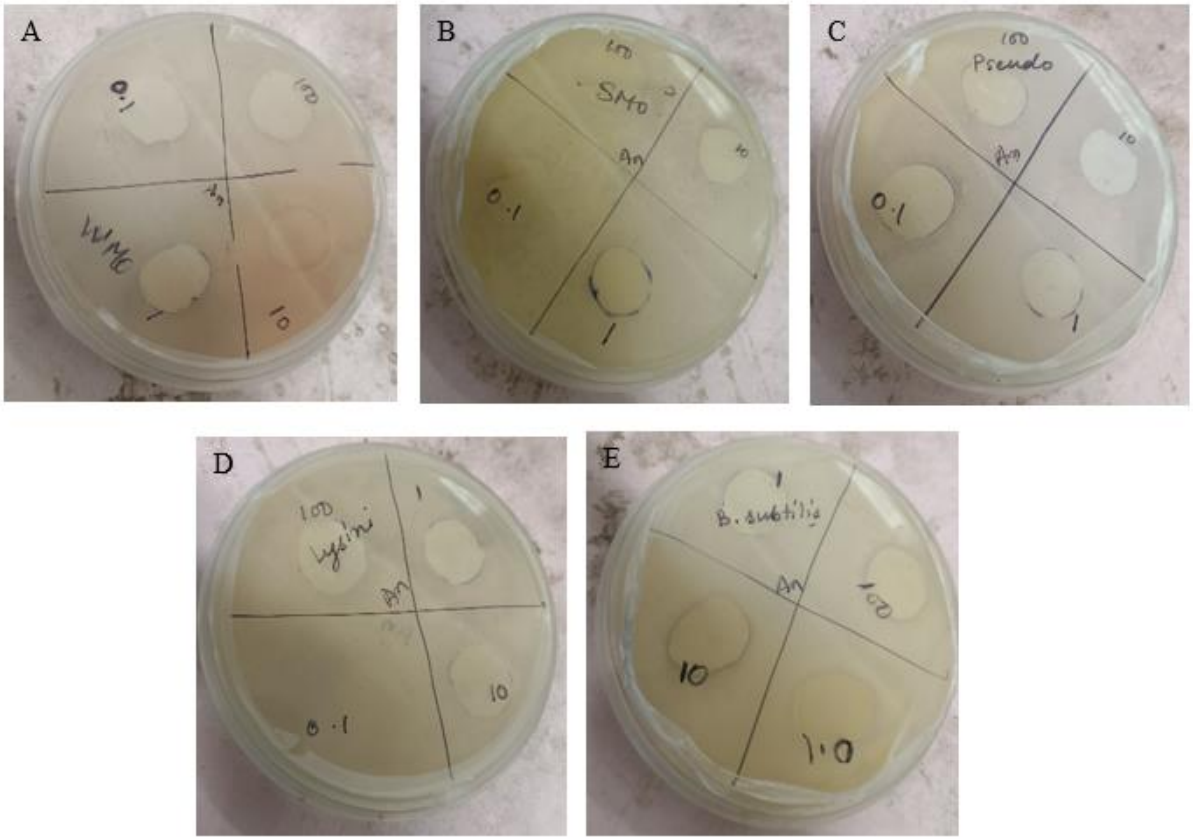


Fig 28: 4) Concentration-dependent inhibition of A) WMO, B) SMO, C) *Pseudomonas sp.*, D) *Lysinibacillus sp.*, and E) *Bacillus subtilis* against Anthracene

6.5. Bioremediation of Pollutants:

Bacteria grown in Nutrient Broth media were incubated for 7 days for full growth of the microbial samples, which were then further used for degradation studies of the pollutants with varieties of Concentration, dose, temperature, pH, and contact time. After regular intervals of time, two 2ml of the samples were taken, of which 2ml of the sample was centrifuged and degradation of the dyes was examined, and the remaining 2ml of the sample was taken for observation of bacterial growth at the wavelength of 600nm.

Calculating the degradation percentage of the pollutants can be determined by Eq 6 mentioned in the “Adsorption section”.

6.5.1. Effect of Different Parameters on Bioremediation:

6.5.1.1. Effect of Contact Time:

Longer contact times generally allow for more contact of the pollutants with the microbial surface along with more microbial growth, adaptation, and the development of more microbial colonies which is better suitable for microbial degradation of specific pollutants (Abd El-Rahim et al., 2009). Extended exposure can lead to increased microbial diversity and metabolic capabilities, enhance the efficiency of the bioremediation, and often higher results of contaminant removal (Bosco et al. 2002). Fig 29. Shows the relation of bioremediation rate with the contact time for different bacterial solutions and the bacterial growth with time in that medium.

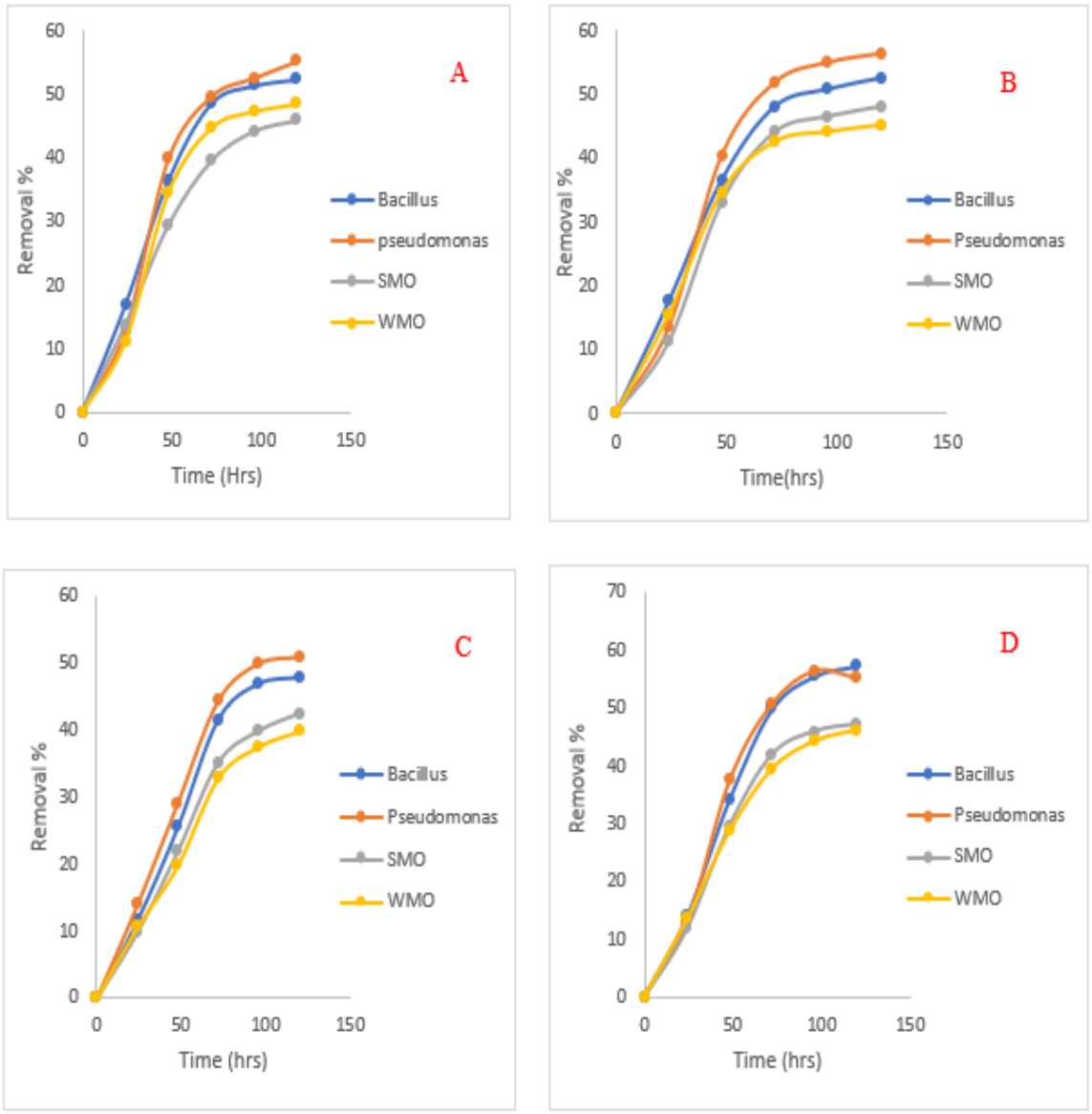


Fig 29: Effect of contact time with the Removal % of (A) Congo Red (B) Methylene Blue (C) Pyrene and (D) Anthracene using bioremediation process by bacterial strain culture *Bacillus subtilis*, *Pseudomonas sp.*, Soil white Micro-organism and Water Micro-organism. Conditions: concentration 5 mg/L, temperature 30^0C and pH-7.

6.5.1.2. Effect of Temperature:

Bioremediation of the Pollutants is influenced by the Temperature of the Bacterial Growth. Mostly at higher temperatures metabolism of the bacteria is enhanced which enhances the degradation of pollutants by microorganisms but at extreme temperatures growth of the microbes is reduced (Iqbal et al, 2007). However, with every micro-organism, there is an optimum temperature, and at the optimum temperature, the growth is enhanced (Sanscartier, David, et al., 2011). Most of the Mesophilic bacterial optimal growth and activity can be seen at a temperature range of 25-35^{0}C (Topp E et al., 1997). Also, because of the optimum growth and activities of the microbes, the bioremediation rate is enhanced on the pollutants.

A graphical representation of the bacterial growth dependency is shown in Fig 30. where the range of the temperature is 20-40^{0}C. From this data, it can be easily observed that at 30^{0}C bacterial growth is the maximum, and in this condition, dye degradation is the highest than other experimental conditions of temperature. However, the removal is also dependent on the bacterial strain used in the removal process. As an example, *Bacillus subtilis* can withstand an extreme range of temperatures, but *Pseudomonas sp.* bacteria contain a wide variety of enzymes that allow them to break down pollutants and for that reason, high-temperature change can affect the bioremediation process by affecting the reaction mechanism and the structure of the enzyme. So, the removal rate of the pollutants by the *Bacillus subtilis* strain is more than *Pseudomonas sp.* in very high and very low temperatures where the removal at 30^{0}C Bacillus gave less removal percentage of pollutants than *Pseudomonas sp.* strain.

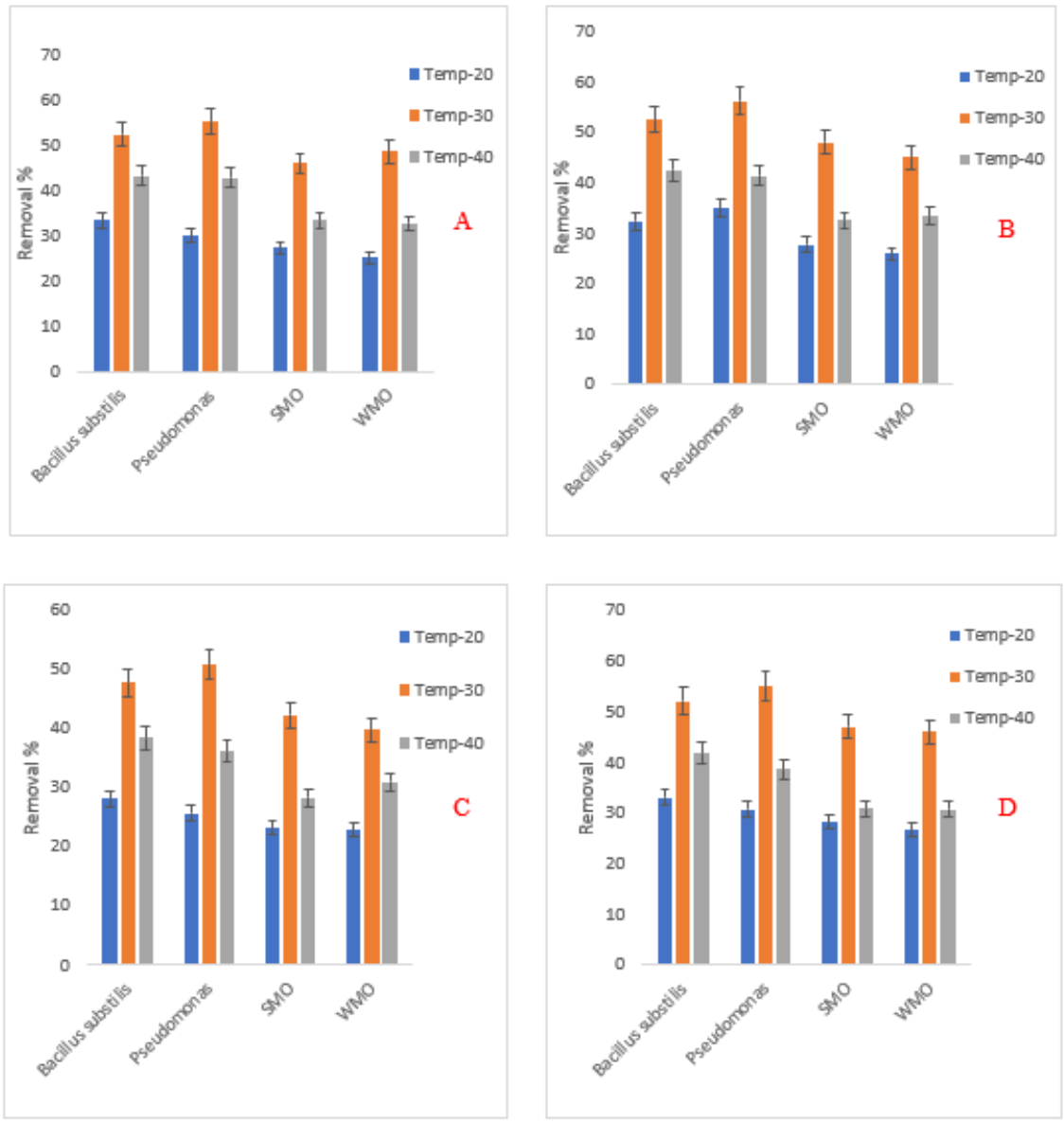


Fig 30: Effect of temperature on the Removal of (A) Congo Red (B) Methylene Blue (C) Pyrene and (D) Anthracene using bioremediation process by bacterial culture *Bacillus subtilis*, *Pseudomonas sp.*, Soil white Micro-organism and Water Micro-organism. Conditions: concentration 5 mg/L, temperature 20^0C, 30^0C, 40^0C and pH-7 with microbial dosage of 10 µl/L.

6.5.1.3. Effect of pH:

Solution pH directly impacts the activities and growth of the microbes involved in the bioremediation. Different microbial species have specific pH ranges at which they thrive and function optimally. Extreme pH of the solution can inhibit the microbial activities of degradation of the pollutants by denaturing the enzyme responsible for the bioremediation of the sample and even disrupting microbial cells (Megharaj et al., 2011). Therefore, maintaining the pH within the optimal range for the target micro-organisms is essential for maximizing the bioremediation rate. In Fig 31. a graphical representation of the bioremediation rate with the change of pH was shown with a range of pH-2 and pH-10 with pH, and from the graphical representation it can be determined that using of extreme pH in the solution, inhibits the growth of the bacterial strain by denaturing the cell wall components and the functionality of the enzyme which are responsible for the degradation process of the pollutants. Still, the bacterial surfaces charges are sometimes affected during the treatment of pH. That's why at high-pH Methylene blue and low-pH Congo Red was attracted by the surface of the bacteria. However, the removal of the Pyrene and Anthracene were highest in optimal pH which is neutral (7) as the biomass concentration in this condition was more than other pH conditions.

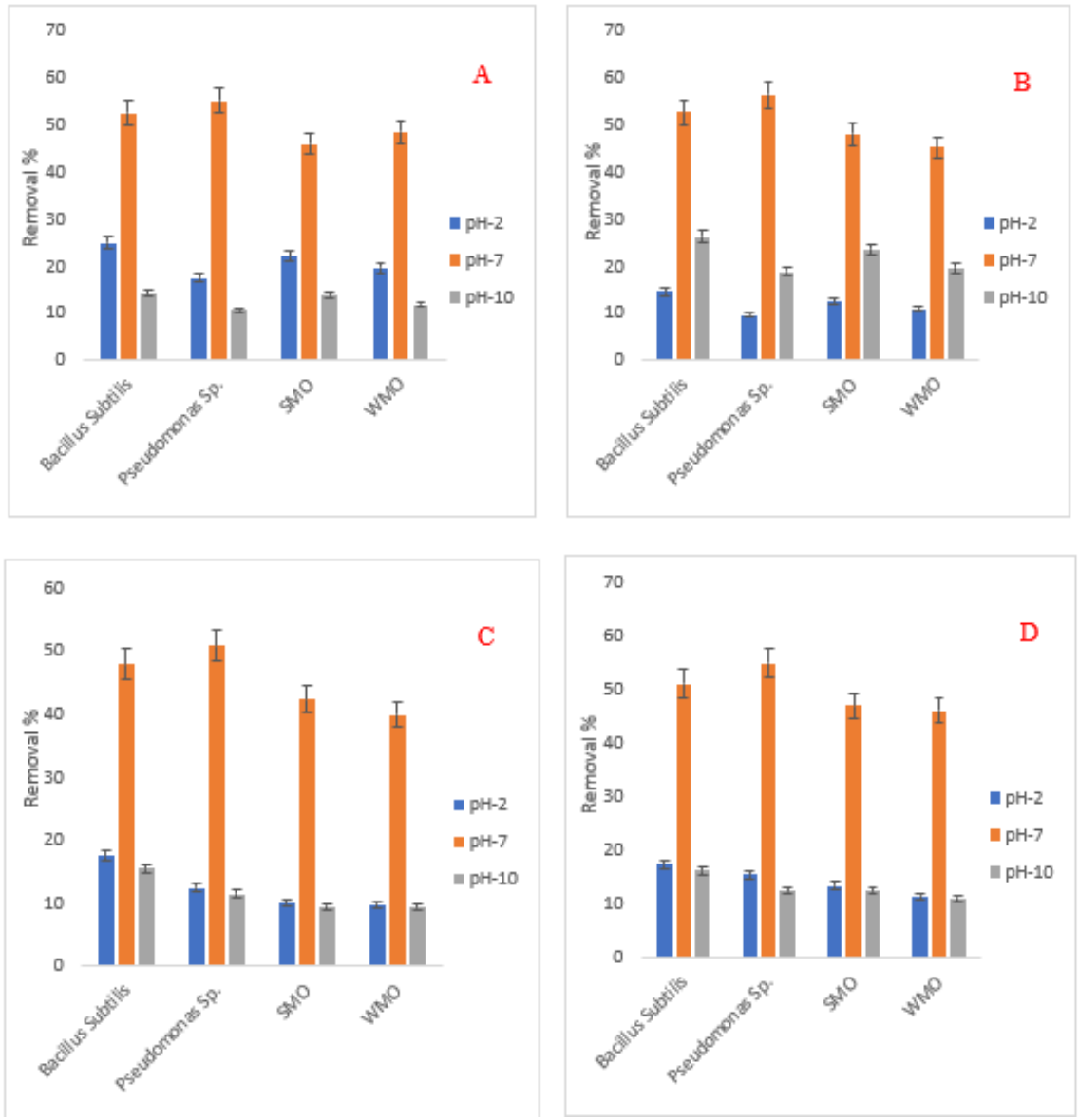


Fig 31: Effect of pH on the Removal of (A) Congo Red (B) Methylene Blue (C) Pyrene and (D) Anthracene using bioremediation process by bacterial culture *Bacillus subtilis*, *Pseudomonas sp.*, Soil white Micro-organism and Water Micro-organism. Conditions: concentration 5 mg/L, temperature 30^0C, microbial dosage 1 µl/L and pH-2, 7, 10.

6.5.1.4. Effect of Pollutant Concentration:

Pollutant concentration has an influence directly on the bioremediation process. Generally, higher concentrations of pollutants provide more microbial growth and metabolic activities (Sayara et al., 2010). Microorganisms utilize pollutants as a source of energy and carbon for their growth and reproduction. However, after threshold limit further increasing of substrate concentration may lead to saturation effects (Nocentini et al., 2000). Saturation occurs when the available of the micro-organisms and enzymes are unable to keep up with the rate of pollutant influx, resulting the diminishing the bioremediation rates. Even in extreme cases, high pollutant concentrations can inhibit microbial activities or even lead to toxicity, and limiting the effectiveness of the bioremediation process (Sharma and Indu, 2020). In Fig 32. Graphical comparative representation of the bioremediation rate change is shown with change of the concentration of pollutants of 5 mg/L and 20 mg/L. And from the graphical representation it can be easily observed that with increase of pollutant concentration the removal rate is decreased. Also decreasing rate of removal from 20 mg/L to 10 mg/L is more than 10 mg/L to 5 mg/L behind this phenomenon pollutants inhibitory effect on bacteria growth is responsible.

6.5.1.5. Effect of Microbial Dose:

The microbial dose indicates the initial population of density of the bioremediation agents introduced to the contaminated environment (Marin et al., 2005). A higher microbial dose typically results in a greater initial population density, which accelerate the onset of the biodegradation and enhance the overall bioremediation rates. Higher microbial doses provide more microbial mass and metabolism capabilities and enable faster degradation rate (Lahel, Abu, et al., 2016; Santini et al., 2016). However, the higher dose of the microbial strains removal percentage of the biodegradation is enhanced but after increasing of dose may cause the lack of substrate in the medium which is the energy and carbon

source for their growth along with lowering the microbial dose may cause opposite and after extreme threshold level may cause toxic effect on the enzyme responsible for the bioremediation process (Liu et al., 1993). In Fig 33. a graphical representation of comparative studies of the bioremediation rate change was shown with the change of the Dose of 300µl and 1ml with 100µl.

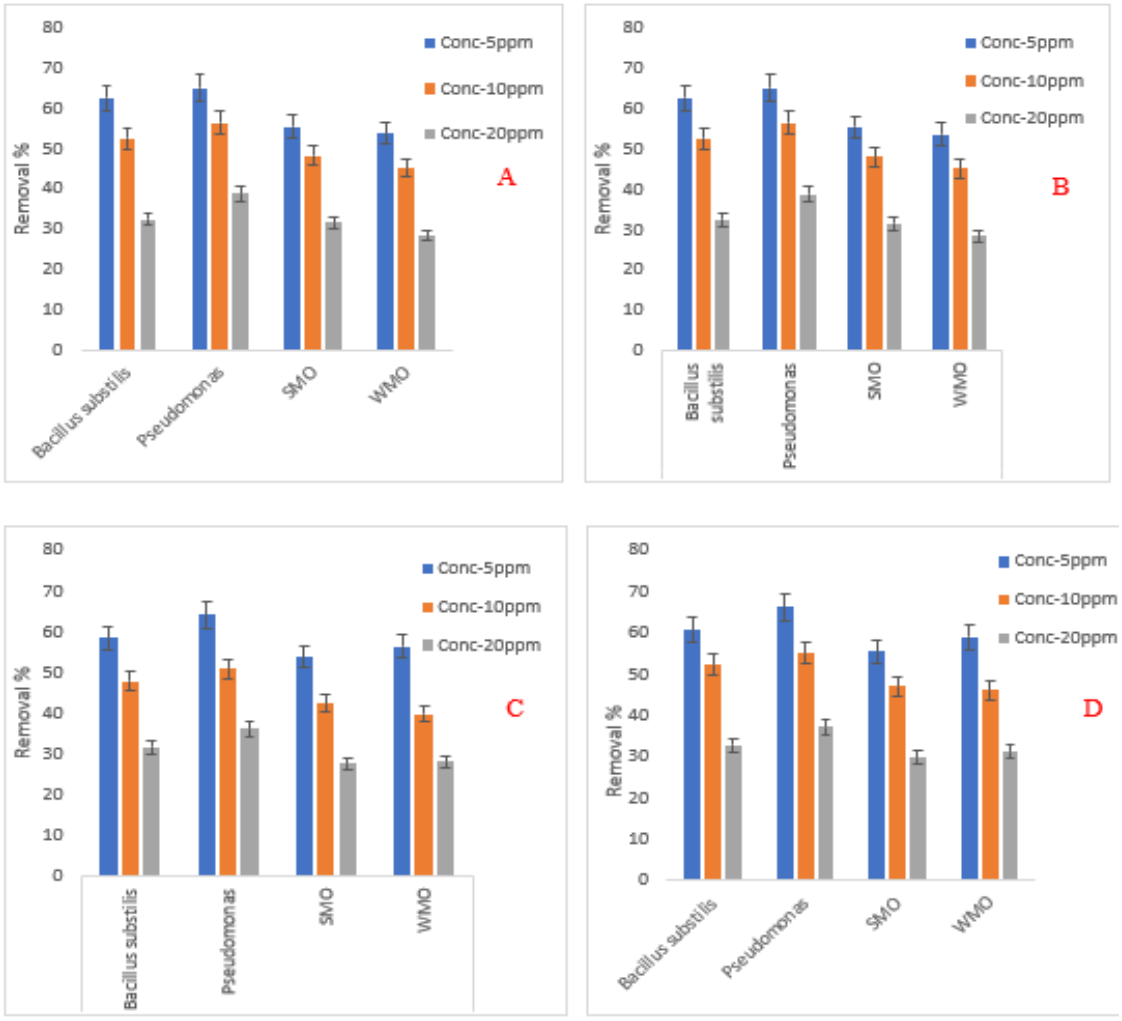


Fig 32: Effect of Pollutants Concentration on the Removal of (A) Congo Red (B) Methylene Blue (C) Pyrene and (D) Anthracene using bioremediation process by bacterial culture *Bacillus subtilis*, *Pseudomonas sp.*, Soil white Micro-organism and Water Micro-organism with variable Concentration of 5 mg/L (ppm) , 10 mg/L (ppm) , and 20 mg/L (ppm) where other parameters maintained at same condition Dosage of Bacteria: 10 µl/L , pH-7 and Temp-30^{0}C.

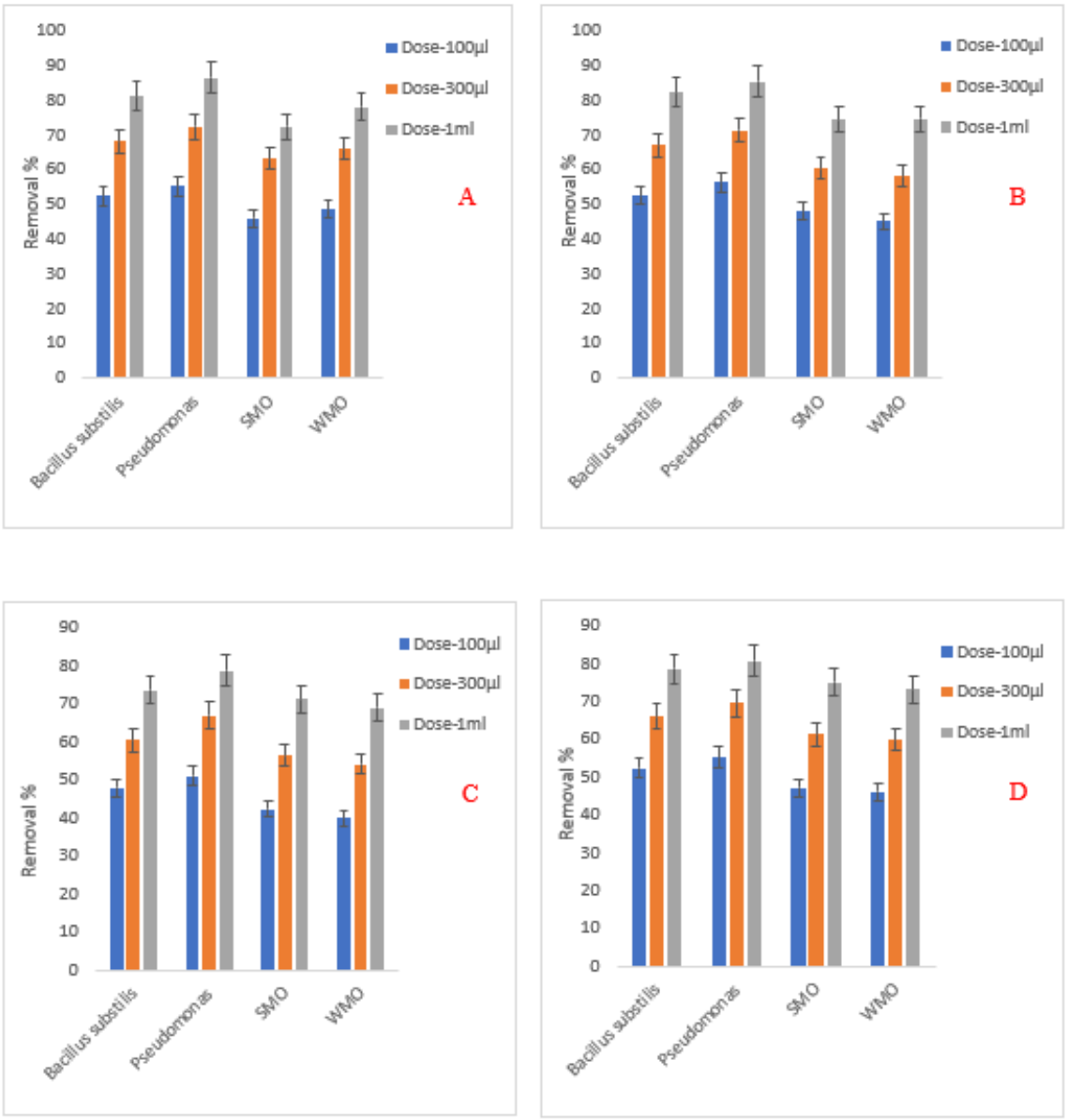


Fig 33: Effect of Bacterial Dose on the Removal of (A) Congo Red (B) Methylene Blue (C) Pyrene and (D) Anthracene using bioremediation process by bacterial culture *Bacillus subtilis*, *Pseudomonas sp.*, Soil white Micro-organism and Water Micro-organism with variable dosage of 100 µl, 300 µl and 1 ml where other parameters maintained at same condition Concentration of pollutants: 5 mg/L, pH-7 and Temp-30^{0}C.

6.5.2. Sorting of bacteria for immobilization in Aerogel Matrix:

From the parameters effects on bioremediation over the pollutants mentioned before it can be clearly observed that *Pseudomonas sp.* have highest removal rate than other bacterial stains used throughout the process. However, *Bacillus subtilis* has more tolerance against extreme temperature and pH still in normal condition removal rate of *Bacillus subtilis* is less than *Pseudomonas sp.*, in other hand *Pseudomonas sp.* can easily immobilized in Gel matrix from other stains used in process of bioremediation. As a result, *Pseudomonas sp.* is sorted out for the further process of pollutants removal using adsorption of aerogel along with bioremediation by bacteria stains in an encapsulated form.

6.6. Removal of Pollutants using Bacteria-doped Aerogel:

6.6.1. Effects of various parameters on removal of pollutants:

Removal of pollutants by Bacteria doped aerogel is a combined effect of adsorption and bioremediation because of these reasons, parameters viz. contact time, concentration of the pollutants, dosage of the adsorbents, pH etc. have various effects on the biosorption of the pollutants. Effect of the parameters are described below by PVA and its derivatives aerogel immobilized with bacteria stain *Pseudomonas sp.* Removal percentage of the pollutants are determined by the Eq 6 mentioned in “Adsorption section”.

5.6.1.1. Effect of Contact Time:

Longer contact time gives higher removal rate of the pollutants by adsorbents but in removal graph by bacteria-doped aerogels some parts indicate the mechanism behind the removal. As shown in Fig 34. PVA and its derivatives aerogels immobilized with *Pseudomonas sp.* bacteria graphical representation of pollutants removal where it can be clearly observed and examined that mechanism of the removal is followed by adsorption,

bioremediation of bacteria situated in lag phase, then bioremediation of bacteria with exponential growth rate and finally with death growth phase bacteria where the removal rate become equilibrium after reaching maximum value.

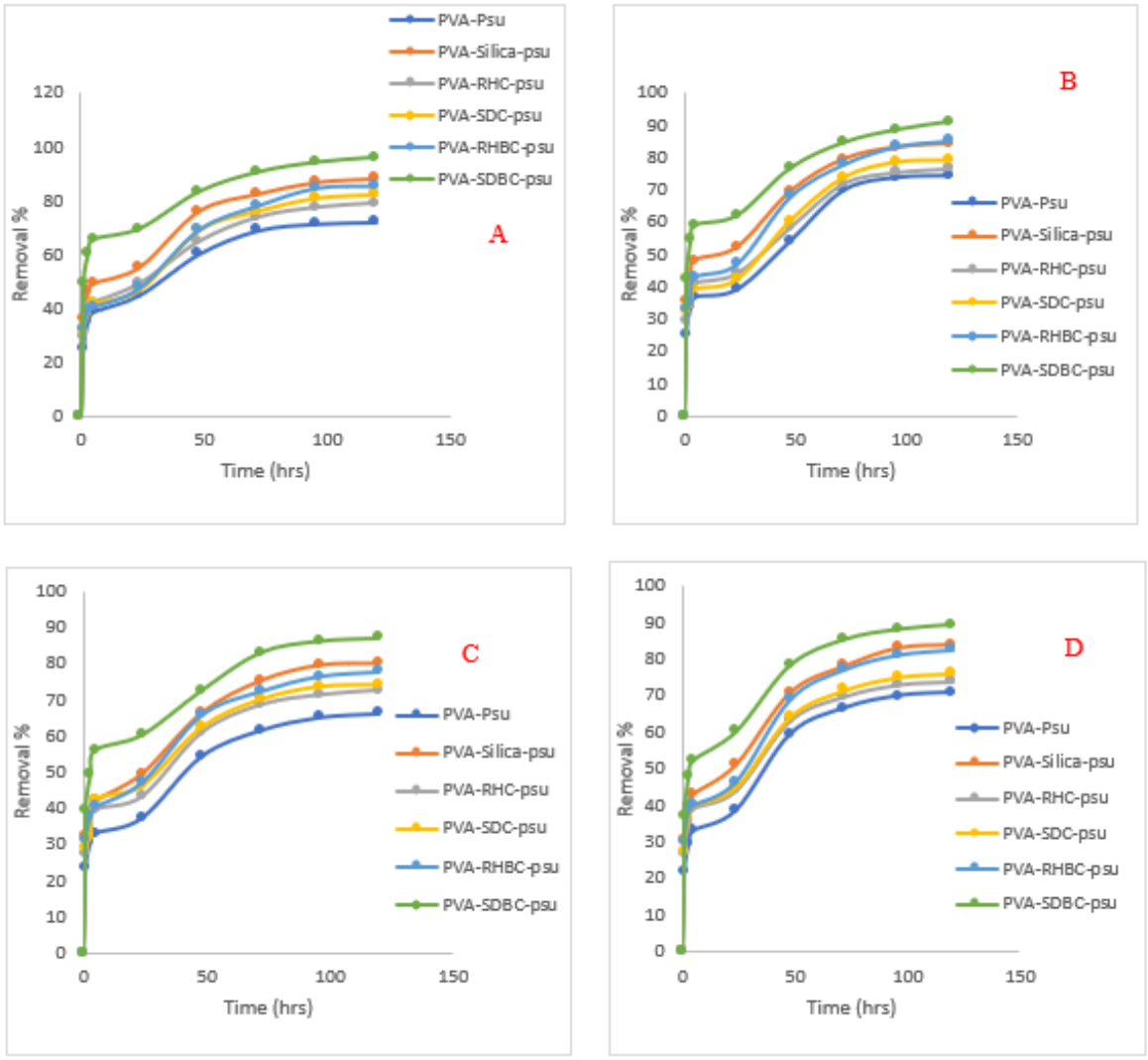


Fig 34: Effect of contact time on removal of the Pollutants: (A) Congo Red, (B) Methylene Blue, (C) Pyrene, and (D) Anthracene using PVA and derivatives aerogels immobilized by *Pseudomonas sp.* bacteria while maintaining conditions viz. Pollutants concentrations 5 mg/L, Dosage- 1 g/L and Temperature-30^{0}C and pH-7.

6.6.1.2. Effect of Temperature:

Both bioremediation and Adsorption were affected by Temperature of the solution. From the perspective of bioremediation, there was an optimum temperature of bacteria stain growth which were responsible for the removal of the pollutants using various enzymes and surface interaction and for specially *Pseudomonas sp.* bacterial stain the with variation of temperature the enzyme excreted from the cells can be denatured or the cell wall can be raptured. On another hand, in adsorption process the removal rate is varied based on the change of the molecular entropy, impurities by increasing the surface activities and kinetics energy of the adsorbates.

There are two possibilities of the adsorption rate changes one is increases of removal rate with increase of temperature and in another hand decreasing of removal rate with increasing of temperature. And both of them shows two mechanisms as below:

- One is increase of adsorption rate with increase of temperature because of presence of Chemisorption where value of ΔH is appx. 200kJ/mol.
- Another one is decrease of adsorption rate with increase of Temperature due to physisorption with value of ΔH is appx. 20kJ/mol.

Overall, the removal rate is quite dependent over temperature due to various factors. In Fig 35. The graphical representation of pollutants removal by bacterial immobilized PVA and its derivatives aerogel are shown with the change of temperature from 20 to 40^0C maintaining the remain parameters constant viz. pH at 7, Pollutants concentration of 5 mg/L and Dosage of the adsorbents 1g/L.

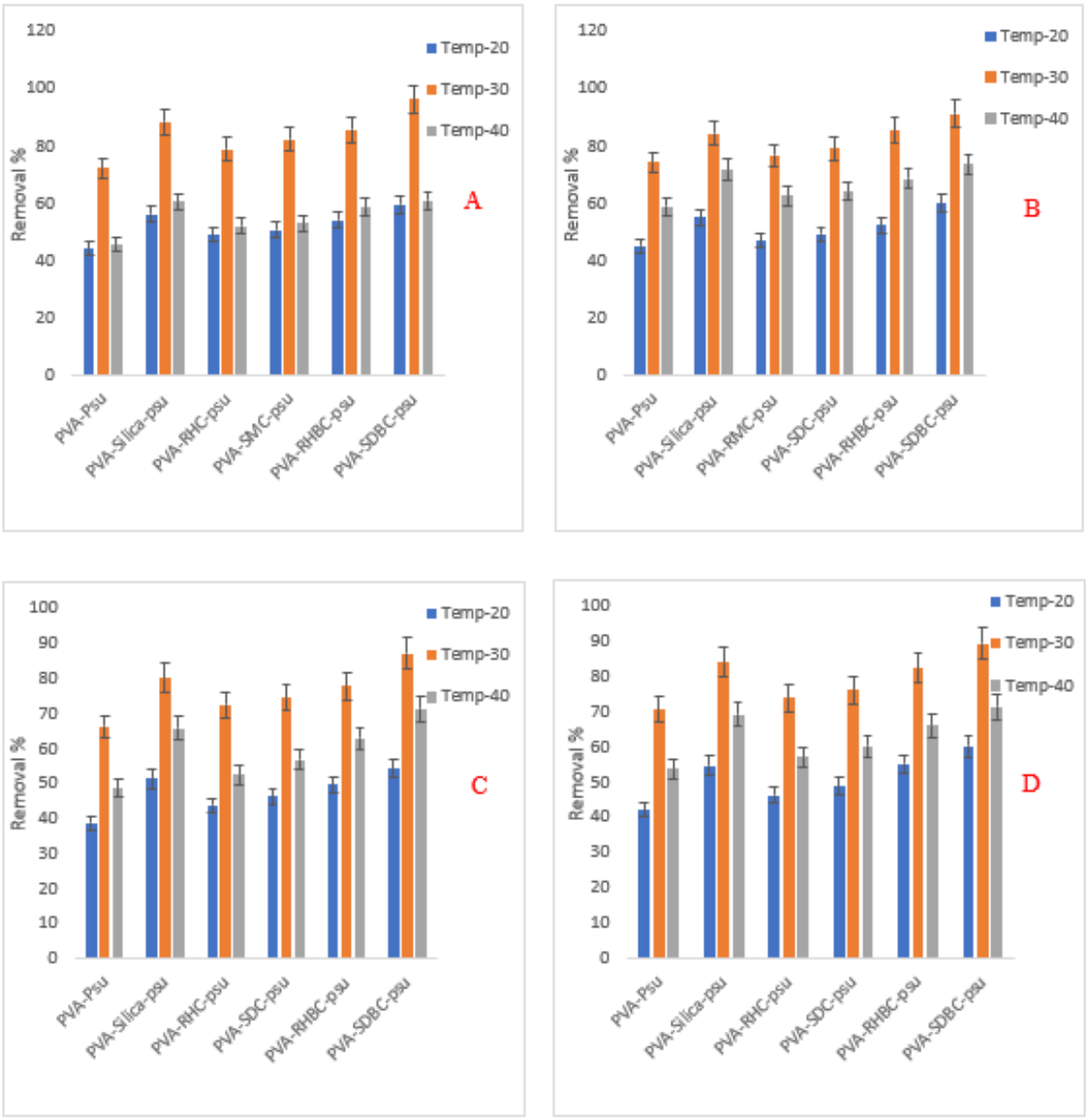


Fig 35: Effect of Solution temperature on the Removal of (A) Congo Red (B) Methylene Blue (C) Pyrene and (D) Anthracene using *Pseudomonas sp.*-doped PVA and its derivatives Aerogel with variable Temperature of 20^0C and 40^0C where other parameters maintained at same condition Adsorbent Dosage: 1 g/L, pH-7 and Conc-5 mg/L.

6.6.1.3. Effect of solution pH:

Solution pH is one of the main important parameters responsible for affecting the removal of pollutants by adsorption and bioremediation process. From the perspective of bioremediation process, pH directly affects the growth of bacteria and because of low bacterial density, removal rate is also decreased. During adsorption pH of the solution can alter the adsorbents' surface charge which sometime results the increase of pollutants removal specially the ionic dyes. As an example, for Congo Red and Methylene Blue the removal rate by adsorption is quite different than bioremediation by micro-organism. From the practical application of pH during adsorption process in Fig 36. it can be easily determined that the dyes during binding on the surface of adsorbents the presence of H^+ and OH^- ions may be increased or decreased. When the acid added to the solution the surface of the adsorbents is promoted for allowing to binding the anionic dyes with the surface easily but repulse cationic dyes and in case of basic solution the result show quite opposite due to presence of electrostatic force between the surface and adsorbates. In other hand for organic non-polar molecules pH didn't give much effects on the removal because of their low affinity toward the adsorbent surface by electrostatic force.

In the Fig. 36. the effect of pH on the removal of the pollutants by PVA and its derivatives aerogel immobilized with *Pseudomonas sp.* bacteria are shown maintaining the other conditions constants viz. Temp 30^0C, Pollutants concentration 5 mg/L and Dosage 1 g/L.

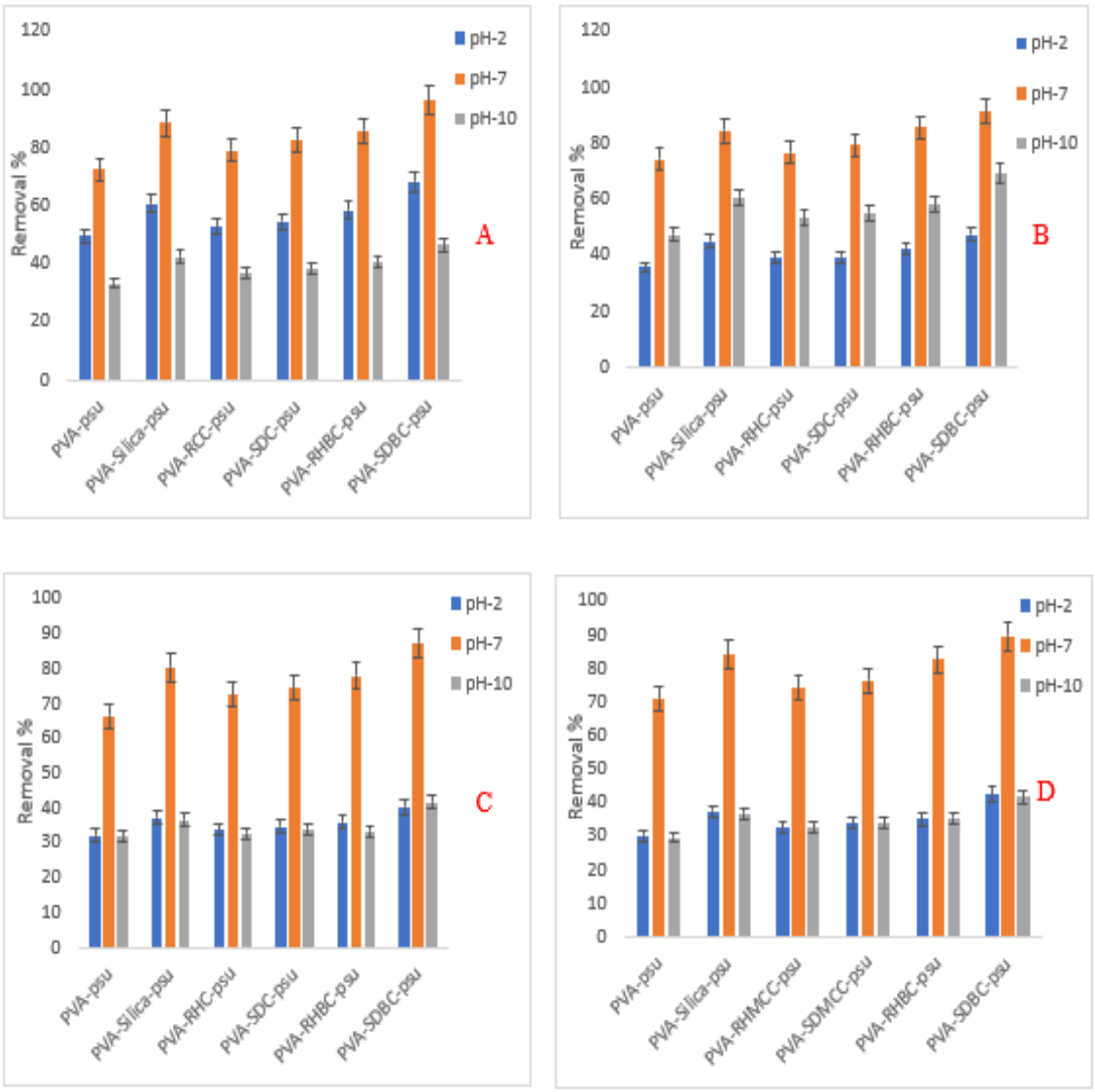


Fig 36: Effect of Solution pH on the Removal of (a) Congo Red (b) Methylene Blue (c) Pyrene and (d) Anthracene using *Pseudomonas sp.*-doped PVA and its derivatives Aerogel with variable pH of 2 and 10 where other parameters maintained at same condition Adsorbent Dosage: 1 g/L, temperature-30^{0}C and Conc-5 mg/L.

6.6.1.4. Effect of Pollutants Concentration:

In Fig 37. Removal of the pollutants are shown with the variation of Pollutants concentration from 5 mg/L to 20 mg/L maintaining the other parameters constant viz. Dosage 1 g/L, temp-30^{0}C and pH-7. And it can be easily determined that with increasing of concentration of pollutants the removal rate by adsorption and bioremediation decreased. From the perspective of adsorption processes the surface of adsorbents are saturated by pollutants or adsorbates. Also, in case of Bioremediation the increase of pollutants concentration sometime gives inhibitory effect during the growth of micro-organism present in the immobilized aerogel used for removal of the pollutants even the surface of bacteria also acts as adsorption friendly surface but more pollutants particle attach make them less available to new particles cause reduction of removal %.

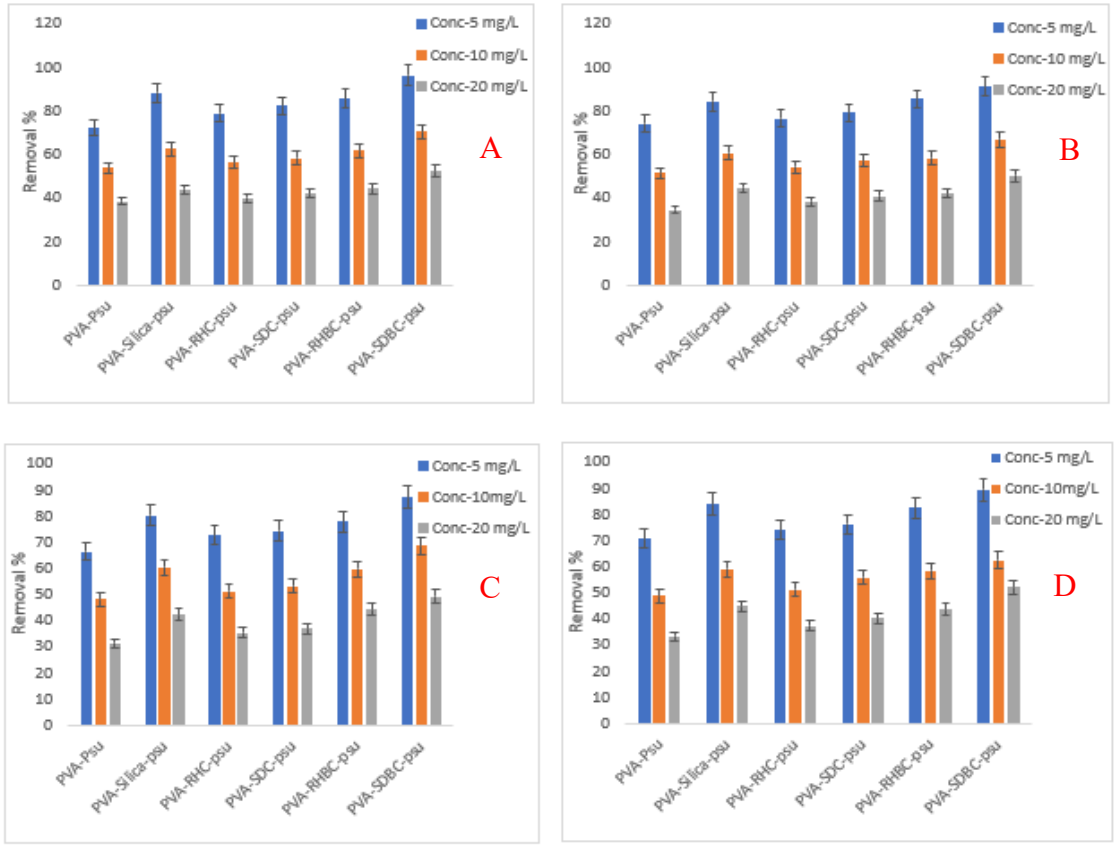


Fig 37: Effect of Pollutants concentration on the Removal of (A) Congo Red (B) Methylene Blue (C) Pyrene and (D) Anthracene using *Pseudomonas sp.*-doped PVA and its derivatives Aerogel with variable conc 5, 10 and 20 mg/L where other parameters maintained at same condition Dosage: 1 g/L, temperature-30^{0}C and pH- 7.

6.6.1.5. Effect of Adsorbent dosage:

In Fig 38. Removal of the pollutants are shown with the variation of adsorbent dosage from 0.5, 1 and 2 g/L and maintaining other parameters viz. pH-7 (neutral), temperature 30^0C and Concentration of pollutants 5 mg/L. And it can be easily determined that with increasing of dosage removal rate of the pollutants are also increased because of the presence of more adsorption side on adsorbent surface and from the perspective of bioremediation, low dose may suffer the inhibition of pollutant toxicity which become low in case of high dose of bacteria strain presence in the immobilized aerogel.

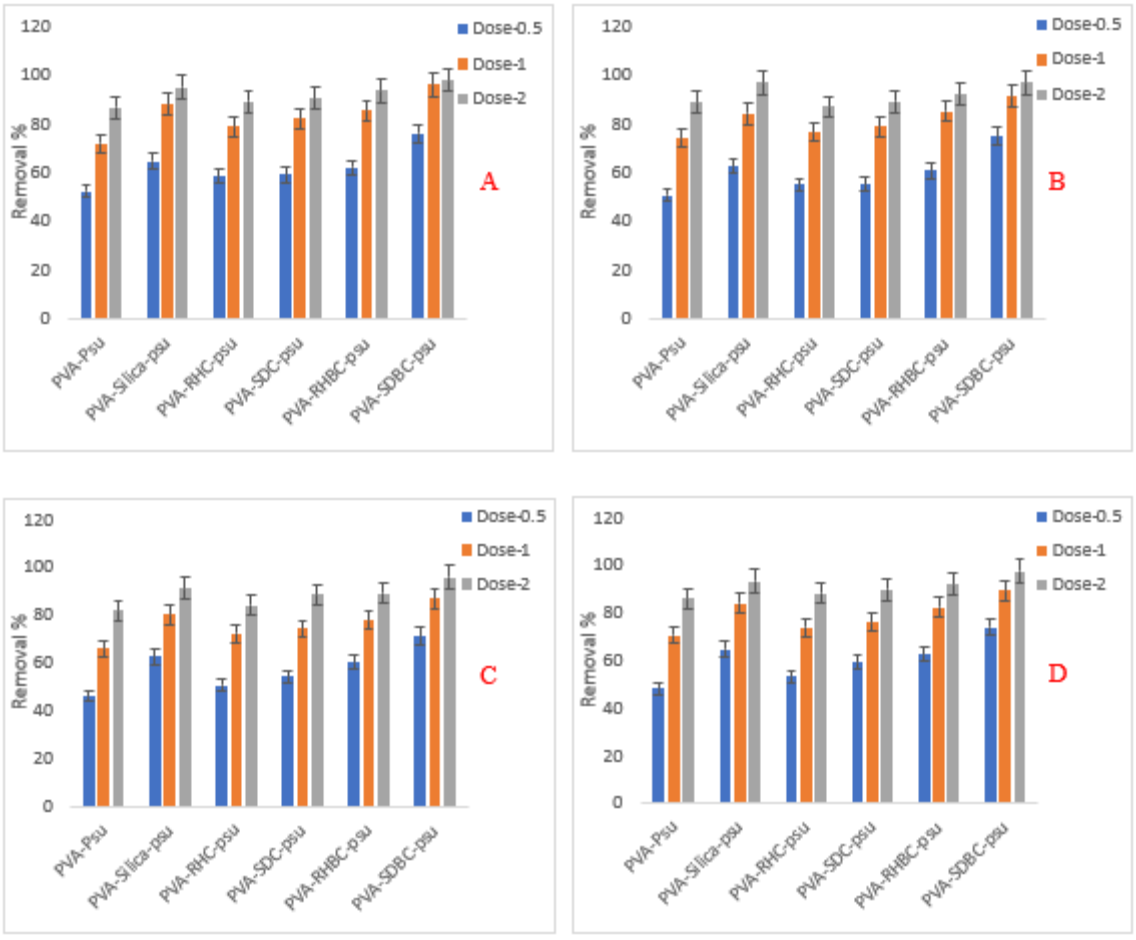


Fig 38: Effect of Adsorbent dosage on the Removal of (A) Congo Red (B) Methylene Blue (C) Pyrene and (D) Anthracene using *Pseudomonas sp.*-doped PVA and its derivatives Aerogel with variable dosage of 0.5, 1, 2 g/L and where other parameters maintained at same condition Concentration- 5 mg/L, temperature-30^0C and pH- 7.

6.7. Comparative Analysis of Bacteria immobilized Aerogel with Base Aerogel on the removal process of pollutants:

In Fig 39. The comparative study of removal process of pollutants are shown between Bacteria-doped Aerogel and normal adsorption process carried out by Base Aerogel which have the highest removal percentage of pollutants. The graphically analysis data are shown in Fig 39. (A) of pollutants removal by Bacteria-doped aerogel can be divided into three consecutive parts:

(1) Adsorption,
(2) Adsorption overlapped with Bioremediation, and
(3) Biodegradation of pollutants by immobilized Micro-organisms.

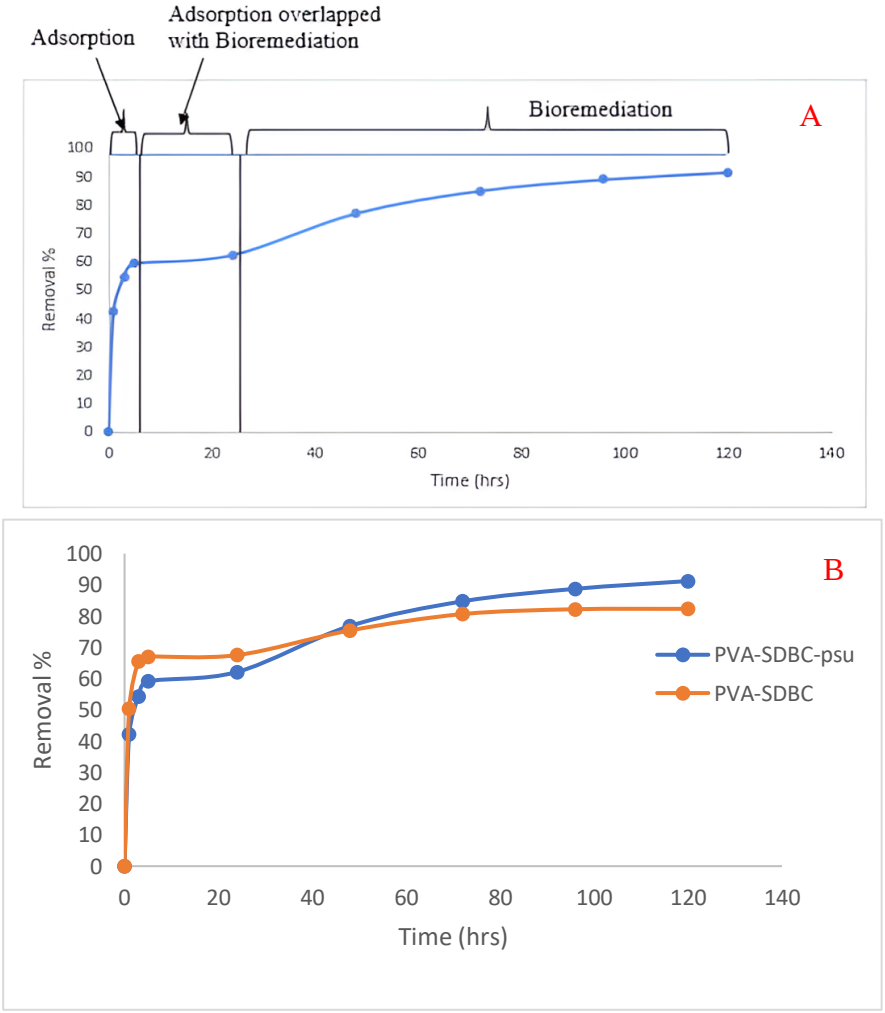


Fig 39. (A) Methylene Blue Dye removal by PVA-SDBC immobilized with *Pseudomonas sp.* with mechanism of removal process with time difference. (B) comparative analysis of Bacteria-immobilized aerogel with Base aerogel.

From the graphical analysis it can be easily observed that final removal percentage of pollutants by Bacteria-doped Aerogel (91.23%) is higher than the normal aerogel (82.39%) due to encapsulating bioremediation process with adsorption. However, the initial stages of the treatment by bacteria-doped Aerogel exhibit lower pollutants removal rate than Base Aerogel. The reason behind the result can be explained by the theory of pore occupied by immobilized Micro-organism inside the matrix and reduce the surface area of the functional site which are responsible for pollutants removal by Adsorption.

6.8. Modelling of Adsorption Process:

Modelling in adsorption processes involves creating mathematical representations or simulations to understand adsorption occurs on a given material's surface and prediction of how adsorbents interact with adsorbates. Modelling of the adsorption involves some key aspects and mathematical solution of the adsorption process:

1. Adsorption Isotherm
2. Kinetics Models
3. Thermodynamics Models

Other of these models there are some other key aspects present viz. Mass transfer models, and Surface Chemistry Models etc.

6.8.1. Adsorption Isotherm:

Adsorption is a surface phenomenon that involves adhesion of atoms, ions, or molecules of any fluids on a surface of any adsorbents. Still based on the molecular interactions there are two types of adsorptions one is chemical adsorption and another on is physical adsorption (Al-Ghouti, Mohammad A., and Dana A. Da'ana, 2020). Where in physical adsorption mono-layer interaction of adsorbate on the adsorbent's surface happened and in case of chemical adsorption multilayer adsorption occurs. The relation in adsorption isotherm explains the phenomena and interactions between adsorbate and adsorbent. Generally, the adsorption performance can be predicted by modeling the adsorption isotherm data because the adsorption isotherm model can provide information about the adsorbent capacity, the adsorption mechanism, and the evaluation of the adsorption process performance (Raya, Indah, et al., 2016).

Isotherm Modelling are various types which are Langmuir Isotherm, Freundlich Isotherm, Temkin Isotherm, Halsey Isotherm, Dubinin-Radushkevich Isotherm, Harkin-Jura Isotherm etc. Out of them Langmuir and Freundlich Isotherm are most important.

6.8.1.1. Langmuir Isotherm:

Langmuir isotherm is one of the models for describing the binding between the adsorbate and adsorbents at a given and constant Temperature. It assumes that adsorption occurs on a homogeneous surface with a finite number of identical sites available for adsorption. According to this model, adsorption proceeds in two steps: first, adsorbate molecules approach the surface, and then they either bind to the surface or desorb back into the gas phase. There are four assumptions in this type of isotherm namely (Irving Langmuir, 1918):

1. The molecules are adsorbed by a fixed site (the reaction site at the adsorbents surface).
2. Each site can "hold" one adsorbate molecule.
3. All sites have the same energy.
4. There is no interaction between the adsorbed molecules and the surrounding sites. Adsorption process from the monolayer.

Langmuir isotherm representation can be expressed by Eq 7:

$$\frac{1}{Qe} = \frac{1}{QmaxKL} \cdot \frac{1}{Ce} + \frac{1}{Qmax} \quad \text{.....(7)}$$

And from the equation of Langmuir isotherm graph (Ce vs Ce/Qe) of Q_{max} and b value can be evaluated which are the maximum monolayer adsorption capacity and binding energy or affinity parameters respectively.

The important factor of Langmuir Isotherm Application is the dimensionless factor or separation factor (R_L) (Irving Langmuir, 1918) which can be represented using Eq 8:

$$R_L = \frac{1}{1+KLCe} \quad \text{.....(8)}$$

This separation factor has some value with various significances:

1. $R_L > 1$, unfavorable adsorption process (allows the adsorption process to occur, most desorption processes occur).
2. $R_L = 1$, linear adsorption process (depending on the amount adsorbed and the concentration adsorbed).
3. $R_L = 0$, Irreversible adsorption process (strong adsorption).
4. $0 < R_L < 1$, Favorable adsorption process (normal adsorption).

In table 11. Significance of Langmuir Isotherm of highest removal pollutant (Methylene Blue) using Aerogel PVA-SDBC is shown with the Q_{max}, K_L, R_L and R^2 value.

Table 11. Langmuir isotherm significance of Methylene Blue removal by PVA-SDBC aerogel:

Aerogel	Pollutant	Q_{max} (mg. g^{-1})	K_L (L.mg^{-1})	R_L (g/L)	R^2
PVA-SDBC	Methylene Blue	18.33	1.85	0.029	0.781

6.8.1.2. Freundlich Isotherm:

The Freundlich Isotherm is a mathematical model used to describe the adsorption of a solute onto a solid surface. This type of adsorption in which the adsorption occurs in several layers and the bonds are not strong (multilayer). Freundlich isotherm also assumes that the sites of adsorption are heterogeneous (Dada, A. O., et al., 2012). The empirical relationship for expressing Freundlich isotherm is given in Eq 9:

$$lnQe = lnKf + \frac{1}{n} lnCe \quad \text{.....(9)}$$

where K_f is Freundlich constant, Ce is the concentration of adsorbate under equilibrium conditions (mg/L), Qe is the amount of adsorbate absorbed per unit of adsorbent (mg/g), and n is the value indicating the degree of linearity between the adsorbate solution and the adsorption process (Dada et al., 2012).

The value of n has various significance:

1. n = 1, linear adsorption.
2. n < 1, adsorption process with chemical interaction.
3. n > 1, adsorption process with physical interaction.
4. Favorable adsorption process is declared when 0 < 1/n < 1, and a cooperative adsorption process occurs when 1/n > 1.

In table 8. Freundlich isotherm significance of PVA and its derivatives aerogel are shown using R^2 value and it can be easily determined that except Congo Red removal Freundlich isotherm show more significance.

In Table 12. The significance of Freundlich Isotherm of highest removed pollutants (Methylene Blue) using PVA-SDBC aerogel is shown using K_f, n and R^2 value.

Table 12. Freundlich Isotherm significance of Methylene Blue by PVA-SDBC aerogel:

Aerogel	Pollutant	K_f	n	R^2
PVA-SDBC	Methylene Blue	8.24	2.54	0.993

6.8.1.3. Significance of Isotherm analysis of Adsorption process by aerogel:

Isotherm analysis plays a very crucial role in adsorption studies to provides the essential information about the interaction between adsorbates molecules and adsorbent surface under equilibrium conditions along with the mechanism of adsorption. By plotting experimental data obtained from the adsorption studies by PVA-Saw Dust Biochar on Methylene Blue pollutants it can be easily determined that the Freundlich isotherm shows more significance due to higher R^2 (0.997) value than Langmuir isotherm (0.781) which show multilayer adsorption on the sites of adsorbent surface.

6.8.2. Adsorption Kinetics:

Same as Adsorption Isotherm, kinetics give a crucial role for understanding the mechanism and dynamics of the adsorption and by this kinetics show how quickly and efficiently molecules (adsorbates) accumulate on a surface (adsorbent) over time. It's particularly important in fields like environmental remediation, separation processes, and heterogeneous catalysis. There are various types kinetics can be used to determine the dynamics of Adsorption but out of them Pseudo first Order and Pseudo second Order kinetics are more importance.

6.8.2.1. Pseudo first Order kinetics:

Pseudo first order kinetics refers to a situation where a reaction that is actually higher-order, such as second order or more, appears to follow first order kinetics under certain conditions. And this typically occurs when one reactant is present in excess compared to other

reactants, causing its concentration to remain nearly constant throughout the reaction. As a result, the reaction becomes dependent over only the concentration of the limiting reactant, giving the appearance of first order kinetics.

The empirical relation for pseudo first order kinetics can be expressed by Eq 10:

$$\log(qe - qt) = logqe - \left[\left(\frac{k1}{2.303}\right) t\right] \quad \text{.....(10)}$$

To evaluate the significance of the pseudo first order k_1, q_e and R^2 need to be determined using the graph of $\log(q_e\text{-}q_t)$ vs time, In table 13. value of parameters were evaluated of the pollutants (Methylene Blue) with highest removal of adsorbents (PVA-SDBC).

Table 13. Significance of pseudo first order kinetics of Methylene Blue by PVA-SDBC:

Adsorbent	Pollutant	$K_1(min^{-1})$	q_e (mg/L)	R^2
PVA-SDBC	Methylene Blue	0.233	6.282	0.953

6.8.2.2. Pseudo second order kinetics:

As pseudo first order kinetics pseudo second order kinetics is also a mathematical model used to describe the rate of the chemical reactions, particularly those involving the adsorption process. In pseudo second kinetics, through equation it can be behaved as second order kinetics. The empirical relation for expressing pseudo second order kinetics can be determined by Eq 11:

$$\frac{t}{qt} = \frac{1}{(k2 * qe^2)} + \frac{t}{qe} \quad \text{.....(11)}$$

To evaluate the significance of the pseudo second order k_2, qe and R^2 need to be determined using the graph of t/q_t vs time, In table 14. value of parameters were evaluated of the pollutants (Methylene Blue) with highest removal of adsorbents (PVA-SDBC).

Table 14. Significance of pseudo second order kinetics of Methylene Blue removal by PVA-SDBC:

Adsorbent	Pollutant	K_2 (g/(mg·min)	q_e	R^2
PVA-SDBC	Methylene Blue	0.488	8.091	0.997

6.8.2.3. Analysis of Adsorption Kinetics of Adsorption process by Aerogel:

With respect to the range of values of R^2, some generalizations can be made. The values of $R^2 < 0.5$ indicate a weak relation between the predictor (or independent) variable(s) and the response variable, while $0.5< R^2 < 0.8$ indicate that the model is not adequate. This implies that $R^2 > 0.8$ indicate good fit between the data and the model. Having this range of R^2, if two models have $R^2 > 0.8$, why is the one with a higher R^2 (closer to 1) can be considered as the possible. From the data given in the Table 9 and 10. The parameters for initial concentration of 1 mg/L results the value of R^2 are evaluated 0.953 and 0.997 which can be determined that the mechanism of the adsorption is PSO is good fit for the mechanism of adsorption.

6.8.3. Adsorption Thermodynamics:

As isotherm and Kinetics thermodynamics is one of the important parameters in adsorption process. Thermodynamic considerations of an adsorption are necessary to conclude whether the process is spontaneous or not. The Gibb's free energy change, ΔG^0, is an indication of spontaneity of chemical reaction which is an important criterion for spontaneity (Bering et al., 1972). Both enthalpy (ΔH^0) and entropy (ΔS^0) factors must be considered in order to determine the Gibb's free energy of the process. Reactions occur spontaneously at a given temperature if ΔG^0 is a negative quantity (Myers, A. L., 2002). The free energy of an adsorption process is related to Van't Hoff equation (Eq 12):

$$\Delta G^0 = - RT \ln Kc \quad \text{.....(12)}$$

Where the ΔG^0 is the Gibb's free energy change (kJ. mol^{-1}), R is the ideal gas constant (8.314 J. mol^{-1}. K^{-1}), and Temperature is T with K_c which is the single point or the linear sorption distribution co-efficient defined by Eq. 13 (Guggenheim et al, 1933):

$$Kc = \frac{Ca}{Ce} \quad \text{.....(13)}$$

where Ca is the equilibrium adsorbate concentration on the adsorbent (mg. L^{-1}) and Ce is the equilibrium adsorbate concentration is the solution (mg. L^{-1}).

There is also an equation between ΔG^0, ΔH^0, ΔS^0 and T it will be linear with the slope and intercept giving the value of ΔH^0 and ΔS^0 respectively which was evaluated by Eq 14.

$$\Delta G^0 = \Delta H^0 - T\Delta S^0 \quad \text{.....(14)}$$

In Table 15. The values of parameters are evaluated of the pollutant (Methylene Blue) with the value highest removal by PVA-SDBC (adsorbent).

Table 15. Thermodynamics analysis on Methylene Blue removal by PVA-SDBC aerogel:

Aerogel	Pollutants	Temperature (K)	ΔG^0 (J/mol)	ΔH^0 (kJ/mol)	ΔS^0 (J/K.mol)
PVA-SDBC	Methylene Blue	293	-795.299	-14.908	56.364
		303	-1114.998		
		313	-1872.201		
	Congo Red	293	-3163.73	25.019	-74.28
		303	-2700		
		313	-1665.38		

6.8.3.1. Conclusion of Thermodynamics analysis of the adsorption process:

From the Table 15. It can be easily analyzed that the removal of the pollutants has an increasing negative ΔG^0 value with increasing of temperature of the solution indication spontaneity, except the removal of Congo Red where from the graphical representation of Fig 23. with the increasing of Temperature deceased the removal of pollutants, gives the increasing ΔG^0 value with positive ΔH^0 and negative value of ΔS^0 indicates endothermic reaction throughout the process.

6.9. Kinetics of Bioremediation:

Modelling of Bioremediation is one of the important processes of mathematical, computation or statistical models of simulate and predict the behavior of bioremediation systems, in which the micro-organisms are used to degrade the organic compounds. Modelling of the bioremediation represent the growth kinetics of microbes used to degrade the pollutants. For the growth of the microbes, some key aspects are involved and mathematical solution are involved viz.

1. Monod Model
2. Logistic Model
3. Modified logistic Model
4. Leudeking-Piret Model

However, Monod model is the most important and widely used model of the out others described.

6.9.1. Monod Model:

Monod modelling is a mathematical model for the growth of micro-organisms. As noted by Bailey and Oils (1986) this model is probably called a great oversimplified equation for expressing the microbial growth. This model is expressed by showing a functional relationship between the specific growth (μ_g) and an essential substrate concentration (S), also the Eq 15. can be expressed as an empirically as below (Alexander, M., 1999; Ferenci, Thomas, 1999):

$$\mu g = \mu max.(\frac{S}{S+Ks}) \quad \text{.....(15)}$$

In which the maximum specific growth is μ_{max} and Ks is called Monod Constant (AF Gaudy and ET Gaudy, 1980).

In Fig 40. The graphical representation of Monod equation and Double reciprocating plot are shown with the value of μ_{max} and Ks value of the bioremediation of highest removed pollutant (Methylene Blue) using the bacteria of *Pseudomonas sp.* shown in Table 16:

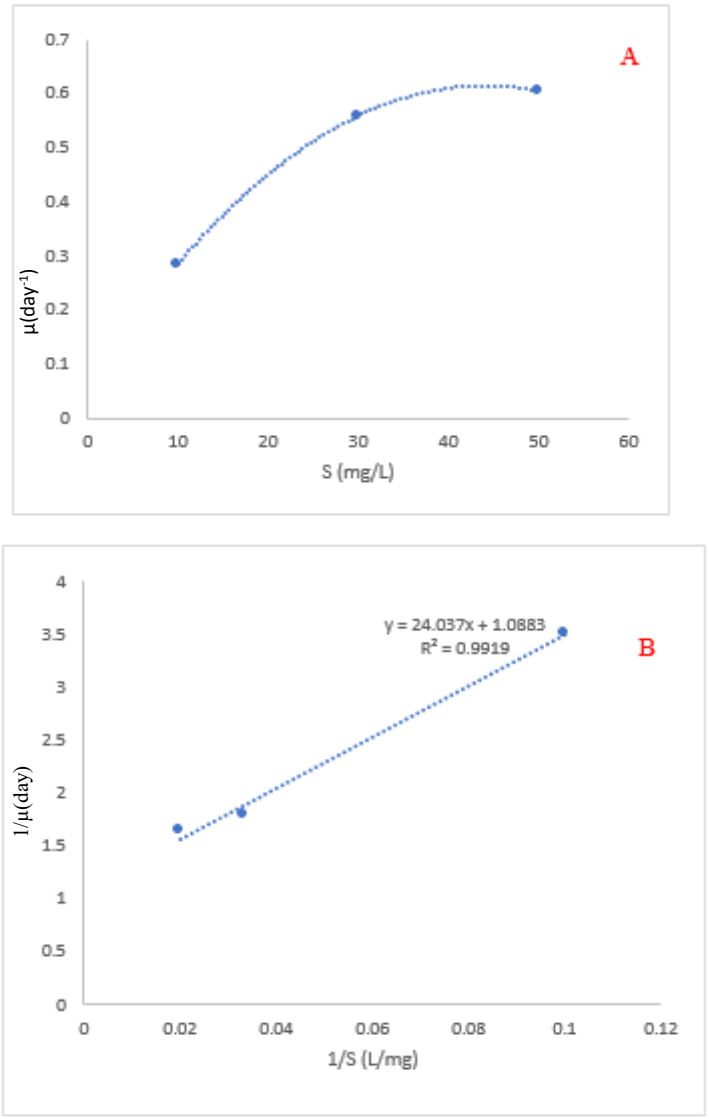


Fig 40: A) Monod equation of Methylene Blue bioremediation using *Pseudomonas sp.* Bacteria, B) Lineweaver-Burk plot (Double-reciprocal plot)

Table 16. Parameters analysis of Methylene Blue bioremediation by *Pseudomonas sp.* using Monod Eq:

Pollutant	Micro-organism	μ_{max} (day^{-1})	Ks (mg/L)
Methylene Blue	*Pseudomonas sp.*	0.919	22.07

6.10. Toxicity analysis:

Toxicity analysis is a critical aspect of ensuring the safety and efficacy of adsorbents for various applications, including environmental remediation, water treatments, and industrial processes (Burgess, Robert M., et al., 2013). Adsorbents are substances capable of attracting and binding to other molecules or particles onto their surface (Ruthven, Douglas M., 1984). The introduction of new adsorbents into these applications requires thorough evaluation to determine their potential impact on human health, the environment, and non-target organisms (Neagu, Monica, et al., 2023; Kong, Hao, et al., 2022). Toxicity tests assess the adverse effects of adsorbents and any leachable substances they may release. These tests involve exposing relevant biological systems, such as cell cultures, aquatic organisms or soil micro-organisms, to the adsorbent or its leachates and monitoring for changes in growth, viability, physiological functions, and genetic integrity. By conducting comprehensive toxicity test there are various methods but out of them experimental analysis based on germination of seeds is most important because of easy accessibility and process simplicity.

6.10.1. Toxicological analysis based on germination of Moong Dal (*Vigna radiata*) seeds:

The toxicological analysis based on seed germination is a significant measure in plant neology, reflecting the allocation of biomass between roots and shoots and germination rate of seed in presence of solution containing pollutants. It's often indicative of a plant's adaptation to its environment, resource availability, and growth strategies (Cheung, Y. H.et al., 1989).

Pollutant solution can significantly impede the germination process of seed by disrupting essential physiological processes critical for early plant growth. These solutions containing various pollutants viz. various dyes, organic pollutants and heavy metals. Upon exposure,

seeds may experience reduced water uptake , altered enzymatic activity, and oxidative stress, all of which inhibit germination. Heavy metals can interfere with cellular metabolism and cause structural damage to cellular components, while organic pollutants may disrupt hormonal balance crucial for germination initiation. Consequently, the presence of pollutants solutions in the germination environment can severely diminish seed viability and compromise overall plant establishment, highlighting the detrimental impact of pollutants on seeding development and ecosystem health.

However, the root-to-shoot ratio of the seed can show the presence of nutrition in water solution. Presence of low-nutrient medium, where the plant invests more in root development to forage for resources (Agathokleous, E. et al, 2019). Conversely, a low root-to-shoot ratio indicates a high nutrient medium. Even it can indicate the presence of any toxic agents in the solution used for seed germination. It is also seen in the case of pollutant removal by the adsorption process seed germination process is delayed or sometimes permanently inhibited because of the production of many by-products or the release of toxic fillers from the adsorbent structure (Shahnaz, Tasrin, et al., 2022). This process also indicates the interaction of micro-organisms with the adsorbents in the bacterial doping process as weak interaction releases microbes in the solution used for seed germination which may alter the root-to-shoot ratio (Asati et al, 2024).

In Table 17: The effect of the pollutants on the seed germination are determined based on Moong Dal seeds using pollutants viz. Congo Red, Methylene Blue, Pyrene and Anthracene. Environmental condition is kept optimal and suitable for seed germination viz. Temp-30^0C, pH-7, concentration of Pollutants 10mg/L, and Dose of the adsorbent is 1g/L of the pollutants sample. Along with data is compared with the data from the seed germination in normal water. However, fungal growth is prevented by 4% of Sodium Hypochlorite solution by which seeds were pretreated and washed vigorously to remove excess antifungal chemicals present in the seed sample (Şen, B. H. et al., 1999). And Form

the Table 17. It can be easily determined that due to use of the microbes immobilized aerogels as adsorbents during the process of adsorption and also present of bioremediation for biodegradation pollutants cause low toxic effects on moong seeds during the germination process. And from the data represented in Table 17. It can be easily determined that the due to biodegradation of pollutants using Micro-organisms and adsorption by aerogel the effect on the germination of seeds are reduced which enhance the root and shoot length along with germination rate, and these values are quite opposite in control solution (without the presence of bacteria-doped aerogel).

Table 17. Toxicity analysis of bacteria immobilized PVA and its derivatives aerogel on germination process of Moong seeds.

Micro-organism used in immobilized aerogel	Pollutants	Germinated rate (%)	Root length (cm)	Shoot Length (cm)	Seedling length (cm)	Root-shoot Ratio index	Seed vigor Index
Bacillus subtilis	Congo Red	50	1	0.4	1.4	5:2	85
	Methylene Blue	60	1.3	0.9	2.2	13:9	114
	Pyrene	40	1.2	0.1	1.3	12:1	52
	Anthracene	50	1.2	0.3	1.5	4:1	75
Pseudomonas sp.	Congo Red	80	1.6	0.9	2.5	16:9	200
	Methylene Blue	60	1.5	0.5	2.0	3:1	120
	Pyrene	40	1.5	0.2	1.7	15:2	68
	Anthracene	50	1.7	0.3	2.0	17:3	100

Water Microorganism	Congo Red	50	1.5	0.9	2.4	5:3	120
	Methylene Blue	80	1	0.5	1.5	2:1	120
	Pyrene	30	1.3	0.2	1.5	13:2	45
	Anthracene	40	1.4	0.3	1.7	14:3	56
Soil Microorganism	Congo Red	90	1.6	0.7	2.3	16:7	207
	Methylene Blue	70	1.3	0.5	1.8	13:5	126
	Pyrene	50	1.1	0.3	1.4	11:3	70
	Anthracene	60	1.5	0.4	1.9	15:4	114
Control*	Congo Red	70	0.8	0	0.8	_	49
	Methylene Blue	70	0.4	0.1	0.5	4:1	35
	Pyrene	40	0.2	0.1	0.3	2:1	12
	Anthracene	60	0.3	0.1	0.4	3:1	24
	Water (no pollutants)	90	4.5	3.2	7.7	45:32	693

* Without presence of any immobilized Aerogel

Chapter 7: Conclusion and Future Perspective

7. Conclusion and Future Perspective

Following the increasing amount of waste-biomass generation, it is necessary to study the removal of such pollutants from wastewater to maintain eco-system balance. In this study, PVA and its derivatives aerogel immobilized with micro-organism was evaluated as a potential-adsorbents in removal of various types of soluble waste from aqueous solution. Without bacterial immobilization, PVA Aerogels showed the less removal throughout the process. But after doping with bacterial strain, the removal efficiency increases vigorously. Characterization results revealed successful surface chemistry modification for the Aerogels, while little change in structural properties. Due to encapsulation of bioremediation and adsorption process simultaneously effect the removal percentages of pollutants from aqueous solution. Freundlich isotherm model and pseudo-second order kinetics model fitted well to the data of PVA and its derivatives aerogels adsorption data on the removal of the pollutants. The thermodynamics analysis suggested that the removal processes are spontaneous and exothermic to nature with the entrapped bacteria can grow maintaining Monod Kinetics throughout the process giving higher removal percentages than normal aerogel adsorption and using of only bioremediation. This study shows that the immobilizing of microbes is a simple cost-effective method to enhance the adsorption performance of soluble waste removal process. Furthermore, finding cost-effective strategies in the fields of storage and reusability of used adsorbents are other important issues for the future studies. In the way, the safe and economical disposal/reuse of used adsorbents should be considered in future investigations. It is possible to use raw materials and refining materials instead to expensive commercial materials to prepare more economically and environmentally viable production with negligible amount of hazard generation.

References

1. Nagar, A. & Pradeep, T. Clean water through nanotechnology: Needs, gaps, and fulfillment. *ACS Nano* **14**, 6420–6435 (2020).
2. Moussavi, G., Pourakbar, M., Aghayani, E. & Mahdavianpour, M. Investigating the aerated VUV/PS process simultaneously generating hydroxyl and sulfate radicals for the oxidation of cyanide in aqueous solution and industrial wastewater. *Chem. Eng. J.* **350**, 673–680 (2018).
3. Roshan, A. & Kumar, M. Water end-use estimation can support the urban water crisis management: A critical review. *J. Environ. Manage.* **268**, 110663 (2020).
4. Amaly, N., El-Moghazy, A. Y., Nitin, N., Sun, G. & Pandey, P. K. Synergistic adsorption-photocatalytic degradation of tetracycline by Combined treated Cellulose composite aerogel doped with montmorillonite hosted methylene blue. *Chem. Eng. J.* **430**, 133077 (2022).
5. Ma, J. *et al.* Comparative study of graphene hydrogels and aerogels reveals the important role of buried water in pollutant adsorption. *Environ. Sci. Technol.* **51**, 12283–12292 (2017).
6. Prabha, S., Gogoi, A., Mazumder, P., Ramanathan, A. & Kumar, M. Assessment of the impact of textile effluents on microbial diversity in Tirupur district, Tamil Nadu. *Appl. Water Sci.* **7**, 2267–2277 (2017).
7. Gogoi, A. *et al.* Occurrence and fate of emerging contaminants in water environment: A review. *Groundw. Sustain. Dev.* **6**, 169–180 (2018).
8. Rathi, B. S. & Kumar, P. S. Application of adsorption process for effective removal of emerging contaminants from water and wastewater. *Environ. Pollut.* **280**, 116995 (2021).

9. Kumar, M. *et al.* Review of perspective, problems, challenges, and future scenario of metal contamination in the urban environment. *J. Hazard. Toxic Radioact. Waste* **21**, 1–16 (2017).
10. Parmar, B., Bisht, K. K., Rajput, G. & Suresh, E. Recent advances in metal-organic frameworks as adsorbent materials for hazardous dye molecules. *Dalt. Trans.* **50**, 3083–3108 (2021).
11. Wan, Y. *et al.* Ionic liquid groups modified 3D porous cellulose microspheres for selective adsorption of AO7 dye. *J. Clean. Prod.* **240**, 118201 (2019).
12. Bani-Atta, S. A. Potassium permanganate dye removal from synthetic wastewater using a novel, low-cost adsorbent, modified from the powder of *Foeniculum vulgare* seeds. *Sci. Rep.* **12**, 1–13 (2022).
13. Wang, S., Zhang, Q., Wang, Z. & Pu, J. Facile fabrication of an effective nanocellulose-based aerogel and removal of methylene blue from aqueous system. *J. Water Process Eng.* **37**, 101511 (2020).
14. Drumond Chequer, F. M. *et al.* Textile dyes: Dyeing process and environmental impact eco-friendly text. *Dye. Finish.*
15. Chowdhury, S., Mishra, R., Saha, P. & Kushwaha, P. Adsorption thermodynamics, kinetics and isosteric heat of adsorption of malachite green onto chemically modified rice husk. *Desalination* **265**, 159–168 (2011).
16. Geyikçi, F., Kiliç, E., Çoruh, S. & Elevli, S. Modelling of lead adsorption from industrial sludge leachate on red mud by using RSM and ANN. *Chem. Eng. J.* **183**, 53–59 (2012).
17. Hassani, A., Khataee, A., Karaca, S., Karaca, M. & Kiranşan, M. Adsorption of two cationic textile dyes from water with modified nanoclay: A comparative study by using central composite design. *J. Environ. Chem. Eng.* **3**, 2738–2749 (2015).

18. Mohammed, N., Grishkewich, N. & Tam, K. C. Cellulose nanomaterials: Promising sustainable nanomaterials for application in water/wastewater treatment processes. *Environ. Sci. Nano* **5**, 623–658 (2018).
19. Zhang, L., Yang, L., Xu, Y. & Chang, G. Renewable 4-HIF/NaOH aerogel for efficient methylene blue removal: Via cation-π interaction induced electrostatic interaction. *RSC Adv.* **9**, 29772–29778 (2019).
20. Chen, Y. *et al.* Ultralight aerogel based on molecular-modified poly(:M-phenylenediamine) crosslinking with polyvinyl alcohol/graphene oxide for flow adsorption. *RSC Adv.* **9**, 22950–22956 (2019).
21. Ganesamoorthy, R., Vadivel, V. K., Kumar, R., Kushwaha, O. S. & Mamane, H. Aerogels for water treatment: A review. *J. Clean. Prod.* **329**, 129713 (2021).
22. Malika, M. & Sonawane, S. S. Statistical modelling for the Ultrasonic photodegradation of Rhodamine B dye using aqueous based Bi-metal doped TiO2 supported montmorillonite hybrid nanofluid via RSM. *Sustain. Energy Technol. Assess.* **44**, 100980 (2021).
23. Liu, M. *et al.* Luminescent cellulose-based porous binary metal-organic gels in an adsorption bed for effective adsorption and sensitive detection of chlortetracycline hydrochloride. *J. Hazard. Mater.* **414**, 125473 (2021).
24. Priya, *et al.* RSM-CCD optimized sodium alginate/gelatin based ZnS-nanocomposite hydrogel for the effective removal of biebrich scarlet and crystal violet dyes. *Int. J. Biol. Macromol.* **129**, 214–226 (2019).
25. Liu, Y., Wang, J., Zheng, Y. & Wang, A. Adsorption of methylene blue by kapok fiber treated by sodium chlorite optimized with response surface methodology. *Chem. Eng. J.* **184**, 248–255 (2012).

26. Barrios, E., Fox, D., Li Sip, Y. Y., Catarata, R., Calderon, J. E., Azim, N., et al. (2019). Nanomaterials in advanced, high-performance aerogel composites: a review. *Polymers* 11:726. doi: 10.3390/polym11040726.
27. Nita, L. E., Ghilan, A., Rusu, A. G., Neamtu, I., and Chiriac, A. P. (2020). New trends in bio-based aerogels. *Pharmaceutics* 12:449. doi: 10.3390/pharmaceutics12050449.
28. Katti, A., Shimpi, N., Roy, S., Lu, H., Fabrizio, E. F., Dass, A., et al. (2006). Chemical, physical, and mechanical characterization of isocyanate cross-linked amine-modified silica aerogels. *Chem. Mater.* 18, 285–296. doi: 10.1021/cm0513841.
29. Novak, B. M., Auerbach, D., and Verrier, C. (1994). Low-density, mutually interpenetrating organic-inorganic composite materials via supercritical drying techniques. *Chem. Mater.* 6, 282–286. doi: 10.1021/cm00039a006.
30. Mehrotra, Tithi, et al. "Use of immobilized bacteria for environmental bioremediation: A review." *Journal of Environmental Chemical Engineering* 9.5 (2021): 105920.
31. Singh, Rachana, and B. B. Prasad. "Trace metal analysis: selective sample (copper II) enrichment on an AlgaSORB column." *Process Biochemistry* 35.9 (2000): 897-905.
32. Kang, Moon-Sung, et al. "Highly charged proton exchange membranes prepared by using water soluble polymer blends for fuel cells." *Journal of Membrane Science* 247.1-2 (2005): 127-135.
33. Baksi, Sibashish, et al. "Studies on delignification and inhibitory enzyme kinetics of alkaline peroxide pre-treated pine and deodar sawdust." *Chemical Engineering and Processing-Process Intensification* 143 (2019): 107607.

34. Jenkins, R. W.; Sutton, A. D.; Robichaud, D. J. (2016-01-01), Chuck, Christopher J. (ed.), "Chapter 8 - Pyrolysis of Biomass for Aviation Fuel", *Biofuels for Aviation*, Academic Press, pp. 191–215, ISBN 978-0-12-804568-8, retrieved 2023-12-12.
35. Cory A. Kramer, Reza Loloee, Indrek S. Wichman and Ruby N. Ghosh, 2009, Time Resolved Measurements of Pyrolysis Products From Thermoplastic Poly-Methyl-Methacrylate (PMMA) Archived 2014-11-06 at the Wayback Machine *ASME 2009 International Mechanical Engineering Congress and Exposition*
36. Kistler, Samuel Stephens. "Coherent expanded aerogels and jellies." *Nature* 127.3211 (1931): 741-741.
37. Geyikçi, Feza, et al. "Modelling of lead adsorption from industrial sludge leachate on red mud by using RSM and ANN." *Chemical Engineering Journal* 183 (2012): 53-59.
38. Lankin, A.V., Kreslavski, V.D., Khudyakova, A.Y. *et al.* Effect of naphthalene on photosystem 2 photochemical activity of pea plants. *Biochemistry Moscow* **79**, 1216–1225 (2014). https://doi.org/10.1134/S0006297914110091.
39. Frank, Richard G., Rena M. Conti, and Howard H. Goldman. "Mental health policy and psychotropic drugs." *The Milbank Quarterly* 83.2 (2005): 271-298.
40. Cohen Ph. D, Maimon M. "The interaction of various drugs with human chromosomes." *Canadian Journal of Genetics and Cytology* 11.1 (1969): 1-24.
41. Bishop, Felicity L., and Lucy Yardley. "Constructing agency in treatment decisions: Negotiating responsibility in cancer." *Health:* 8.4 (2004): 465-482.
42. Pignatti, Francesco, et al. "The– European Medicines Agency: an overview of its mission, responsibilities, and recent initiatives in cancer drug regulation." *Clinical Cancer Research* 17.16 (2011): 5220-5225.
43. Kumar, M. Dinesh, and Vishwa Ballabh. "Water management problems and challenges in India: an analytical review." (2000): 32-pp.

44. Alamgir, Jalal (2008). *India's Open-Economy Policy: Globalism, Rivalry, Continuity*. Routledge. p. 176. ISBN 978-1-135-97056-7.

45. Kanungo, Rama P.; Rowley, Chris; Banerjee, Anurag N. (2018). *Changing the Indian Economy: Renewal, Reform and Revival*. *Elsevier*. p. 24. *ISBN 978-0-08-102014-2*.*[permanent dead link]*

46. Chakraborti, Dipankar, Bhaskar Das, and Matthew T. Murrill. "Examining India's groundwater quality management." (2011): 27-33.

47. Mousavi, Sara, et al. "Efficient dye adsorption by highly porous nanofiber aerogels." *Colloids and Surfaces A: Physicochemical and Engineering Aspects* 547 (2018): 117-125.

48. Blanket, Particle, Panel, Monolith), By Product (Silica, Carbon, Polymers), By End Use, By Technology, By Region, And Segment Forecasts. [(accessed on 21 February 2020)]; Available online: https://www.researchandmarkets.com/reports/4613368/aerogel-market-size-share-and-trends-analysis#rela4-4894101.

49. Zuo L., Zhang Y., Zhang L., Miao Y.-E., Fan W., Liu T. Polymer/carbon-based hybrid aerogels: Preparation, properties and applications. *Materials.* 2015;8:6806–6848. doi: 10.3390/ma8105343.

50. De Oliveira J.P., Bruni G.P., El Halal S.L.M., Bertoldi F.C., Dias A.R.G., Zavareze E.D.R. Cellulose nanocrystals from rice and oat husks and their application in aerogels for food packaging. *Int. J. Biol. Macromol.* 2019; 124:175–184.

51. Gurav, Jyoti L., et al. "Silica aerogel: synthesis and applications." *Journal of Nanomaterials* 2010 (2010): 1-11.

52. Sheng, Zhizhi, et al. "The rising aerogel fibers: status, challenges, and opportunities." *Advanced Science* 10.9 (2023): 2205762.

53. Goryunova, Kristina, Yunis Gahramanli, and Rena Gurbanova. "Adsorption properties of silica aerogel-based materials." *RSC advances* 13.27 (2023): 18207-18216.
54. Pete, Amber J., et al. "Chitosan-Coated Lignin Nanoparticles Enhance Adsorption and Proliferation of Alcanivorax borkumensis at the Hexadecane–Water Interface." *ACS ES&T Engineering* 3.9 (2023): 1339-1349.
55. Ihsanullah, Ihsanullah, et al. "Bioremediation of dyes: Current status and prospects." *Journal of Water Process Engineering* 38 (2020): 101680.
56. Hüsing, Nicola, and Ulrich Schubert. "Aerogele–luftige materialien: chemie, struktur und eigenschaften." *Angewandte Chemie* 110.1-2 (1998): 22-47.
57. Lee, Kun-Hong, Sun-Young Kim, and Ki-Poong Yoo. "Low-density, hydrophobic aerogels." *Journal of Non-Crystalline Solids* 186 (1995): 18-22.
58. Zheng, Qifeng, et al. "Highly porous polymer aerogel film-based triboelectric nanogenerators." *Advanced Functional Materials* 28.13 (2018): 1706365.
59. Dorcheh, A. Soleimani, and M. H. Abbasi. "Silica aerogel; synthesis, properties, and characterization." *Journal of materials processing technology* 199.1-3 (2008): 10-26.
60. Lu, Hong, et al. "Degradable composite aerogel with excellent water-absorption for trace water removal in oil and oil-in-water emulsion filtration." *Frontiers I.*
61. Zhang, Yongmin, et al. "Eco-friendly ferrocene-functionalized chitosan aerogel for efficient dye degradation and phosphate adsorption from wastewater." *Chemical engineering journal* 439 (2022): 135605.
62. E.A. Clarke, R. Anliker, Organic dyes and pigments Anthropogenic Compounds, Springer Berlin Heidelberg (1980), pp. 181-215.
63. Hunger, Klaus, ed. *Industrial dyes: chemistry, properties, applications*. John Wiley & Sons, 2007.

64. Djilani, Chahrazed, et al. "Adsorption of dyes on activated carbon prepared from apricot stones and commercial activated carbon." *Journal of the Taiwan Institute of Chemical Engineers* 53 (2015): 112-121.

65. Yagub, Mustafa T., et al. "Dye and its removal from aqueous solution by adsorption: a review." *Advances in colloid and interface science* 209 (2014): 172-184.

66. Rápó E., Szép R., Keresztesi Á., Suciu M., Tonk S. Adsorptive Removal of Cationic and Anionic Dyes from Aqueous Solutions by Using Eggshell Household Waste as Biosorbent. *Acta Chim. Slov.* 2018;65:709–717. doi: 10.17344/acsi.2018.4401.

67. Brito M.J., Veloso C.M., Santos L.S., Bonomo R.C., Fontan R.D. Adsorption of the Textile Dye Dianix® Royal Blue CC onto Carbons Obtained from Yellow Mombin Fruit Stones and Activated with KOH and H_3PO_4: Kinetics, Adsorption Equilibrium and Thermodynamic Studies. *Powder Technol.* 2018;339:334–343. doi: 10.1016/j.powtec.2018.08.017.

68. Kanwal A., Bhatti H.N., Iqbal M., Noreen S. Basic Dye Adsorption onto Clay/$MnFe_2O_4$ Composite: A Mechanistic Study. *Water Environ. Res.* 2017;89:301–311. doi: 10.2175/106143017X14839994522984.

69. Khasri A., Jamir M.R.M., Ahmad A.A., Ahmad M.A. Adsorption of Remazol Brilliant Violet 5R Dye from Aqueous Solution onto Melunak and Rubberwood Sawdust Based Activated Carbon: Interaction Mechanism, Isotherm, Kinetic and Thermodynamic Properties. *DWT.* 2021;216:401–411. doi: 10.5004/dwt.2021.26852.

70. Yeow P.K., Wong S.W., Hadibarata T. Removal of Azo and Anthraquinone Dye by Plant Biomass as Adsorbent—A Review. *Biointerface Res. Appl. Chem.* 2020;11:8218–8232. doi: 10.33263/BRIAC111.82188232.

71. Badawy A.A., Ibrahim S.M., Essawy H.A. Enhancing the Textile Dye Removal from Aqueous Solution Using Cobalt Ferrite Nanoparticles Prepared in Presence of Fulvic

Acid. *J. Inorg. Organomet. Polym.* 2020;30:1798–1813. doi: 10.1007/s10904-019-01355-1.

72. Szende T., Eszter R. *Környezeti Szennyezők, Környezeti Problémák, Környezeti Remediáció.* 1st ed. EXIT Kiadó; Cluj Napoca, Romania: 2020.
73. Şentürk İ., Alzein M. Adsorption of Acid Violet 17 Onto Acid-Activated Pistachio Shell: Isotherm, Kinetic and Thermodynamic Studies. *Acta Chim. Slov.* 2020;67:55–69. doi: 10.17344/acsi.2019.5195.
74. Pernyeszi T., Farkas R., Kovács J. Methylene Blue Adsorption Study on Microcline Particles in the Function of Particle Size Range and Temperature. *Minerals.* 2019;9:555. doi: 10.3390/min9090555.
75. Ma C.M., Hong G.B., Wang Y.K. Performance Evaluation and Optimization of Dyes Removal Using Rice Bran-Based Magnetic Composite Adsorbent. *Materials.* 2020;13:2764. doi: 10.3390/ma13122764.
76. Neag E., Moldovan A., Băbălău-Fuss V., Török A., Cadar O., Roman C. Kinetic, Equilibrium and Phytotoxicity Studies for Dyes Removal by Low Cost Natural Activated Plant-Based Carbon. *Acta Chim. Slov.* 2019;66:850–858. doi: 10.17344/acsi.2018.4924.
77. Esmaeili H., Foroutan R., Jafari D., Aghil Rezaei M. Effect of Interfering Ions on Phosphate Removal from Aqueous Media Using Magnesium Oxide@ferric Molybdate Nanocomposite. *Korean J. Chem. Eng.* 2020;37:804–814. doi: 10.1007/s11814-020-0493-6.
78. Salahshour R., Shanbedi M., Esmaeili H. Methylene Blue Dye Removal from Aqueous Media Using Activated Carbon Prepared by Lotus Leaves: Kinetic, Equilibrium and Thermodynamic Study. *Acta Chim. Slov.* 2021;68:363–373. doi: 10.17344/acsi.2020.6311.

79. Popa S., Radulescu-Grad M.E., Perdivara A., Mosoarca G. Aspects Regarding Colour Fastness and Adsorption Studies of a New Azo-Stilbene Dye for Acrylic Resins. *Sci. Rep.* 2021;11:5889. doi: 10.1038/s41598-021-85452-7.

80. Rápó E., Aradi L.E., Szabó Á., Posta K., Szép R., Tonk S. Adsorption of Remazol Brilliant Violet-5R Textile Dye from Aqueous Solutions by Using Eggshell Waste Biosorbent. *Sci. Rep.* 2020;10:8385. doi: 10.1038/s41598-020-65334-0.

81. Rápó E., Posta K., Suciu M., Szép R., Tonk S. Adsorptive Removal of Remazol Brilliant Violet-5R Dye from Aqueous Solutions Using Calcined Eggshell as Biosorbent. *Acta Chim. Slov.* 2019;66:648–658. doi: 10.17344/acsi.2019.5079.

82. Hamza W., Dammak N., Hadjltaief H.B., Eloussaief M., Benzina M. Sono-Assisted Adsorption of Cristal Violet Dye onto Tunisian Smectite Clay: Characterization, Kinetics and Adsorption Isotherms. *Ecotoxicol. Environ. Saf.* 2018;163:365–371. doi: 10.1016/j.ecoenv.2018.07.021.

83. Fan, K., Zhang, T., Xiao, S., He, H., Yang, J., & Qin, Z. (2022). Preparation and adsorption performance of functionalization cellulose-based composite aerogel. *International Journal of Biological Macromolecules*, *211*, 1-14.

84. Yagub M.T., Sen T.K., Afroze S., Ang H.M. Dye and Its Removal from Aqueous Solution by Adsorption: A Review. *Adv. Colloid Interface Sci.* 2014;209:172–184. doi: 10.1016/j.cis.2014.04.002.

85. Terangpi P., Chakraborty S. Adsorption Kinetics and Equilibrium Studies for Removal of Acid Azo Dyes by Aniline Formaldehyde Condensate. *Appl. Water Sci.* 2017;7:3661–3671. doi: 10.1007/s13201-016-0510-4.

86. Al-Ghouti M.A., Al-Absi R.S. Mechanistic Understanding of the Adsorption and Thermodynamic Aspects of Cationic Methylene Blue Dye onto Cellulosic Olive Stones Biomass from Wastewater. *Sci. Rep.* 2020;10:15928. doi: 10.1038/s41598-020-72996-3.

87. . Seow T.W., Lim C.K. Removal of Dye by Adsorption: A Review. *Int. J. Appl. Eng. Res.* 2016;11:2675–2679.

88. de Farias Silva C.E., da Gama B.M., da Silva Gonçalves A.H., Medeiros J.A., de Souza Abud A.K. Basic-Dye Adsorption in Albedo Residue: Effect of PH, Contact Time, Temperature, Dye Concentration, Biomass Dosage, Rotation and Ionic Strength. *J. King Saud Univ.-Eng. Sci.* 2020;32:351–359.

89. Rodríguez-Arellano G., Barajas-Fernández J., García-Alamilla R., Lagunes-Gálvez L.M., Lara-Rivera A.H., García-Alamilla P. Evaluation of Cocoa Beans Shell Powder as a Bioadsorbent of Congo Red Dye Aqueous Solutions. *Materials.* 2021;14:2763. doi: 10.3390/ma14112763.

90. Benkhaya B., Harfi S.E., Harfi A.E. Classifications, Properties and Applications of Textile Dyes: A Review. *Appl. J. Environ. Eng. Sci.* 2017;3:311–320.

91. Katheresan V., Kansedo J., Lau S.Y. Efficiency of Various Recent Wastewater Dye Removal Methods: A Review. *J. Environ. Chem. Eng.* 2018;6:4676–4697.

92. Farouk R., Gaffer H.E. Simultaneous Dyeing and Antibacterial Finishing for Cotton Cellulose Using a New Reactive Dye. *Carbohydr. Polym.* 2013;97:138–142.

93. Labanda J., Sabaté J., Llorens J. Modeling of the Dynamic Adsorption of an Anionic Dye through Ion-Exchange Membrane Adsorber. *J. Membr. Sci.* 2009;340:234–240. doi: 10.1016/j.memsci.2009.05.036.

94. Prol A.E.A. Study of Environmental Concerns of Dyes and Recent Textile Effluents Treatment Technology: A Review. *Asian J. Fish. Aquat. Res.* 2019;3:1–18. doi: 10.9734/ajfar/2019/v3i230032.

95. Rachakornkij M., Sirawan R., Sumate T. Removal of Reactive Dyes from Aqueous Solution Using Bagasse Fly Ash. *Songklanakarin J. Sci. Technol.* 2004;26:13–24.

96. Lazaridis N.K., Karapantsios T.D., Georgantas D. Kinetic Analysis for the Removal of a Reactive Dye from Aqueous Solution onto Hydrotalcite by Adsorption. *Water Res.* 2003;37:3023–3033. doi: 10.1016/S0043-1354(03)00121-0.

97. Easton R. The dye maker's view. In: Cooper P., editor. *Colour in Dyehouse Effluents.* The Aldren Press; Bradford, UK: 1995. pp. 9–21.

98. Vijayaraghavan K., Won S.W., Yun Y.-S. Treatment of Complex Remazol Dye Effluent Using Sawdust- and Coal-Based Activated Carbons. *J. Hazard. Mater.* 2009;167:790–796. doi: 10.1016/j.jhazmat.2009.01.055.

99. Hassaan M.A., El Nemr A., Madkour F.F. Testing the Advanced Oxidation Processes on the Degradation of Direct Blue 86 Dye in Wastewater. *Egypt. J. Aquat. Res.* 2017;43:11–19. doi: 10.1016/j.ejar.2016.09.006.

100. Irshad S., Sultana H., Usman M., Saeed M., Akram N., Yusaf A., Rehman A. Solubilization of Direct Dyes in Single and Mixed Surfactant System: A Comparative Study. *J. Mol. Liq.* 2021;321:114201. doi: 10.1016/j.molliq.2020.114201.

101. Horng J.Y., Huang S.D. Removal of Organic Dye (Direct Blue) from Synthetic Wastewater by Adsorptive Bubble Separation Techniques. *Environ. Sci. Technol.* 1993;27:1169–1175. doi: 10.1021/es00043a017.

102. Benkhaya B., Harfi S.E., Harfi A.E. Classifications, Properties and Applications of Textile Dyes: A Review. *Appl. J. Environ. Eng. Sci.* 2017;3:311–320. doi: 10.48422/IMIST.PRSM/ajees-v3i3.9681.

103. Benkhaya S., M'rabet S., El Harfi A. A Review on Classifications, Recent Synthesis and Applications of Textile Dyes. *Inorg. Chem. Commun.* 2020;115:107891. doi: 10.1016/j.inoche.2020.107891.

104. Wu J., Li Q., Li W., Li Y., Wang G., Li A., Li H. Efficient Removal of Acid Dyes Using Permanent Magnetic Resin and Its Preliminary Investigation for Advanced

Treatment of Dyeing Effluents. *J. Clean. Prod.* 2020;251:119694. doi: 10.1016/j.jclepro.2019.119694.

105. Raval N.P., Shah P.U., Shah N.K. Malachite Green “a Cationic Dye” and Its Removal from Aqueous Solution by Adsorption. *Appl. Water Sci.* 2017;7:3407–3445. doi: 10.1007/s13201-016-0512-2.

106. Hessel C., Allegre C., Maisseu M., Charbit F., Moulin P. Guidelines and Legislation for Dye House Effluents. *J. Environ. Manag.* 2007;83:171–180. doi: 10.1016/j.jenvman.2006.02.012.

107. Singh P.K., Singh R.L. Bio-Removal of Azo Dyes: A Review. *Int. J. Appl. Sci. Biotechnol.* 2017;5:108–126. doi: 10.3126/ijasbt.v5i2.16881.

108. Chikri R., Elhadiri N., Benchanaa M., El Maguana Y. Efficiency of Sawdust as Low-Cost Adsorbent for Dyes Removal. *J. Chem.* 2020;2020:e8813420. doi: 10.1155/2020/8813420.

109. Crini G. Non-Conventional Low-Cost Adsorbents for Dye Removal: A Review. *Bioresour. Technol.* 2006;97:1061–1085. doi: 10.1016/j.biortech.2005.05.001.

110. Katheresan V., Kansedo J., Lau S.Y. Efficiency of Various Recent Wastewater Dye Removal Methods: A Review. *J. Environ. Chem. Eng.* 2018;6:4676–4697. doi: 10.1016/j.jece.2018.06.060.

111. Samsami S., Mohamadizaniani M., Sarrafzadeh M.-H., Rene E.R., Firoozbahr M. Recent Advances in the Treatment of Dye-Containing Wastewater from Textile Industries: Overview and Perspectives. *Process Saf. Environ. Prot.* 2020;143:138–163. doi: 10.1016/j.psep.2020.05.034.

112. Ghoreishi S, Haghighi R. Chemical catalytic reaction and biological oxidation for treatment of non-biodegradable textile effluent. Chem Eng J 2003;95(1):163–9.

113. Bhatia D., Sharma N.R., Singh J., Kanwar R.S. Biological Methods for Textile Dye Removal from Wastewater: A Review. *Crit. Rev. Environ. Sci. Technol.* 2017;47:1836–1876. doi: 10.1080/10643389.2017.1393263.

114. Madhav S., Ahamad A., Singh P., Mishra P.K. A Review of Textile Industry: Wet Processing, Environmental Impacts, and Effluent Treatment Methods. *Environ. Qual. Manag.* 2018;27:31–41. doi: 10.1002/tqem.21538.

115. Bhardwaj D., Bharadvaja N. Phycoremediation of Effluents Containing Dyes and Its Prospects for Value-Added Products: A Review of Opportunities. *J. Water Process Eng.* 2021;41:102080. doi: 10.1016/j.jwpe.2021.102080.

116. Choudhary A. Removal of Oil from Seawater Using Charcoal and Rice Hull. *IOP Conf. Ser. Mater. Sci. Eng.* 2017;263:032007. doi: 10.1088/1757-899X/263/3/032007.

117. Tan K.L., Hameed B.H. Insight into the Adsorption Kinetics Models for the Removal of Contaminants from Aqueous Solutions. *J. Taiwan Inst. Chem. Eng.* 2017;74:25–48. doi: 10.1016/j.jtice.2017.01.024.

118. Abebe B., Murthy H.C.A., Amare E. Summary on Adsorption and Photocatalysis for Pollutant Remediation: Mini Review. *J. Encapsul. Adsorpt. Sci.* 2018;8:225–255. doi: 10.4236/jeas.2018.84012.

119. Qi Y., Zhu J., Fu Q., Hu H., Huang Q. Sorption of Cu by Humic Acid from the Decomposition of Rice Straw in the Absence and Presence of Clay Minerals. *J. Environ. Manag.* 2017;200:304–311. doi: 10.1016/j.jenvman.2017.05.087.

120. Sims R.A., Harmer S.L., Quinton J.S. The Role of Physisorption and Chemisorption in the Oscillatory Adsorption of Organosilanes on Aluminium Oxide. *Polymers.* 2019;11:410. doi: 10.3390/polym11030410.

121. Al-Ghouti M.A., Da'ana D.A. Guidelines for the Use and Interpretation of Adsorption Isotherm Models: A Review. *J. Hazard. Mater.* 2020;393:122383. doi: 10.1016/j.jhazmat.2020.122383.
122. Ruthven D.M. *Principles of Adsorption and Adsorption Processes.* John Wiley & Sons; New York, NY, USA: 1984.
123. Kamaya Parashar Adsorption, Presentation at University of Johannesburg. [(accessed on 3 September 2021)];2015 Available online: https://www.slideshare.net/Kamyaparashar/adsorption-presentation-44669901 [Ref list]
124. Terry P.A., Noble R.D., editors. *Principles of Chemical Separations with Environmental Applications.* Cambridge University Press; Cambridge, UK: 2004. Adsorption; pp. 182–213. (Cambridge Series in Chemical Engineering).
125. Guo X., Wang J. A General Kinetic Model for Adsorption: Theoretical Analysis and Modeling. *J. Mol. Liq.* 2019;288:111100. doi: 10.1016/j.molliq.2019.111100.
126. Al-Ghouti M.A., Da'ana D.A. Guidelines for the Use and Interpretation of Adsorption Isotherm Models: A Review. *J. Hazard. Mater.* 2020;393:122383. doi: 10.1016/j.jhazmat.2020.122383.
127. Adsorption Techniques|EMIS. [(accessed on 28 July 2021)]; Available online: https://emis.vito.be/en/bat/tools-overview/sheets/adsorption-techniques [Ref list].
128. Erkey, Can. "Synthesis of nanostructured composites of metals." *Supercritical fluid science and technology*. Vol. 1. Elsevier, 2011. 79-120.
129. Kreek, Kristiina, et al. "Preparation of metal-doped carbon aerogels from oil shale processing by-products." *Oil Shale* 31.2 (2014): 185.
130. Lee, Jong-Hoon, and Soo-Jin Park. "Recent advances in preparations and applications of carbon aerogels: A review." *Carbon* 163 (2020): 1-18.

131. J.M. Lynch, A.J. Moffat, Bioremediation–prospects for the future application of innovative applied biological research, Ann. Appl. Biol. 146 (2005) 217–221.

132. K. Vikrant, B.S. Giri, N. Raza, K. Roy, K.-H. Kim, B.N. Rai, R.S. Singh, Recent advancements in bioremediation of dye: current status and challenges, Bioresour. Technol. 253 (2018) 355–367, https://doi.org/10.1016/j.biortech.2018.01.029.

133. Topp E, Vallayes T and Soulas G (1997) Pesticides: Microbial degradation and effects on microorganisms. In: Modern soil microbiology. Van Elsas JD Trevors JT and Wellington EMH (eds.). Mercel Dekker, Inc. New York. USA. Pp. 547–575.

134. Bosco, Francesca, Antonio Capolongo, and Bernardo Ruggeri. "Effect of temperature, pH, ionic strength, and sodium nitrate on activity of LiPs: Implications for bioremediation." *Bioremediation journal* 6.1 (2002): 65-76.

135. Iqbal, Javed, Caroline Metosh-Dickey, and Ralph J. Portier. "Temperature effects on bioremediation of PAHs and PCP contaminated south Louisiana soils: a laboratory mesocosm study." *Journal of Soils and Sediments* 7 (2007): 153-158.

136. Sanscartier, David, et al. "The effect of temperature and aeration rate on bioremediation of diesel-contaminated soil in solid-phase bench-scale bioreactors." *Soil and Sediment Contamination* 20.4 (2011): 353-369.

137. Megharaj, Mallavarapu, et al. "Bioremediation approaches for organic pollutants: a critical perspective." *Environment international* 37.8 (2011): 1362-1375.

138. Sharma, Indu. "Bioremediation techniques for polluted environment: concept, advantages, limitations, and prospects." *Trace metals in the environment-new approaches and recent advances*. IntechOpen, 2020.

139. Sayara, Tahseen, Montserrat Sarrà, and Antoni Sánchez. "Effects of compost stability and contaminant concentration on the bioremediation of PAHs-contaminated soil through composting." *Journal of Hazardous Materials* 179.1-3 (2010): 999-1006.

140. Nocentini, M., D. Pinelli, and F. Fava. "Bioremediation of a soil contaminated by hydrocarbon mixtures: the residual concentration problem." *Chemosphere* 41.8 (2000): 1115-1123.

141. Lahel, Abu, et al. "Effect of process parameters on the bioremediation of diesel contaminated soil by mixed microbial consortia." *International Biodeterioration & Biodegradation* 113 (2016): 375-385.

142. Liu, Shi, and Joseph M. Suflita. "Ecology and evolution of microbial populations for bioremediation." *Trends in Biotechnology* 11.8 (1993): 344-352.

143. Santini, Talitha C., et al. "pH and organic carbon dose rates control microbially driven bioremediation efficacy in alkaline bauxite residue." *Environmental Science & Technology* 50.20 (2016): 11164-11173.

144. Marin, J. A., T. Hernandez, and C. Garcia. "Bioremediation of oil refinery sludge by landfarming in semiarid conditions: Influence on soil microbial activity." *Environmental research* 98.2 (2005): 185-195.

145. Abd El-Rahim, Wafaa M., Ola Ahmed M. El-Ardy, and Fatma HA Mohammad. "The effect of pH on bioremediation potential for the removal of direct violet textile dye by Aspergillus niger." *Desalination* 249.3 (2009): 1206-1211.

146. E.S. Costa-Júnior, E.F. Barbosa-Stancioli, A.A.P. Mansur, W.L. Vasconcelos, H. S. Mansur, Preparation and characterization of chitosan/poly(vinyl alcohol) chemically crosslinked blends for biomedical applications, Carbohydr. Polym. 76 (2009) 472–481, https://doi.org/10.1016/j.carbpol.2008.11.015.

147. El-Shamy, Ahmed G., and H. S. S. Zayied. "New polyvinyl alcohol/carbon quantum dots (PVA/CQDs) nanocomposite films: structural, optical and catalysis properties." *Synthetic Metals* 259 (2020): 116218.

148. Gandhi, Muniyappan Rajiv, and S. Meenakshi. "Preparation and characterization of silica gel/chitosan composite for the removal of Cu (II) and Pb (II)." *International Journal of Biological Macromolecules* 50.3 (2012): 650-657.

149. Zheng, Yian, Dajian Huang, and Aiqin Wang. "Chitosan-g-poly (acrylic acid) hydrogel with crosslinked polymeric networks for Ni2+ recovery." *Analytica chimica acta* 687.2 (2011): 193-200.

150. Habiba, Umma, et al. "Chitosan/(polyvinyl alcohol)/zeolite electrospun composite nanofibrous membrane for adsorption of Cr6+, Fe3+ and Ni2+." *Journal of hazardous materials* 322 (2017): 182-194.

151. Yang, Guanghui, et al. "Luminescent poly (vinyl alcohol)/carbon quantum dots composites with tunable water-induced shape memory behavior in different pH and temperature environments." *ACS Applied Materials & Interfaces* 8.50 (2016): 34744-34754.

152. gamal El-Shamy, Ahmed. "Novel hybrid nanocomposite based on Poly (vinyl alcohol)/carbon quantum dots/fullerene (PVA/CQDs/C60) for thermoelectric power applications." *Composites Part B: Engineering* 174 (2019): 106993.

153. Humphreys, C. J. "The significance of Bragg's law in electron diffraction and microscopy, and Bragg's second law." *Acta Crystallographica Section A: Foundations of Crystallography* 69.1 (2013): 45-50.

154. Al-Ghouti, Mohammad A., and Dana A. Da'ana. "Guidelines for the use and interpretation of adsorption isotherm models: A review." *Journal of hazardous materials* 393 (2020): 122383.

155. Raya, Indah, et al. "Chorella vulgaris and Spirulina platensis: Concentration of protein, Docosahexaenoic Acid Chorella (DHA), Eicosapentaenoic Acid (EPA) and variation concentration of maltodextrin via microencapsulation method." *Int. J. Appl. Chem* 12 (2016): 539-548.

156. Langmuir, Irving. "The adsorption of gases on plane surfaces of glass, mica and platinum." *Journal of the American Chemical society* 40.9 (1918): 1361-1403.

157. Dada, A. O., et al. "Langmuir, Freundlich, Temkin and Dubinin–Radushkevich isotherms studies of equilibrium sorption of Zn2+ unto phosphoric acid modified rice husk." *IOSR Journal of applied chemistry* 3.1 (2012): 38-45.

158. Myers, A. L. "Thermodynamics of adsorption in porous materials." *AIChE journal* 48.1 (2002): 145-160.

159. Guggenheim, Edward Armand, and Neil Kensington Adam. "The thermodynamics of adsorption at the surface of solutions." *Proceedings of the royal society of London. Series A, containing papers of a mathematical and physical character* 139.837 (1933): 218-236.

160. Bering, B. P., M. M. Dubinin, and V. V. Serpinsky. "On thermodynamics of adsorption in micropores." *Journal of Colloid and Interface Science* 38.1 (1972): 185-194.

161. Alexander, M. "Biodegradation and bioremediation. 2nd edn Academic Press." *San Diego, USA* (1999).

162. Ferenci, Thomas. "Growth of bacterial cultures' 50 years on: towards an uncertainty principle instead of constants in bacterial growth kinetics." *Research in microbiology* 150.7 (1999): 431-438.

163. Bailey, James E., and David F. Ollis. *Biochemical engineering fundamentals*. McGraw-Hill, 2018.

164. Gaudy, Anthony F., and Elizabeth T. Gaudy. "Microbiology for environmental scientists and engineers." *Water resources and environmental engineering (USA)* (1980).

165. Meddouri, Malaaz, et al. "Effect of co-solvent on structural and morphological properties of ZnO aerogel prepared by a modified sol-gel process." *The European Physical Journal-Applied Physics* 66.1 (2014): 10402.

166. Burgess, Robert M., et al. "Effects-directed analysis (EDA) and toxicity identification evaluation (TIE): Complementary but different approaches for diagnosing causes of environmental toxicity." *Environmental Toxicology and Chemistry* 32.9 (2013): 1935-1945.

167. Neagu, Monica, et al. "Updated Aspects of Safety Regulations for Biomedical Applications of Aerogel Compounds—Compendia-Like Evaluation." *Safety* 9.4 (2023): 80.

168. Kong, Hao, et al. "Two-dimensional material-based functional aerogels for treating hazards in the environment: synthesis, functional tailoring, applications, and sustainability analysis." *Nanoscale Horizons* 7.2 (2022): 112-140.

169. Ruthven, Douglas M. *Principles of adsorption and adsorption processes*. John Wiley & Sons, 1984.

170. Cheung, Y. H., Ming Hung Wong, and N. F. Y. Tam. "Root and shoot elongation as an assessment of heavy metal toxicity and 'Zn Equivalent Value'of edible crops." *Hydrobiologia* 188 (1989): 377-383.

171. Agathokleous, E., Belz, R. G., Kitao, M., Koike, T., & Calabrese, E. J. (2019). Does the root to shoot ratio show a hormetic response to stress? An ecological and environmental perspective. *Journal of Forestry Research*, *30*(5), 1569-1580.

172. Asati, Himanshu, Raka Mondal, and Kumud Malika Tripathi. "Economically viable N-doped graphene aerogel for the photodegradation of structurally different dyes and a plant-model-based environmental assessment." *Environmental Science: Nano* (2024).

173. Shahnaz, Tasrin, et al. "Magnetic nanocellulose from Cyperus rotundas grass in the absorptive removal of rare earth element cerium (III): Toxicity studies and interpretation." *Chemosphere* 287 (2022): 131912.

174. Cavali, Matheus, et al. "Effect of sequential acid-alkaline treatment on physical and chemical characteristics of lignin and cellulose from pine (Pinus spp.) residual sawdust." *Bioresource Technology* 316 (2020): 123884.

175. Salimian, S., et al. "A review on aerogel: 3D nanoporous structured fillers in polymer-based nanocomposites." *Polymer Composites* 39.10 (2018): 3383-3408.

176. Bezerra, M. A., Santelli, R. E., Oliveira, E. P., Villar, L. S., & Escaleira, L. A. (2008). Response surface methodology (RSM) as a tool for optimization in analytical chemistry. *Talanta*, *76*(5), 965-977.

177. Lenth, R. V. (2010). Response-surface methods in R, using rsm. *Journal of statistical Software*, *32*, 1-17.

178. Şen, B. H., Safavi, K. E., & Spångberg, L. S. (1999). Antifungal effects of sodium hypochlorite and chlorhexidine in root canals. *Journal of Endodontics*, *25*(4), 235-238.

179. Al-Tohamy, R., Ali, S. S., Li, F., Okasha, K. M., Mahmoud, Y. A. G., Elsamahy, T., ... & Sun, J. (2022). A critical review on the treatment of dye-containing wastewater: Ecotoxicological and health concerns of textile dyes and possible remediation approaches for environmental safety. *Ecotoxicology and Environmental Safety*, *231*, 113160.

180. Chen, L., Lu, H., Jiang, X., Qu, N., Hasi, Q., Zhang, Y., ... & Jiang, S. (2024). Microorganisms immobilized hydroxyethyl cellulose/luffa composite sponge for selective adsorption and biodegradation of oils in wastewater. *International Journal of Biological Macromolecules*, 133477.

181. Rápó, E., & Tonk, S. (2021). Factors affecting synthetic dye adsorption; desorption studies: a review of results from the last five years (2017–2021). Molecules, 26(17), 5419.

182. Zhao, Y., Li, Y., & Zhang, R. (2018). Silica aerogels having high flexibility and hydrophobicity prepared by sol-gel method. *Ceramics International*, *44*(17), 21262-21268.

183. Kaya, G. G., & Deveci, H. (2020). Synergistic effects of silica aerogels/xerogels on properties of polymer composites: A review. *Journal of Industrial and Engineering Chemistry*, *89*, 13-27.

184. Kucharek, M., MacRae, W., & Yang, L. (2020). Investigation of the effects of silica aerogel particles on thermal and mechanical properties of epoxy composites. *Composites Part A: Applied Science and Manufacturing*, *139*, 106108.

185. Ferrero, F. (2007). Dye removal by low-cost adsorbents: hazelnut shells in comparison with wood sawdust. *Journal of hazardous materials*, *142*(1-2), 144-152.

186. Wei, J., Yang, Z., Sun, Y., Wang, C., Fan, J., Kang, G., ... & Li, Y. (2019). Nanocellulose-based magnetic hybrid aerogel for adsorption of heavy metal ions from water. *Journal of Materials Science*, *54*(8), 6709-6718.

187. Scherer, George W. "Adsorption in aerogel networks." *Journal of non-crystalline solids* 225 (1998): 192-199.

188. Karami, Davood. "A review of aerogel applications in adsorption and catalysis." *Journal of Petroleum Science and Technology* 8.4 (2018): 3-15.

189. Abramian, Lara, and Houssam El-Rassy. "Adsorption kinetics and thermodynamics of azo-dye Orange II onto highly porous titania aerogel." *Chemical Engineering Journal* 150.2-3 (2009): 403-410.

190. Chen, B., Ding, L., Wang, Y., & Zhang, Y. (2022). High efficient adsorption for thorium in aqueous solution using a novel tentacle-type chitosan-based aerogel:

Adsorption behavior and mechanism. *International Journal of Biological Macromolecules*, *222*, 1747-1757.

191. Yu, B., Xu, J., Liu, J. H., Yang, S. T., Luo, J., Zhou, Q., ... & Liu, Y. (2013). Adsorption behavior of copper ions on graphene oxide–chitosan aerogel. *Journal of Environmental Chemical Engineering*, *1*(4), 1044-1050.

192. Štandeker, Suzana, Zoran Novak, and Željko Knez. "Adsorption of toxic organic compounds from water with hydrophobic silica aerogels." *Journal of colloid and interface science* 310.2 (2007): 362-368.

193. Chong, Mee Yoke, and Yew Joon Tam. "Bioremediation of dyes using coconut parts via adsorption: a review." *SN Applied Sciences* 2 (2020): 1-16.

194. Senan, Resmi C., and T. Emilia Abraham. "Bioremediation of textile azo dyes by aerobic bacterial consortium aerobic degradation of selected azo dyes by bacterial consortium." *Biodegradation* 15 (2004): 275-280.

195. Shah, M. P. (2019). Bioremediation of azo dye. In *Microbial wastewater treatment* (pp. 103-126). Elsevier.

196. Kumar, S. S., Shantkriti, S., Muruganandham, T., Murugesh, E., Rane, N., & Govindwar, S. P. (2016). Bioinformatics aided microbial approach for bioremediation of wastewater containing textile dyes. *Ecological Informatics*, *31*, 112-121.

197. Ghosh, Arpita, Manisha Ghosh Dastidar, and T. R. Sreekrishnan. "Bioremediation of chromium complex dyes and treatment of sludge generated during the process." *International Biodeterioration & Biodegradation* 119 (2017): 448-460.

198. Ajaz, Mehvish, Sana Shakeel, and Abdul Rehman. "Microbial use for azo dye degradation—a strategy for dye bioremediation." *International Microbiology* 23 (2020): 149-159.